

**EFFECTS OF THERMAL SPIKES ON HYGROTHERMALLY  
AND ULTRAVIOLET RADIATION TREATED FIBER  
REINFORCED POLYMER COMPOSITES**

**Thesis submitted to  
NATIONAL INSTITUTE OF TECHNOLOGY, ROURKELA  
In Partial Fulfillment of the Requirements for the Degree of  
Bachelor of Technology**



**Submitted by-  
Soumya Mishra**

**110MM0027**

**Shivangi Sahu**

**110MM0274**

**Under the Guidance of**

**Prof. B. C. Ray**

**Department of Metallurgical & Materials Engineering,**

**National Institute of Technology, Rourkela**

**2014**



**National Institute of Technology  
Rourkela**

**CERTIFICATE**

This is to certify that the thesis entitled, '**Effects Of Thermal Spikes On Hygrothermally And Ultraviolet Radiation Treated Fiber Reinforced Polymer Composites**' submitted by **Soumya Mishra (110MM0027)** and **Shivangi Sahu (110MM0274)** in partial fulfillment of the requirements for the award of Bachelor of Technology Degree in Metallurgical & Materials Engineering at the National Institute Of Technology, Rourkela is a bonafide and authentic research work carried out by them under my supervision and guidance over the last one year (2013-14).

To the best of my knowledge, the work embodied in this thesis has not been submitted earlier, in part or full, to any other university or institution for the award of any Degree or Diploma.

Date:

Dr. B. C. Ray

Dept. of Metallurgical & Materials Engineering

National Institute of Technology, Rourkela

# ACKNOWLEDGEMENT

We would like to convey our heartfelt gratitude and regards to our project supervisor **Dr. B.C. Ray**, Department of Metallurgical & Materials Engineering, National Institute of Technology, Rourkela for his outstanding guidance and for giving us such a mind stimulating and innovative project. He has always bestowed parental care upon us and evinced keen interest in solving our problems. An erudite teacher, a magnificent personality and a strict disciplinarian, we consider ourselves fortunate to have worked under his supervision.

We are highly grateful to Department of Metallurgical & Materials Engineering, NIT Rourkela, for providing required facilities during the course of the work. We admit thanks to **Mrs. Sanghamitra Sethi**, Research scholar, Department of Metallurgical & Materials Engineering, NIT Rourkela for showing us the guideline as well as rendering support and expertise needed for carrying out the work. We also express our deep gratitude to **Mr. Dinesh Kumar Rathore**, Research Scholar, for his continual guidance and support. We also thank **Mr. Kishore Kumar Mahato** for rendering support while conducting experiments. We wish to place our deep sense of thanks to **Mr. Rajesh Pattnaik** and **Mr. S. Hembram** for their cooperation and critical suggestions during our experimental work.

Soumya Mishra  
110MM0027

Shivangi Sahu  
110MM0274

Date:  
Place:

## List of Symbols

F	Rate of transfer of water molecules per unit area of cross-section of the material ( $\text{kg/m}^2\text{s}$ )
D	Diffusion coefficient or diffusivity of the moisture in the material ( $\text{m}^2/\text{s}$ )
C	Moisture concentration in the material ( $\text{kg/m}^3$ )
l	Height of the material (mm)
w	Width of the material (mm)
h	Thickness of the material (mm)
t	Exposure time (s)
M	Percentage moisture content in the material
k	Boltzmann's constant ( $1.38 \cdot 10^{-23} \text{ J/K}$ )
n	Number density of mobile water molecules ( $\text{molecules/cm}^3$ )
N	Number density of bound water molecules ( $\text{molecules/cm}^3$ )
$\mu$	Dimensionless hindrance coefficient
$\beta$	Probability per unit time that a bound water molecule becomes mobile ( $\text{days}^{-1}$ )
$\gamma$	Probability per unit time that a mobile water molecule becomes bound ( $\text{days}^{-1}$ )
$\kappa$	Characteristic diffusion constant
I	Positive odd integer

## Subscripts

$x, y, z$  in  $x, y$  and  $z$  directions

$t$  at time  $t$

$\infty$  at saturation level

$o$  when concentration dependence is neglected

$\gamma$  for mobile water molecules

$F$  Fickian term

$R$  Resin relaxation term

## List of Tables

Table 1.1: Chemical composition of different of glass fibers

Table 1.2: Properties of different of carbon fibers

Table 1.3: Properties of different grades of Kevlar fibers

Table 4.1: Properties of epoxy resin, glass fibers and carbon fibers

## List of Figures

Fig. 1.1: History of use of composite materials (a) straw reinforced mud bricks for building houses in Egypt in 4000 BC (b) 12<sup>th</sup> century Mongolian composite bows (c) first manned hot air balloon in 1783 (d) de Havilland DH.98 Mosquito, World War II

Fig. 1.2: Classification of the various types of composites

Fig. 1.3: Schematic representation of the various geometrical and spatial arrangements of reinforcements (a) concentration (b) size (c) shape (d) distribution (e) orientation

Fig. 1.4: Chemical structure of diglycidyl ether of bisphenol A (DGEBA)

Fig. 1.5: Glass fibers available for use in a variety of forms (a) chopped strand (b) continuous yarn (c) roving (d) fabric

Fig. 1.6: Schematic representation of fiber/matrix interface

Fig. 1.7: Comparison of FRP materials with conventional materials

Fig. 1.8: (a) Debonding failure of Young America boat in 1999 (b) broken wing of American Airlines Flight 587

Fig. 2.1: Typical linear Fickian diffusion model

Fig. 2.2: Experimental data fitting with linear Fickian diffusion model of carbon/ epoxy composites aged at 70°C and 85% RH

Fig. 2.3: Typical linear Fickian and non-Fickian diffusion models

Fig. 2.4: Langmuirian model applied to moisture absorption data of glass/epoxy composite exposed to humid ageing at 70°C and 85% RH

Fig. 2.5: (a) Typical 3D hindered diffusion model and (b) fitting of experimental data of carbon-fiber reinforced bismaleimide composites (immersed in distilled water) with hindered diffusion model and linear Fickian model

Fig. 2.6: Theoretical moisture uptake curves showing combined effect of Fickian diffusion and polymeric relaxation

Fig. 2.7: Experimental data following the dual-stage diffusion model in (a) glass fiber reinforced polyester composite, immersed in water and (b) glass fibers reinforced isophthalic polyester composite exposed to water and humidity

Fig. 2.8: Typical diffusion path in polymeric composites composed of (a) permeable fibers and (b) impermeable fibers

Fig. 2.9: Structure dependence of stability of epoxy resins in boiling water

Fig. 2.10: Effect of silanization on the moisture uptake profile of glass fiber/epoxy composites

Fig. 2.11: Schematic diagram of plasticization caused by moisture in polymer matrix

Fig. 2.13: Scanning electron micrographs of fracture surfaces of glass/polyester samples exposed to humid environment for (a) 0 hours (b) 500 hours (c) 1000 hours (d) 2000 hours

Fig. 2.14: Scanning electron micrographs of carbon/epoxy composites exposed to humidity, showing (a) matrix cracking and (b) fiber breakage

Fig. 5.1: Moisture uptake kinetics of (a) GFRP composite samples with post-curing treatment (b) GFRP composite samples without post-curing treatment (c) GFRP composite with alumina nano-fillers (d) CFRP composite samples and (e) Hybrid composite

Fig. 5.2: Comparison of moisture uptake kinetics of (a) GFRP composite samples with and without post-curing treatment (b) GFRP composite samples with and without post-curing treatment and GFRP with alumina nano-fillers (c) GFRP composite samples with and without post-curing treatment, GFRP composite with alumina nano-fillers, CFRP composite samples and Hybrid composite

Fig. 5.3: Variation of ILSS of GFRP composites with post-curing treatment with spiking temperature for times (a) 5 minutes (b) 20 minutes

Fig. 5.4: Variation of ILSS of GFRP composites without post-curing treatment with spiking times at 60°C

Fig. 5.5: Variation of ILSS of CFRP composites (a) with spiking times at temperature 60°C (b) with no treatment, hygrothermal treatment for 2000 hours and UV treatment

Fig. 5.6: Variation of ILSS of Hybrid composites (a) with spiking times at temperature 60°C (b) with no treatment, hygrothermal treatment for 2000 hours and UV treatment



Fig. 5.7: FTIR plot for GFRP specimens subject to hygrothermal treatment for 2000 hours and thermal spike for 15 minutes

Fig. 5.8 FTIR plot for CFRP specimens subject to hygrothermal treatment for 2000 hours and thermal spike for 20minutes

Fig. 5.9 FTIR plot for CFRP specimens subject to hygrothermal treatment for 2000 hours and thermal spike at 60°C

Fig. 5.10 FTIR plot for GFRP specimens subject to hygrothermal treatment for 2000 hours and thermal spike at 60°C

Fig. 5.11 FTIR plot for Glass-Carbon-Epoxy composite specimens subject to hygrothermal treatment for 2000 hours and ambient specimens

Fig. 5.12 FTIR plot for GFRP+3 wt%  $\text{Al}_2\text{O}_3$  nano composite specimens subject to hygrothermal treatment, UV treatment and ambient conditions

Fig. 5.13 FTIR plot for Glass-Carbon-Epoxy composite and GFRP specimens subject to UV conditioning

Fig. 5.14: Variation of glass transition temperature of GFRP composites with hygrothermal treatment and thermal spiking at different temperatures.

Fig. 5.15: Variation of glass transition temperature of CFRP composites with hygrothermal treatment and thermal spiking at different temperatures.

Fig. 5.16: Variation of glass transition temperature of Hybrid composites with hygrothermal treatment and thermal spiking at different temperatures.

Fig. 5.17: Variation of glass transition temperature of GFRP composites with nano fillers with hygrothermal treatment and UV treatment

Fig. 5.18: Scanning electron micrographs of fractured E-glass fiber surfaces of GFRP samples tested at ambient temperature with (a) no treatment (b) hygrothermal treatment for 400 hours (c) thermal spiking at 60°C after hygrothermal treatment (d) thermal spiking at 100°C after hygrothermal treatment (e) thermal spiking at 200°C after hygrothermal treatment

Fig. 5.19: Scanning electron micrographs of epoxy matrix of GFRP samples tested at ambient temperature with (a) no treatment (b) hygrothermal treatment for 400 hours (c) thermal spiking at 60°C after hygrothermal treatment (d) thermal spiking at 100°C after hygrothermal treatment (e) thermal spiking at 150°C after hygrothermal treatment (f) thermal spiking at 200°C after hygrothermal treatment

Fig. 5.20: Scanning electron micrographs of fractured E-glass fiber surfaces of GFRP samples tested at ambient temperature with (a) no treatment (b) hygrothermal treatment for 400 hours (c) thermal spiking at 60°C after hygrothermal treatment (d) thermal spiking at 100°C after hygrothermal treatment (e) thermal spiking at 200°C after hygrothermal treatment

Fig. 5.21: Scanning electron micrographs of fractured CFRP samples tested at ambient temperature subjected to hygrothermal treatment for 2000 hours showing (a) matrix failure modes (b) brittle failure of fibers and interfacial debonding (c) massive fiber imprints on matrix

Fig. 5.22: Scanning electron micrographs of fractured hybrid composite samples tested at ambient temperature subjected to hygrothermal treatment for 2000 hours showing (a) brittle failure of fibers and interfacial debonding (b) matrix cracking (c) matrix degradation

Fig. 5.23: Scanning electron micrographs of fractured GFRP samples with alumina nano-fillers, tested at ambient temperature with (a) brittle failure of fibers and interfacial debonding (b) matrix degradation (c) agglomerated nano-particles

# Table of Contents

Certificate.....	ii
Acknowledgement.....	iii
List of Symbols.....	iv
List of Tables.....	vi
List of Figures.....	vii
Abstract.....	xiv
1. Introduction.....	1
1.1.Overview and History.....	1
1.2.Matrix.....	3
1.2.1. Polymer Matrix.....	4
1.2.1.1.Thermosets and thermoplastics.....	4
1.2.1.2.Epoxy resin.....	5
1.3.Reinforcements.....	6
1.3.1. Fibers.....	6
1.3.1.1.Glass fibers.....	6
1.3.1.2.Carbon fibers.....	8
1.3.1.3.Kevlar fibers.....	8
1.3.2. Nano-fillers.....	9
1.4.Interface/Interface.....	11
1.5.Promise of FRP Materials.....	12
1.6. Application of FRP Materials.....	13
1.7.Limitation of FRP Materials.....	17
2. Literature Review.....	19
2.1.Moisture Ingression in FRP Composites.....	19
2.1.1. Moisture Ingression models.....	19
2.1.1.1. Linear Fickian diffusion model.....	19

2.1.1.2. Deviation from Fickian behaviour: Anomalous behaviour.....	22
2.1.1.3. Langmuirian diffusion model.....	23
2.1.1.4. Hindered diffusion model.....	25
2.1.1.5. Dual-stage diffusion model.....	27
2.1.2. Factors affecting moisture ingress kinetics.....	29
2.1.2.1. Effect of Fiber system.....	29
2.1.2.2. Effect of Resin structure.....	30
2.1.2.3. Effect of interfacial adhesion.....	31
2.1.3. Effect of Moisture Ingression on Mechanical Properties of FRP Composites...	32
2.1.4. Effect of Moisture Ingression on Failure Modes of FRP Composites.....	33
2.2. Effect of Thermal Spiking on FRP Composites.....	36
2.3. Effect of UV Radiation on FRP Composites.....	36
3. Motivation.....	37
4. Experimental Details.....	39
4.1. Effect of Hygrothermal Treatment and Thermal Spiking on FRP Composites.....	41
4.1.1. Glass Fibre Reinforced Composites.....	41
4.1.2. Glass Fibre Composites with Nano-fillers.....	42
4.1.3. Carbon Fibre Reinforced Composites.....	43
4.1.4. Glass and Carbon Fibre Reinforced Hybrid Composites.....	44
4.2. Effect of UV Treatment on FRP Composites.....	45
5. Results and Discussion.....	46
5.1. Moisture Ingression Behaviour in FRP Composites.....	46
5.2. Effect of Moisture Ingression and UV radiation exposure on Interlaminar Shear Strength (ILSS) in FRP Composites.....	51

5.3. Effect of Moisture Ingression and UV conditioning on Bond Structure in FRP Composites.....	54
5.4. Effect of Moisture Ingression and UV conditioning on Glass Transition Temperature of FRP Composites.....	59
5.5. Effect of Moisture Ingression on Failure Modes in FRP Composites.....	62
5.5.1. Glass/Epoxy Composites.....	62
5.5.1.1. Failure Mode of Glass Fibers.....	62
5.5.1.2. Failure Mode of Epoxy Matrix.....	63
5.5.1.3. Failure Mode of Glass Fiber/Epoxy Interphase.....	65
5.5.2. Carbon/Epoxy Composites.....	67
5.5.3. Glass/Carbon/Epoxy Hybrid Composites.....	68
5.5.4. Glass/Epoxy Composites with alumina nano-fillers.....	69
6. Conclusion.....	70
7. Scope of Future Work.....	72
References.....	73
Appendix I	
List of papers presented/communicated based on this project.....	78

## Abstract

Nowadays fiber reinforced polymer (FRP) composites are in massive demand for applications in diversified fields owing to their unique combination of properties. Despite numerous advantages over conventional metallic materials, polymeric composites suffer from the limitation of being susceptible to degradation when exposed to harsh environmental attacks. During their fabrication, storage and service period, components made up of these polymeric materials are subjected to heat and moisture, when operating under changing environments. Such environmental exposures affect the reliability and predictability of the short term as well as the long term properties and also the in-service performance of these components. The fiber/matrix interphase plays a key role in deciding the moisture diffusion kinetics as well as response of the FRP composites to different environments. Although moisture uptake theory and mechanism in polymeric composites has been an active area of research for last few decades, but still accurate predictability of moisture absorption kinetics is under question due to complex sorption kinetics and scattered experimental data. The present investigation aims to study the moisture ingress kinetics and to evaluate the synergistic mechanisms of degradation caused by moisture and temperature on the performance of fibrous polymeric composites. Also, polymer matrix degradation caused by ultraviolet radiation exposure is evaluated. Mechanical properties are found to be degraded and the failure modes are observed to change with moisture uptake, thermal spiking and ultraviolet radiation exposure.

**Keywords:** Polymer Composites, Hygrothermal Ageing, Thermal Spike, UV exposure, Moisture uptake kinetics, Interphase, Adhesion, Mechanical Properties, Inter-laminar shear strength.

# Chapter 1

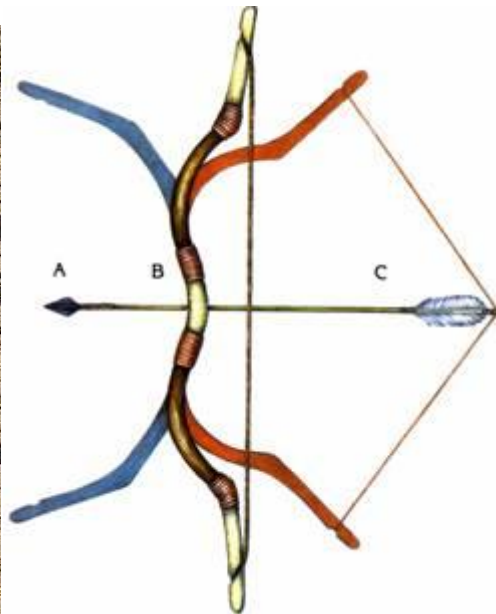
## Introduction

### 1.1.Overview and history

Many applications in the present day world especially aerospace, structural and underwater applications require a combination of various properties which are available in conventional materials like metals, alloys, ceramics, polymers, etc. The concept of composite materials has helped fulfil this requirement by providing the liberty to have tailor-made properties according to the desired efficiencies. A composite material is a judicious combination of two or more different materials, which maintain their distinct identities, to give rise to a material possessing a unique combination of exceptional properties. It generally consists of two basic chemically dissimilar components- the matrix, or the continuous phase, and the reinforcement, or the dispersed strengthening phase. The overall properties of composite materials depend on the individual properties of its constituents, their relative proportions in the composite and the geometry of the reinforcing phase.



(a)



(b)





(c)



(d)

**Fig. 1.1 History of use of composite materials (a) straw reinforced mud bricks for building houses in Egypt in 4000 BC(b) 12<sup>th</sup> century Mongolian composite bows(c) first manned hot air balloon in 1783 (d) *de Havilland DH.98 Mosquito*, World War II**

The maiden use of composite dates back to 4000 BC when the early Egyptians and Mesopotamians used straw reinforced mud bricks to build strong and reliable building structures [1]. Around the turn of the 12<sup>th</sup> century, the Mongols exhibited their vast understanding of the advantages of using composite materials in their weaponry. They have been known to have utilized various materials like wood, cattle sinew, antlers, silk and resin glue to design stronger and more effectively used bows in their time [2]. The first ever manned balloon flight in 1783 was possible because of composite technology. The balloon was made up of linen fabric and paper composite material [3]. The modern era of composites was heralded when scientists during the late 19<sup>th</sup> century developed synthetic polymers like polyester, polystyrene and vinyl. The lack of strength in these man-made plastics led to the idea of using strengthening reinforcements for structural applications. The major development was in 1935 when Owens Corning produced the first ever glass fiber: fiberglass. Thus, modern day FRPs (fiber-reinforced polymer) came into being. During the Second World War there was an urgent need for strong, light-weight materials to build fighter planes. Wood-composite laminates were used for weight saving in *de Havilland DH.98 Mosquito*, a Fighter aircraft of British Air Force. And since then, composite materials



have been in used almost everywhere – from ordinary toys to super-critical structures such as missiles and spacecrafts

A general classification of composites can be depicted as follows:

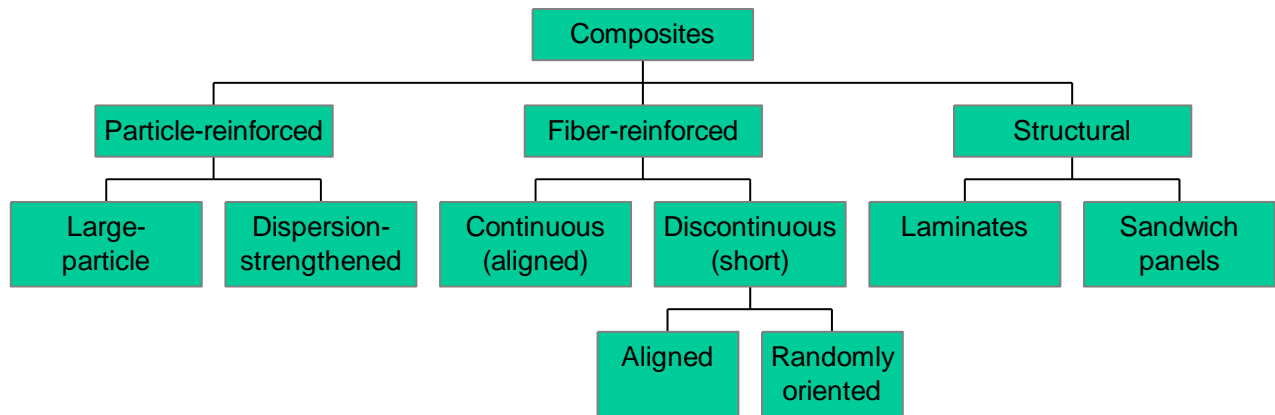


**Fig. 1.2 Classification of the various types of composites [4]**

The various geometrical variations of composite materials have a profound effect on the final combination of properties in the composites.

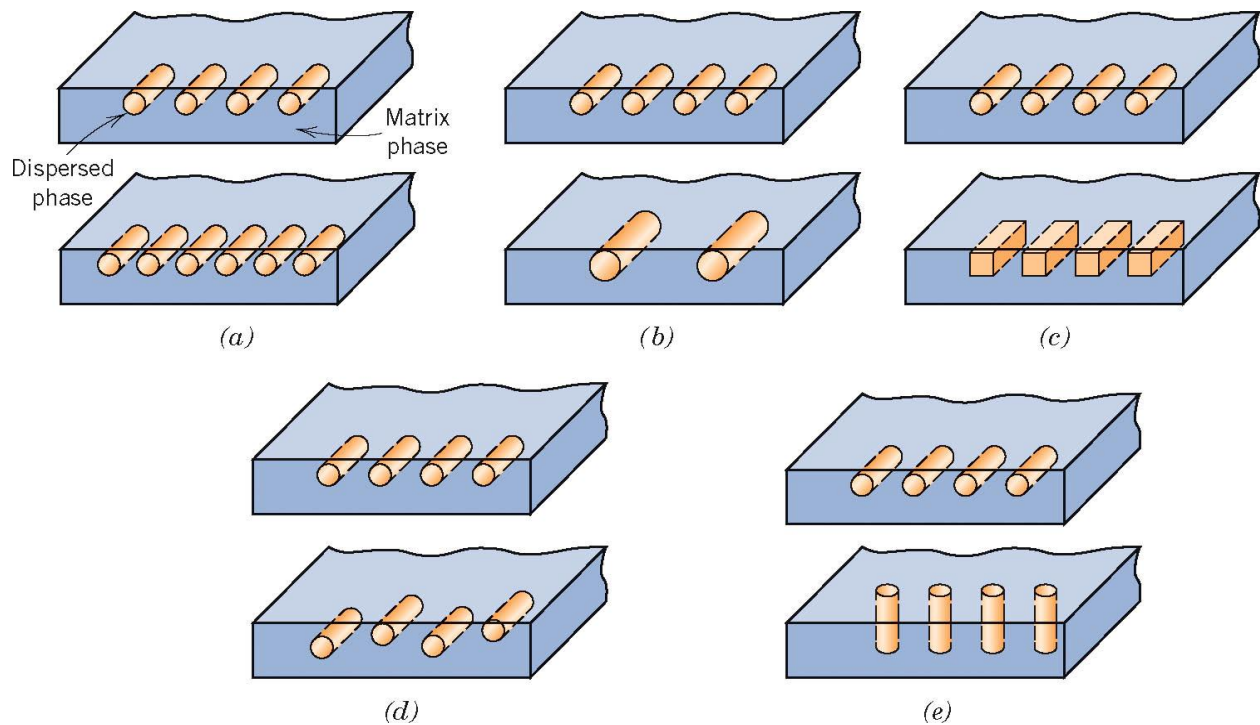


**Fig. 1.3 Schematic representation of the various geometrical and spatial arrangements of reinforcements (a) concentration (b) size (c) shape (d) distribution (e) orientation [4]**

## **1.2.Matrix**

The matrix in a composite is the continuous phase in a multiphase composite material. Its chief functions are as follows

1. It binds together the reinforcement materials to maintain integrity of the composite.
2. It keeps the fibers/particles distinct from one another
3. The most important function of a matrix phase is the transfer of load to the strengthening phase
4. It also protects the dispersed phase from damage and degradation due to external factors.

Commonly used matrix materials can be polymers, metals and ceramics. Accordingly composites can be categorised as polymer matrix composites (PMC), metal matrix composites (MMC) and ceramic matrix composites (CMC).

### **1.2.1. Polymer matrix**

Polymers are the most commonly used matrix material in spite of their lower strength and modulus, low temperature tolerance, poor electrical and thermal conductivity, etc. This is due to their resistance to chemical attack, tenacity, cheap availability and low production costs. Polymers are generally giant chain-like molecules joined together by a process of polymerization. There are two types of polymers used as composite matrices –thermosets and thermoplastics.

#### **1.2.1.1. Thermosets and thermoplastics**

Thermoplastics are those polymers which soften and melt on heating. They are characterised by their amorphous structure and random arrangement of chain molecules and are suitable for easy forming operations by liquid-flow on heating. Examples of thermoplastics are low and high density polystyrene, PMMA and polyethylene.

Thermosetting polymers consist of cross-linked polymer macro molecules in the form of a network structure. Due to this cross-linking the molecules do not slide over each other resulting in strong and rigid polymers which do not soften but decompose on heating. Some examples of thermosets include epoxy, polyester, vinyl ester and phenolic.

#### 1.2.1.2. Epoxy resin

One of the most commonly used polymeric matrix material is thermosetting epoxy resin. They are available in a wide range of varieties from low viscosity liquids to high melting solids and are quite amenable to a range of modifications and processes for tailored use. They offer high strength, low shrinkage, easy curing by a variety of chemical agents, better electrical insulation, proper adhesion and wetting of surfaces. Such properties make them ideal for use in composites. In epoxy resins, cross-linking occurs of epoxide groups (one oxygen and two carbon atoms). For use at elevated temperatures, epoxy resins are cured by addition of chemical agents to yield an inflexible molecular structure. Epoxies that are primarily used for composite applications include the following classes – phenolic glycidyl ethers, aromatic glycidyl amines and cycloaliphatics. The most commonly used epoxy is diglycidyl ether of bisphenol A (DGEBA) which is a type of phenolic glycidyl ether.

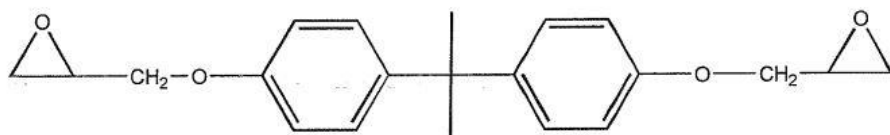


**Fig. 1.4 Chemical structure of diglycidyl ether of bisphenol A (DGEBA) [5]**

The chief curing agents used as hardeners for epoxy resins are amines, amine derivatives or anhydrides. Certain curing agents used at room temperature are polyamides, aliphatic amines and amidoamines. Certain chemicals called modifiers can be used to alter the mechanical and physical functionality of cure or uncured resins. These include rubbers, thermoplastics, fillers, flame retardants and pigments.

## 1.3.Reinforcement

### 1.3.1. Fibers

Most commonly used reinforcements in composite materials are in the form of fibers – short or long, continuous or discontinuous- because of their high stiffness and strength. Advanced fibres like glass, carbon and aramid fibers are more widely accepted for use because of their high strength and low density combination. Natural fibers like cotton, hemp, jute, etc. can also be used due to the low cost factor involved. For effective reinforcing action of fibers, they must possess high aspect ratio ( $l/d$  ratio) for better load transfer to the fibers, small diameter to attain higher theoretical strength and a high degree of flexibility to allow ease of variation in production techniques.

#### 1.3.1.1. Glass fibers

Glass fibers are the most common type of fiber reinforcements used in FRP composites. General chemical compositions of glass fibers include 50-60% silica and other oxides of calcium, boron, sodium, etc. Glass fibers are mainly of three types:

- **E-glass fiber :**  
Good electrical insulator, good strength and average modulus.
- **S-glass fiber:**  
High silica content which makes it ideal for use at elevated temperatures.
- **C-glass fiber:**  
Better resistance to chemical corrosion than other types of fibers.

The common chemical compositions of these types of glass fibers are given in the table listed below.

Composition	E glass	C glass	S glass
SiO <sub>2</sub>	55.2	65.0	65.0
Al <sub>2</sub> O <sub>3</sub>	8.0	4.0	25.0
CaO	18.7	14.0	–
MgO	4.6	3.0	10.0
Na <sub>2</sub> O	0.3	8.5	0.3
K <sub>2</sub> O	0.2	–	–
B <sub>2</sub> O <sub>3</sub>	7.3	5.0	–

**Table 1.1 Chemical composition of different of glass fibers [5]**

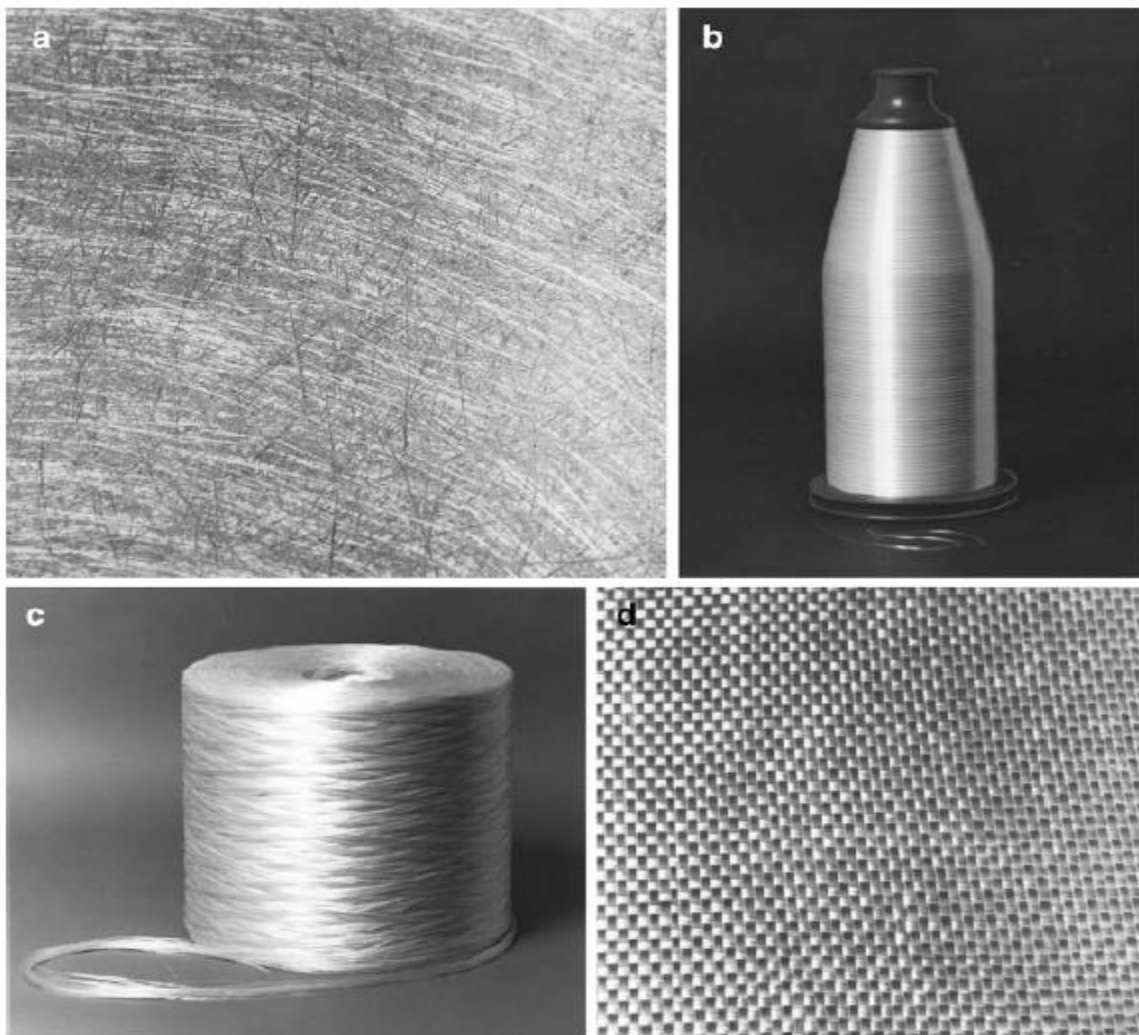


**Fig.1.5 Glass fiber are available for use in a variety of forms (a) chopped strand (b) continuous yarn (c) roving (d) fabric [6]**

### 1.3.1.2. Carbon fibers

Carbon, a highly anisotropic and high directional modulus element in its graphitic form, is very light weight and is a material of choice for reinforcements in FRP composites. Better homogeneous modulus along all axes can be obtained by carbonisation and graphitisation of precursor fibers at elevated temperatures. Carbon are usually obtained by processing of poly acrylonitrile (PAN), cellulose, rayon and pitch (from poly vinyl chloride, petroleum asphalt and coal tar) by the routine process of fiberization, stabilization, carbonisation and graphitization. The properties of carbon fibers obtained from various sources are listed below.

Precursor	Density (g/cm <sup>3</sup> )	Young's modulus (GPa)	Electrical resistivity (10 <sup>-4</sup> Ω cm)
Rayon <sup>a</sup>	1.66	390	10
Polyacrylonitrile <sup>b</sup> (PAN)	1.74	230	18
Pitch (Kureha)			
LT <sup>c</sup>	1.6	41	100
HT <sup>d</sup>	1.6	41	50
Mesophase pitch <sup>e</sup>			
LT	2.1	340	9
HT	2.2	690	1.8
Single-crystal <sup>f</sup> graphite	2.25	1,000	0.40

<sup>a</sup>Union Carbide, ThomeI 50

<sup>b</sup>Union Carbide, ThomeI 300

<sup>c</sup>LT low-temperature heat-treated

<sup>d</sup>HT high-temperature heat-treated

<sup>e</sup>Union Carbide type P fibers

<sup>f</sup>Modulus and resistivity are in-plane values

Source: Adapted with permission from Singer (1979)

**Table 1.2 Properties of different of carbon fibers [7]**

### 1.3.1.3. Kevlar fibers

Kevlar was the first ever organic fiber synthesized by DuPont in 1970s with appropriate strength and modulus for use in composites. It is a type of aramid (aromatic polyamide) fiber whose chemical composition is poly para-phenyleneterephthalamide and is also popularly known as para-aramid. Three grades of Kevlar are commercially available: Kevlar 29, Kevlar 49, and Kevlar 149. Kevlar fibers have comparable strength and modulus values to E-glass fibers but

have lighter weight. Hence, for low density applications, Kevlar is a better substitute for glass fibers in FRP composites. The properties of various Kevlar grades are listed below.

<b>Grade</b>	<b>Density g/cm<sup>3</sup></b>	<b>Tensile Modulus GPa</b>	<b>Tensile Strength GPa</b>	<b>Tensile Elongation %</b>
<b>29</b>	<b>1.44</b>	<b>83</b>	<b>3.6</b>	<b>4.0</b>
<b>49</b>	<b>1.44</b>	<b>131</b>	<b>3.6--4.1</b>	<b>2.8</b>
<b>149</b>	<b>1.47</b>	<b>186</b>	<b>3.4</b>	<b>2.0</b>

**Table 1.3 Properties of different grades of Kevlar fibers [8]**

### **1.3.2. Nano-fillers**

Nano-fillers are particles used as dispersed phase for conventional polymeric applications and composite materials which are nano dimensioned in at least one dimension [9]. One very important feature of nano fillers is their surface area. Their specific areas are known to be one to two orders of magnitude higher than that of conventional fillers. This significantly higher surface area has a profound effect on the properties of the polymer matrix in the vicinity which may alter the properties of the composite significantly. In addition to this, deleterious effects like poor stabilisation of the composite is also to be expected because of such high specific areas. Nano fillers can be regular, rod-like or plate-like depending on their relative dimensions. Nano-clay particles, CNTs etc are mostly used as fillers in the polymer matrix.

The addition of mineral fillers such as silica to a resin usually reduces the thermal expansion coefficient considerably [11]. Epoxy resin filled with the hard filler, titanium diboride, TiB<sub>2</sub>, show enormous but reversible changes in electrical resistivity (by eight orders of magnitude) on heating from ambient temperature to the cure temperature. This is a consequence of thermal expansion affecting inter-particle contacts.



## 1.4.Interface/Interphase

The interface is the two-dimensional boundary region between the matrix and the reinforcements which is of paramount importance in determining the properties of the composite materials. An interphase is the three dimensional form of an interface. Several characteristic properties like concentration of element, elastic modulus, coefficient of thermal expansion, etc. vary across the interface depending on the combination of matrix and reinforcement used.

The high amount of surface area on part of the interface makes its understanding so important for evaluation of composite materials. Factors to be considered for better understanding of the interface include type and extent of bonding between fiber and matrix, wetting of fiber by matrix, load transfer across the interface and so on.

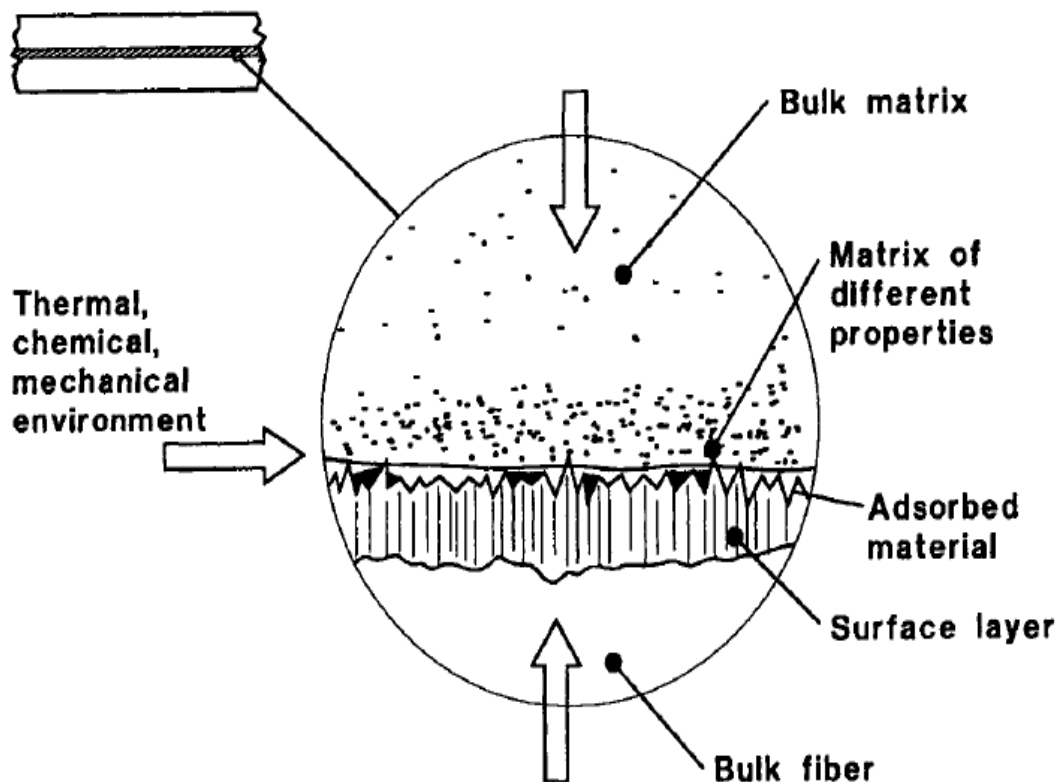


Fig.1.6 Schematic representation of fiber/matrix interface [10]



## 1.5. Promises of FRP Materials

Fiber-reinforced polymers (FRP) are composites which have fibers embedded as reinforcements in a resin matrix.

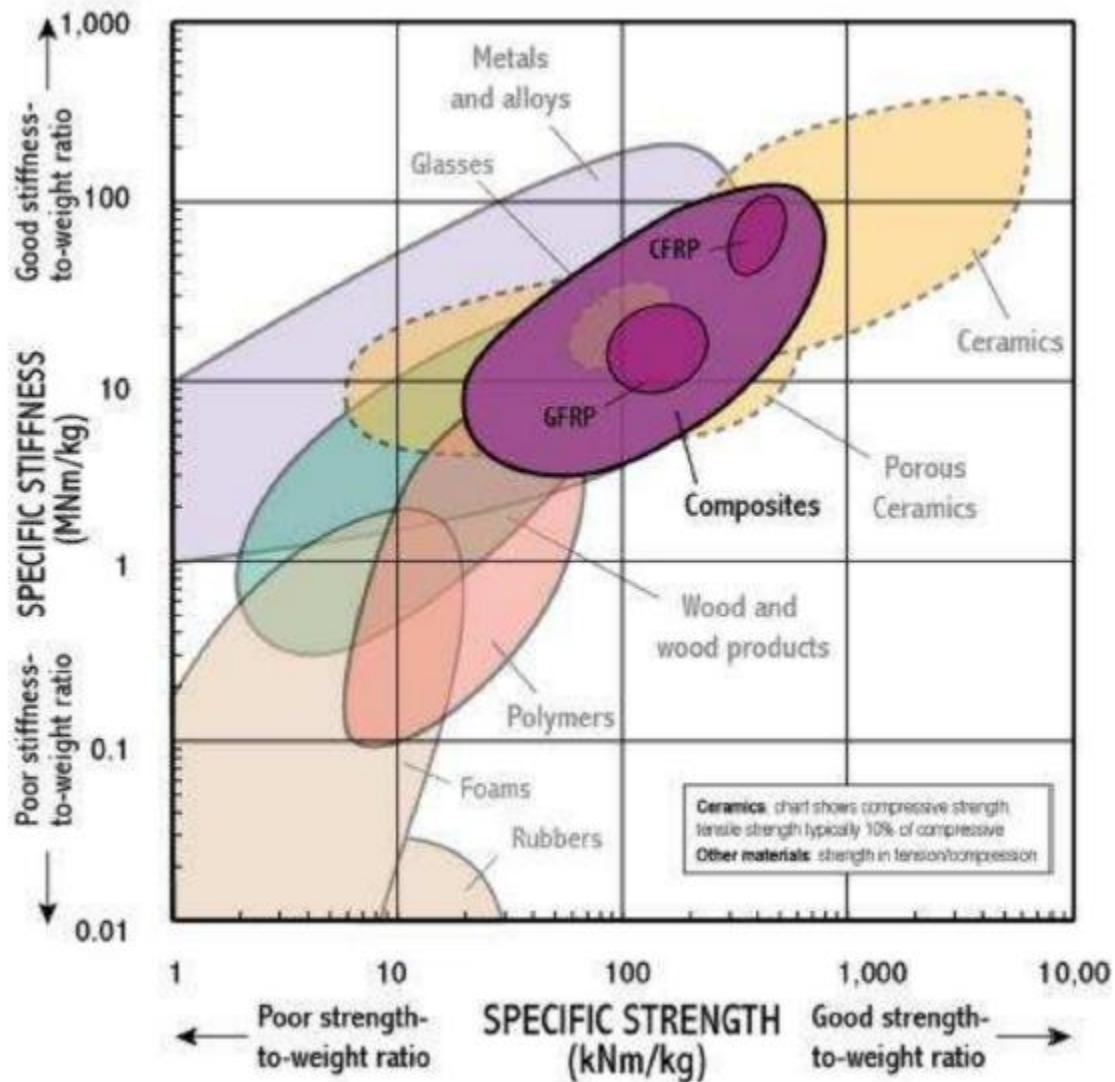


Fig.1.6 Comparison of FRP materials with conventional materials

They are the most widely used type of polymer composite as they offer several advantages like-

- High strength to weight ratio especially critical for structural and aeronautical application

- Anisotropic properties can be easily attained which are used for efficient utilisation for specific applications
- Excellent fatigue resistance and predictable damage
- Tailorable damping properties can be used to control mechanical-induced vibrations
- Excellent wear resistance
- Excellent corrosion resistance
- Flexibility in processing leads to simplicity in design and part manufacturing

## 1.6.Applications of FRP Materials

Even in day-to-day life, composites can be seen in every aspect of life. The most common examples of natural composites include muscles, bones, wings of birds, leaves, etc. Composites find widespread applications in the following fields-

- **Aircraft/military**

Commercial, military and aerospace aircraft and their parts



- **Appliance/ Business**

Household and office appliances, tools, etc.

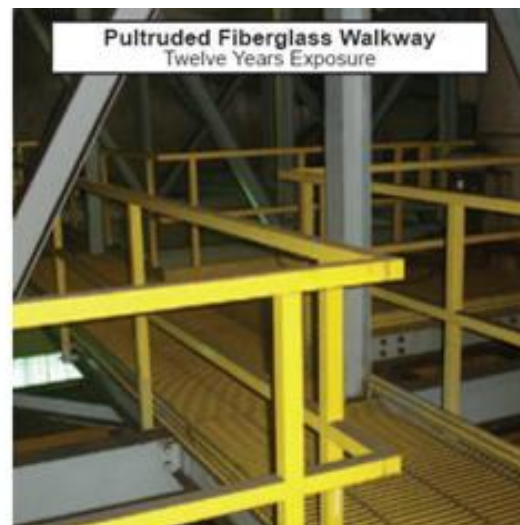
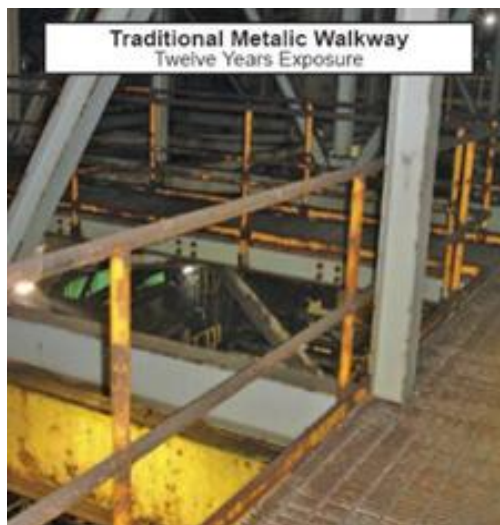
- **Automobiles/ Transportation**

Parts for automobiles, trucks, sports vehicles etc.



➤ **Structural/ Infrastructure**

Material for building buildings, bridges, and architectural components and cladding



➤ **Electrical and electronics**

Antennas, wiring boards, line hardware, substation equipment etc.

➤ **Electrical and electronics**

➤ **Energy Production**

Wind turbine blades



➤ **Consumer**

Goods like golf clubs, tennis rackets, cookware, furniture, etc.

➤ **Marine equipment**

Naval boats, ships, submarines, etc.



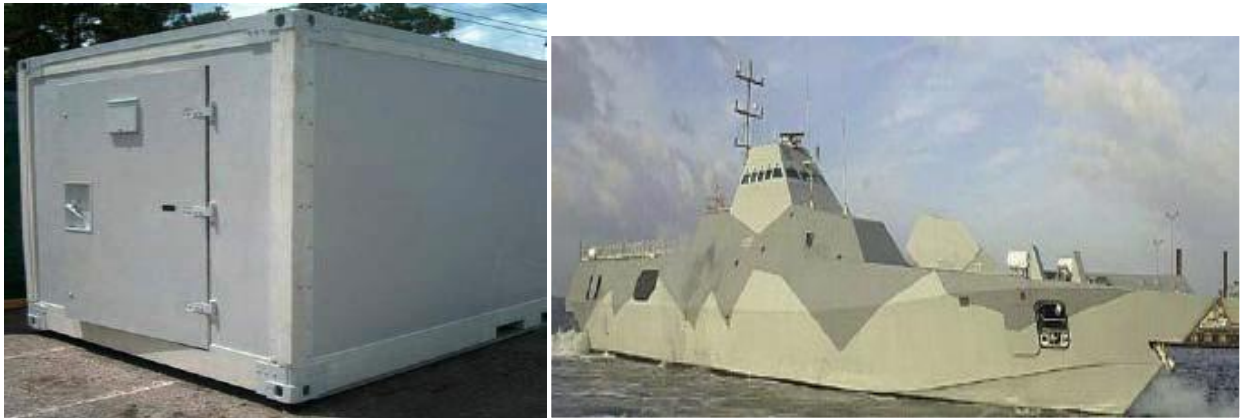


➤ **Pipeline Application**



➤ **Military Application**

Stealth and Blast resistant structure



➤ **Olympics**



London Olympics Aquatic Centre,  
Olympics 2012

Bridge-in-a-Backpack, Olympics  
2014



Fire resistant FRP jackets for steel columns, Olympics 2016

## 1.7. Limitations of FRP materials

Despite their promises of superior performance, polymeric composites suffer from limitations of being susceptible to degradation under environmental attacks (humid environments, high temperature, thermal spikes and shocks, cryogenic environments, vacuum and different radiation environments such as UV and microwave).



(a)



(b)

**Fig.1.8 (a) Debonding failure of Young America boat in 1999 (b) broken wing of American Airlines Flight 587**

Failure of composite structures in past have made the material science fraternity alarmed about the limited understanding of the material due overshadowing increase in its usage over research involved in this field. Two such instances are shown in Fig. 1.8. A boat named “Young America” broke in two parts during sailing in 1991 due to debonding in its sandwich structure .In 2001, American Airlines Flight 587 broke apart in New York, causing the death of 265 passengers.

Since delamination is the major cause of failure in composites structure as predicted by theory and evident by practical experience, the study of interfacial properties are highly crucial in order to evaluate and assess the FRP composite material in any application. Interlaminar shear strength (ILSS) is indicative of interfacial adhesion and delamination tendency of a composite material.

## Chapter 2

### Literature Review

#### 2.1. Moisture Ingression in FRP Composites

##### 2.1.1. Moisture Ingression Models

Over decades, different models have been developed with an aim of accurately predicting the moisture ingress phenomenon in such polymeric composites. Alfrey et.al [12] was the first to propose three distinct types classification of diffusion processes in polymeric materials. This classification was based on the relative rates of diffusion of penetrant molecules and relaxation of polymeric chains. The first category is that of Fickian diffusion in which the rate of relaxation is much higher than that of diffusion. Non-Fickian diffusion comes under the second category in which the rate of relaxation is nearly same as diffusion rate. The third category pertains to a case, where rate of relaxation is much lower than that of diffusion.

Many models have also been proposed to quantitatively describe the moisture absorption characteristics of different FRP systems. Some of the diffusion models relevant to moisture diffusion in fibrous polymeric composites, which have evolved over last few decades, are discussed below.

##### 2.1.1.1. Linear Fickian Diffusion Model

The simplest model which is applicable to most polymeric composites, was developed by Fick long back in 1855 [13], basing his work on the foundation set by Fourier [14].

Fick's first law of diffusion is based on hypothesis that for an isotropic medium, rate of diffusion through any cross-section is directly proportional to the concentration gradient normal to it and is quantitatively represented as -

$$F = -D \frac{\partial C}{\partial x} \quad (1)$$

However, Fick's second law is considered as the fundamental law of diffusion and can be represented by equation (2) when  $D$  is dependent on moisture concentration.

$$\frac{\partial C}{\partial t} = \frac{\partial (D \frac{\partial C}{\partial x})}{\partial x} \quad (2)$$



However, in case of moisture concentration independent D, equation (2) becomes –

$$\frac{\partial C}{\partial t} = D \frac{\partial^2 C}{\partial x^2} \quad (3)$$

The most accepted classical solution of Fick's second law for that of a plate, which is given below [15] -

$$\frac{M_t}{M_\infty} = 1 - \frac{8}{\pi^2} \sum_{n=0}^{\infty} \frac{(-1)^n}{(2n+1)^2} \exp \left[ \frac{-(2n+1)^2 \pi^2 D t}{4h^2} \right] \quad (4)$$

Often, for simplicity, the above equation is often approximated as proposed by Springer [16]-

$$\frac{M_t}{M_\infty} = 1 - \exp \left[ -7.3 \left( \frac{D t}{h^2} \right)^{0.75} \right] \quad (5)$$

Also, the solution for moisture desorption is as follows-

$$\frac{M_t}{M_0} = - \frac{8}{\pi^2} \sum_{n=0}^{\infty} \frac{(-1)^n}{(2n+1)^2} \exp \left[ \frac{-(2n+1)^2 \pi^2 D t}{4h^2} \right] \quad (6)$$

When the moisture diffusion is Fickian in nature, the diffusion coefficient is alone sufficient to describe the behaviour of the FRP composite [16]. The diffusion coefficient in this case is independent of concentration of penetrating molecules and can be found out by the following equation –

$$D = \pi \left( \frac{h}{4M_\infty} \right)^2 \left( \frac{M_1 - M_2}{\sqrt{t_1} - \sqrt{t_2}} \right)^2 \quad (7)$$

Typical linear Fickian behaviour is shown in Fig. 2.1, which can be roughly divided into two parts - an initial linear region which is the consequence of concentration independent diffusion coefficient and a saturation region in which no more moisture is absorbed even if the sample is kept in same humid condition for a very long time. Fickian behaviour is reported to be more pronounced when the polymer composites are exposed to humid air and at lower temperatures [17].

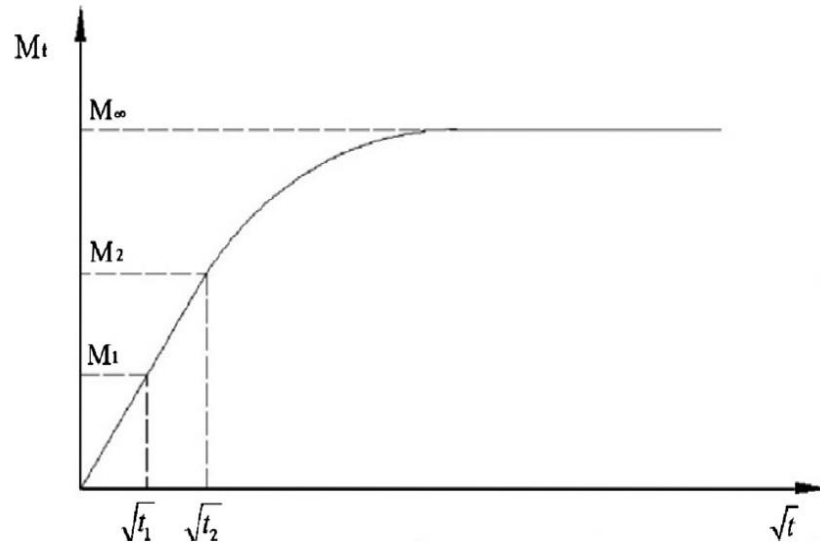


**Fig. 2.1: Typical linear Fickian diffusion model[18]**

Moisture diffusion in many FRP composites has been reported to follow Fick's law [19-27, 30]. In Fig. 2.2, the gravimetric moisture ingress curve of carbon/epoxy composite is shown, which follows Fick's law.

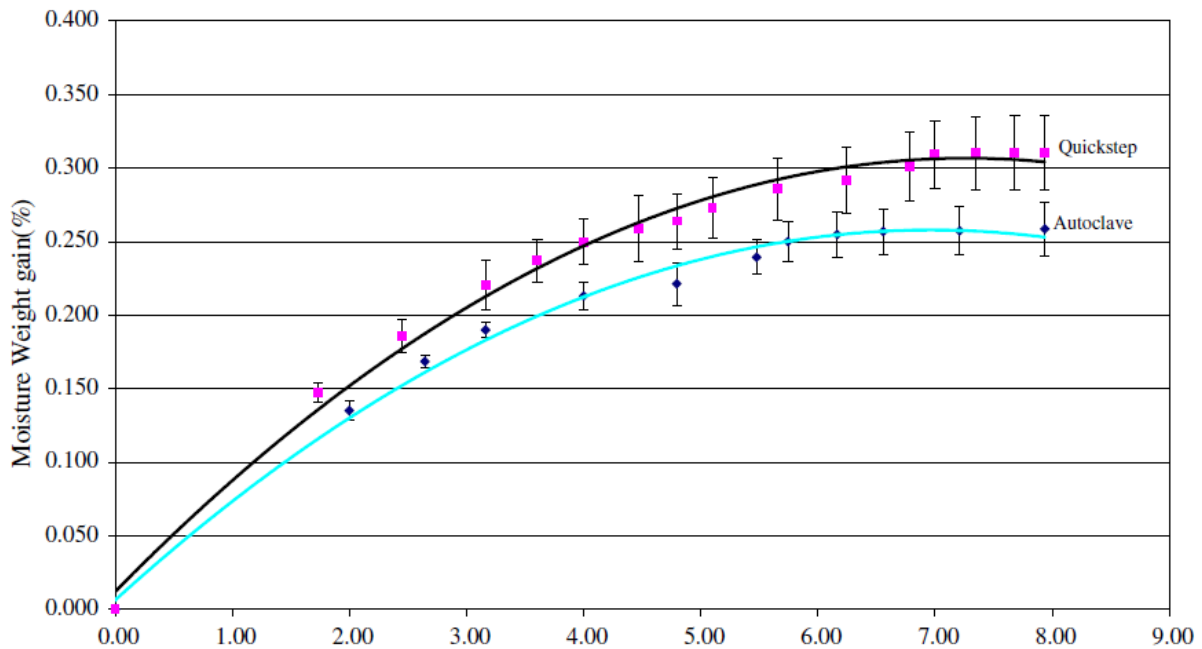


**Fig. 2.2: Experimental data fitting with linear Fickian diffusion model of carbon/epoxy composites aged at 70°C and 85% RH [28]**

### 2.1.1.2.Deviation from Fickian Behaviour: Non-Fickian Diffusion Models

Glass transition temperature is an important parameter when it comes to study the polymeric systems. Although polymers follow Fick's law of moisture absorption in their rubbery state but, in glassy state, polymers show deviation from Fickian behaviour. Such non-Fickian behaviour is due to different reasons such as negligible swelling of the composites, development of cracks and voids and moisture diffusion along fiber matrix interface [92]. Also, polymer matrix itself has an important role to play in deciding the moisture diffusion behaviour. For example, epoxy resin based composites are usually found to follow non-Fickian moisture absorption kinetics [18].

Different non-Fickian moisture absorption curves observed in polymeric composites are shown in Fig. 2.3.

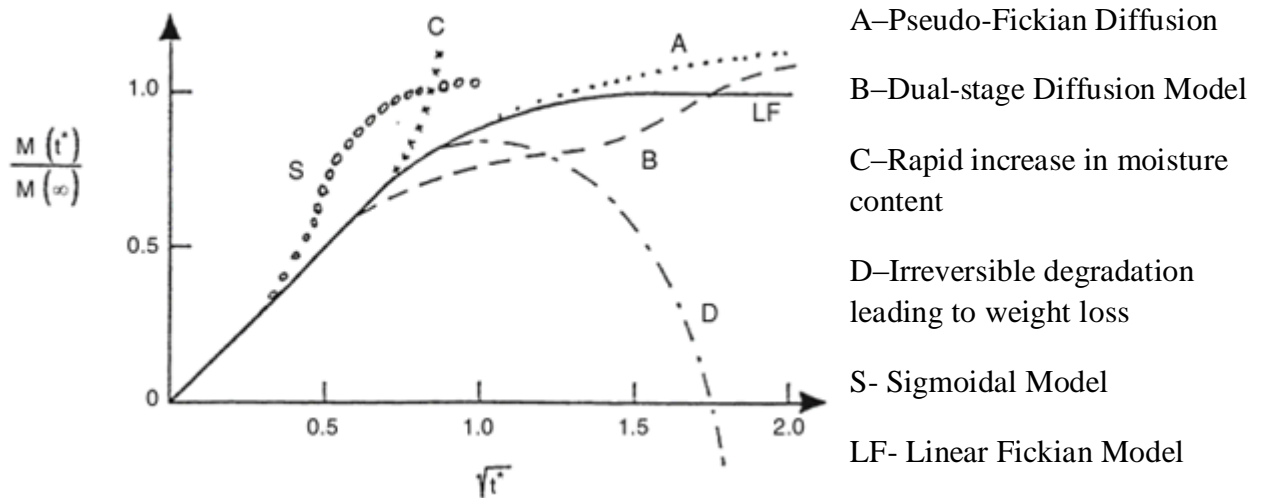


**Fig 2.3: Typical linear Fickian and non-Fickian diffusion models [29]**

Curve “A” shows the pseudo-Fickian diffusion in which true equilibrium is never achieved. The curve can be divided into two linear regions – the initial region being similar to Fickian curve and the other region having a lower but non-zero slope. Such behaviour is mostly observed in polymeric composites in which both fiber and matrix absorb moisture, for example - glass/epoxy composites for a variety of humidity and temperature condition [30, 31], glass/epoxy in water at different temperatures [32-34], glass/urethane composite in distilled water at different

temperatures [35], glass/polyester composites in water and sea water [36] and so on. But this is not always the case. Many polymeric composites in which the fiber has no role in moisture absorption also show similar behaviour [38, 40]. This might be due to involvement of fiber/matrix interface in moisture absorption. Also, on varying the environment, moisture diffusion kinetics of the same system changes noticeably [30, 35-38].

Curve “C” shows the case of rapid increase in moisture content in the polymer composite, which usually results from induced damage in the material, which might sometimes lead to large deformations, and even failure. Under certain conditions, polymer composites are reported to switch to such kind of irreversible behaviour, although usually they tend to have quite different moisture absorption characteristics [33, 34, 40-43].

Curve “D” accounts for the physical (swelling) or chemical (leaching and hydrolysis) degradation of the composite material which causes weight loss. This irreversible behaviour threatens the loss of structural integrity and might even lead to failure of the composite.

Such behaviour of fibrous polymeric composites has been reported in many literatures [44-47].

In fact, whenever moisture ingress characteristics of a composite material is found to be in resemblance with either curve “C” or “D”, it raises question on the decision of material selection for that particular environment.

Curve “S” represents the sigmoidal type moisture diffusion in the polymer composite and is reported to be related to a moving diffusion front [30, 32, 48, 49].

Many researchers have reported that polymeric composites recover their original strength, either partly or even entirely, on drying [30, 37, 48]. In general, in case of curves “LF”, “A” and “B”, which are associated with reversible changes upon moisture absorption, complete regaining of original strength is possible, but for curves “C” and “D”, permanent loss of strength is observed [29].

### **2.1.1.3. Langmuirian Diffusion Model**

Langmuirian model, also known as the dual-mode sorption model or the two-phase diffusion model, is based on the assumption that the penetrant molecules are divided into two populations- one consists of the mobile molecules which are dissolved in the matrix and hence are free to diffuse; while the other molecules are locally immobilized as they occupy the micro-voids [51]. However, there exists a possibility of exchange between mobile and bound molecules over time.

Langmuirian model of diffusion is a modification of Fick's law, proposed by Carter and Kibler [51] and can be quantitatively described as -

$$D_{\gamma} \frac{\partial^2 n}{\partial z^2} = \frac{\partial n}{\partial t} + \frac{\partial N}{\partial t} \quad (8)$$

$$\frac{\partial N}{\partial t} = \gamma n - \beta N \quad (9)$$

The solution for the above set of equation is given below-

$$\frac{M_t}{M_{\infty}} = \frac{\beta}{\gamma + \beta} e^{-\gamma t} \left( 1 - \frac{8}{\pi^2} \sum_{h=1}^{\infty (\text{odd})} \frac{e^{-\kappa i^2 t}}{i^2} \right) + \frac{\beta}{\gamma + \beta} (e^{-\beta t} - e^{-\gamma t}) + (1 - e^{-\beta t}) ; 2\gamma, 2\beta \ll \kappa \quad (10)$$

For shorter exposure times, equation (11) can be approximated to-

$$\frac{M_t}{M_{\infty}} \approx \frac{4}{\pi^{3/2}} \left( \frac{\beta}{\gamma + \beta} M_{\infty} \right) \sqrt{\kappa t} ; 2\gamma, 2\beta \ll \kappa, t \leq 0.7\kappa \quad (11)$$

And for longer exposure times, the same equation can be modified as follows-

$$\frac{M_t}{M_{\infty}} \approx 1 - \frac{\gamma}{\gamma + \beta} e^{-\beta t} ; 2\gamma, 2\beta \ll \kappa, t \gg \frac{1}{\kappa} \quad (12)$$

This model of two-phase diffusion has been adopted by many researchers to explain the moisture absorption kinetics of FRP composites [52-58]. Moreover, Fickian and Langmuirian models could be statistically equivalent in case of certain conditioning environments [91]. However, the Langmuirian model has been reported to be able to accurately predict the moisture uptake of certain systems in certain environments such as carbon/epoxy conditioned in anti-icing additive [59].

A comparison between Fickian and Langmuirian fitting of experimental data of moisture absorption kinetics of glass/epoxy composite is shown in Fig. 2.4 [55]. It can be clearly seen that anomalous Carter-Kibler or Langmuirian fitting gives a more accurate approximation for the observed data than the Fickian fitting.

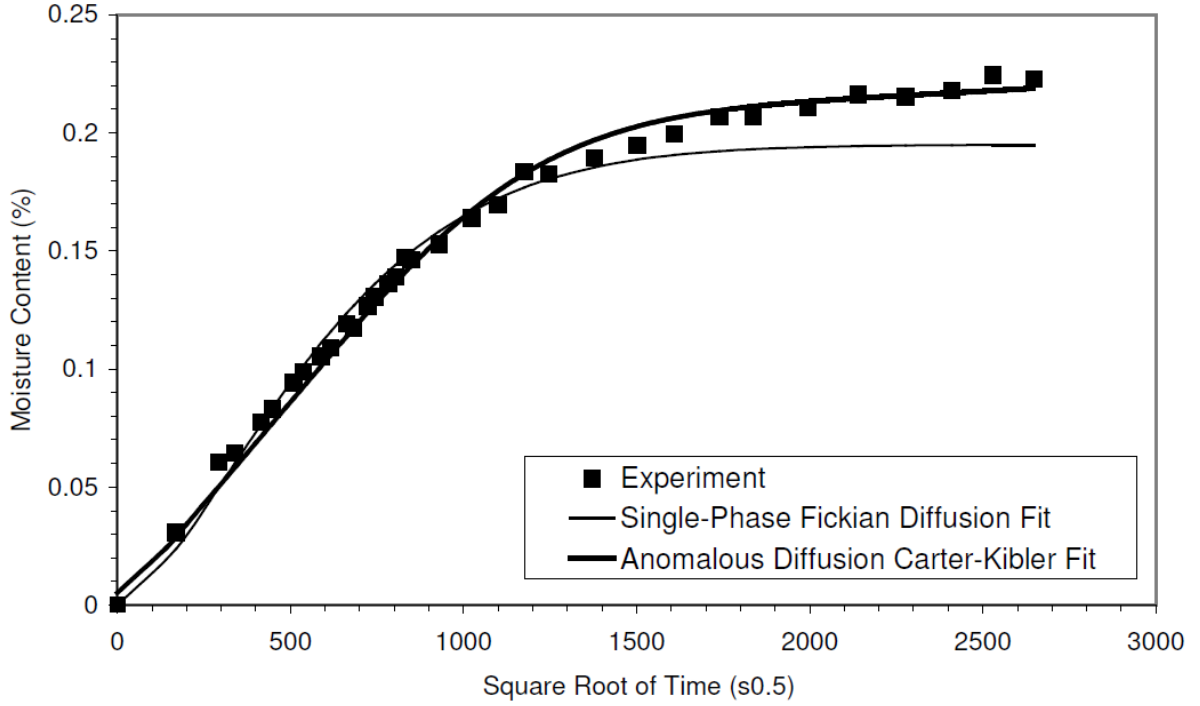


**Fig-4: Langmuirian model applied to moisture absorption data of glass/epoxy composite exposed to humid ageing at 70°C and 85% RH [55]**

#### 2.1.1.4. Hindered Diffusion Model

The one-dimensional hindered diffusion model is equivalent to the 1D Langmuirian model [60, 61]. The three dimensional hindered diffusion model of moisture diffusion in polymeric composites is an extended form of the one-dimensional model to incorporate diffusion through multiple surfaces and interaction between water molecules and the polymeric composite. This model can be described by the following equation -

$$D_x^* \frac{\partial^2 n^*}{\partial (x^*)^2} + D_y^* \frac{\partial^2 n^*}{\partial (y^*)^2} + D_z^* \frac{\partial^2 n^*}{\partial (z^*)^2} = \mu \frac{\partial n^*}{\partial t^*} + (1 - \mu)(n^* - N^*) \quad (13)$$

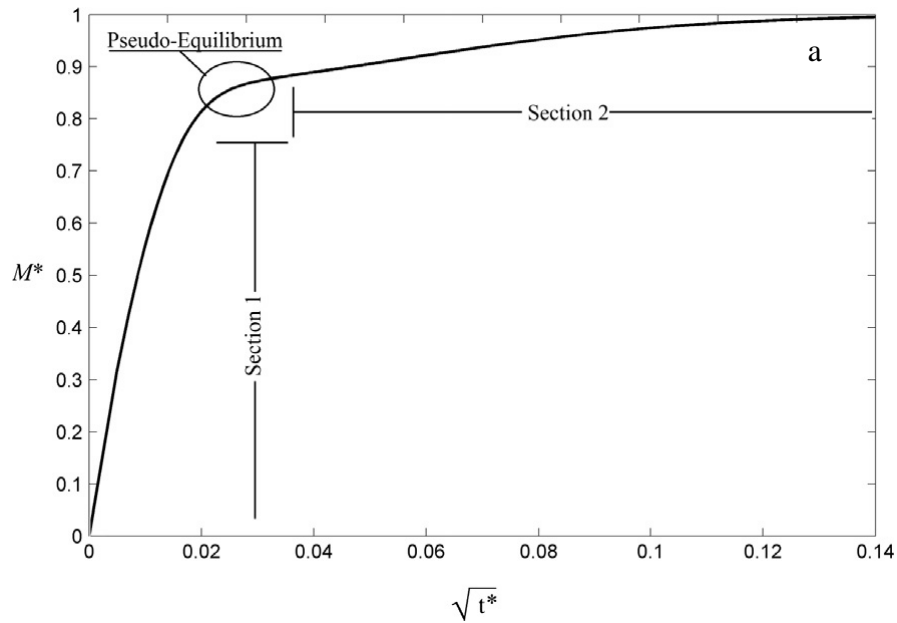
Where

$$n^* = \frac{n_t}{n_\infty} N^* = \frac{N_t}{N_\infty} t^* = \beta t$$

$$x^* = \frac{x}{h} y^* = \frac{y}{w} z^* = \frac{z}{l}$$

$$D_x^* = \frac{D_x}{h^2(\gamma + \beta)} D_y^* = \frac{D_y}{w^2(\gamma + \beta)} D_z^* = \frac{D_z}{l^2(\gamma + \beta)} \quad \mu = \frac{\beta}{\gamma + \beta}$$

Moisture absorption in fibrous polymeric composites subjected to hindered diffusion is shown in Fig. 2.5(a). The initial part is linear, after which “pseudo-equilibrium” is attained, where moisture absorption rate slows down noticeably [60]. One can compare this “pseudo-equilibrium” to be equal with the saturation moisture content in case of Fickian diffusion. In case of Fickian diffusion, there is no further increase in moisture content after “pseudo-equilibrium”. Hence, it is important to distinguish between the two types of diffusion processes as one might arrive at the incorrect conclusion by assuming the slow moisture uptake rate in hindered diffusion to be Fickian diffusion behavior. Fig. 2.5(b) shows the clear distinction between the two diffusion processes, while fitting with the experimental data of carbon-fiber reinforced bismaleimide composites subjected to distilled water immersion.



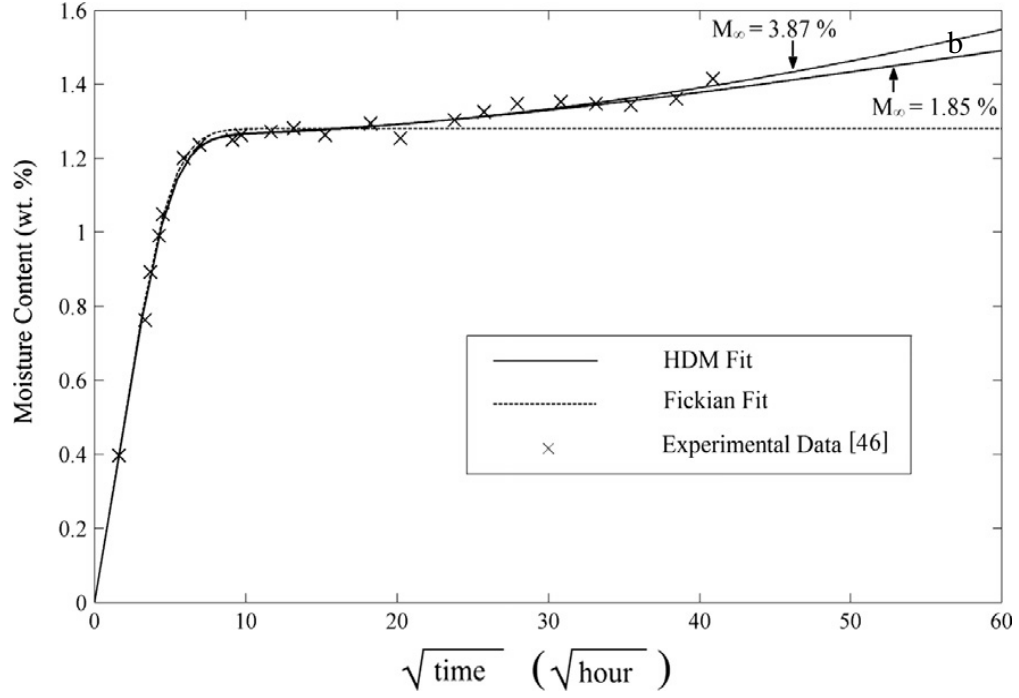


**Fig. 2.5: (a) Typical 3D hindered diffusion model and (b) fitting of experimental data of carbon-fiber reinforced bismaleimide composites (immersed in distilled water) with hindered diffusion model and linear Fickian model [60]**

#### 2.1.1.5. Dual-stage Diffusion Model

In Fig. 2.3, Curve “B” shows the dual-stage moisture diffusion model. The dual-stage diffusion model can be quantitatively described by dividing concentration of moisture in the polymeric composite into two parts, namely - the polymer chain relaxation behaviour and the Fickian diffusion behaviour.

$$M_t = M_{t,F} + M_{t,R} \quad (13)$$

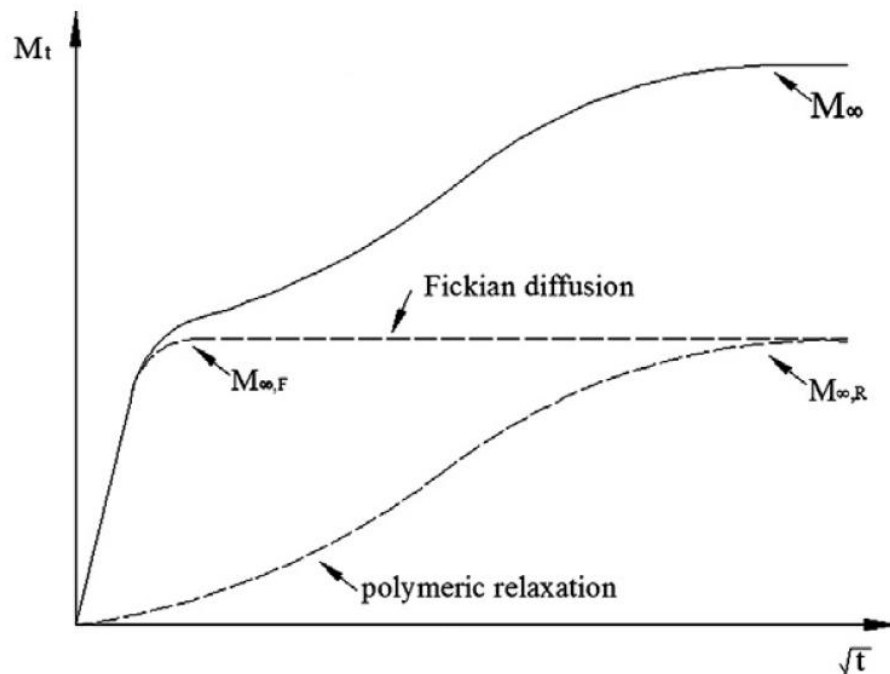
The solution to the equation (16) is given by the following equation -

$$M_t = M_{\infty,F} \left\{ 1 - \exp \left[ -7.3 \left( \frac{Dt}{h^2} \right)^{0.75} \right] \right\} + M_{\infty,R} [1 - \exp(-kt)] \quad (14)$$

Equation (14) is plotted in Fig. 2.6, which shows that the two-stage moisture diffusion is the combined effect of the classical Fickian diffusion and polymer matrix relaxation. The initial linear part of the curve is identical to the Fickian curve and hence, it can be said that polymeric

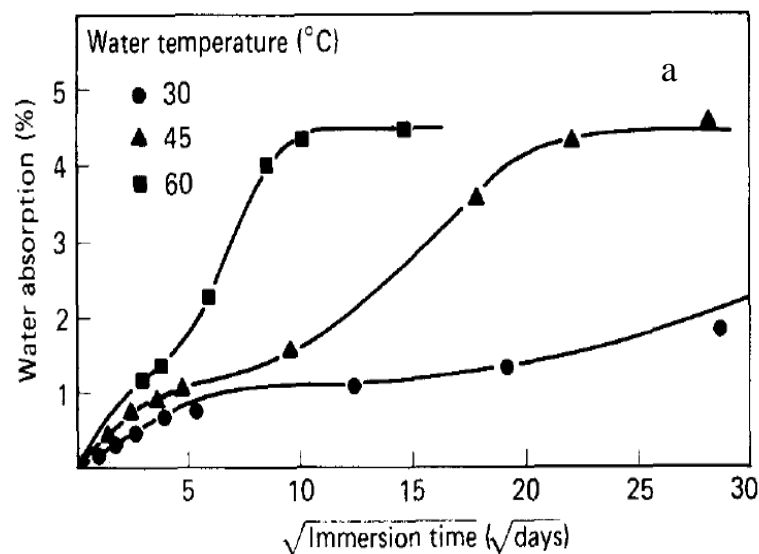


relaxation has no influence on it, while polymeric relaxation plays decisive role in determining the second part, in which diffusion rate decreases to attain final saturation moisture level.



**Fig. 2.6: Theoretical moisture uptake curves showing combined effect of Fickian diffusion and polymeric relaxation [64]**

Experimental data of some polymeric composite systems, which are reported follow dual-stage diffusion are shown in Fig. 2.7.



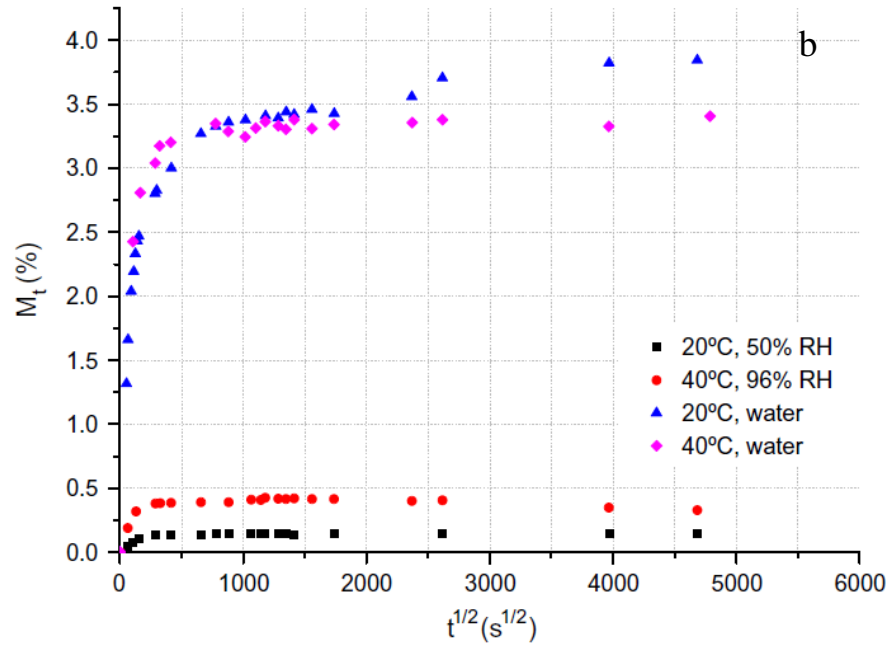


**Fig. 2.7: Experimental data following the dual-stage diffusion model in (a) glass fiber reinforced polyester composite, immersed in water [62] and (b) glass fibers reinforced isophthalic polyester composite exposed to water and humidity [63]**

## 2.1.2. Factors affecting moisture ingress kinetics in polymeric composites

### 2.1.2.1. Effect of Fiber system

On the basis of moisture absorption tendency, fibers can be broadly classified into two groups – permeable and impermeable fibers – as shown in Fig. 2.8.

Glass and aramid fibers are permeable in nature and hence, moisture absorption in polymeric composites containing these fibers is affected by both the fiber and resin. On the contrary, carbon fibers are resistant to moisture absorption and therefore, moisture absorption in carbon fiber reinforced polymer composites depends only on the resin phase.

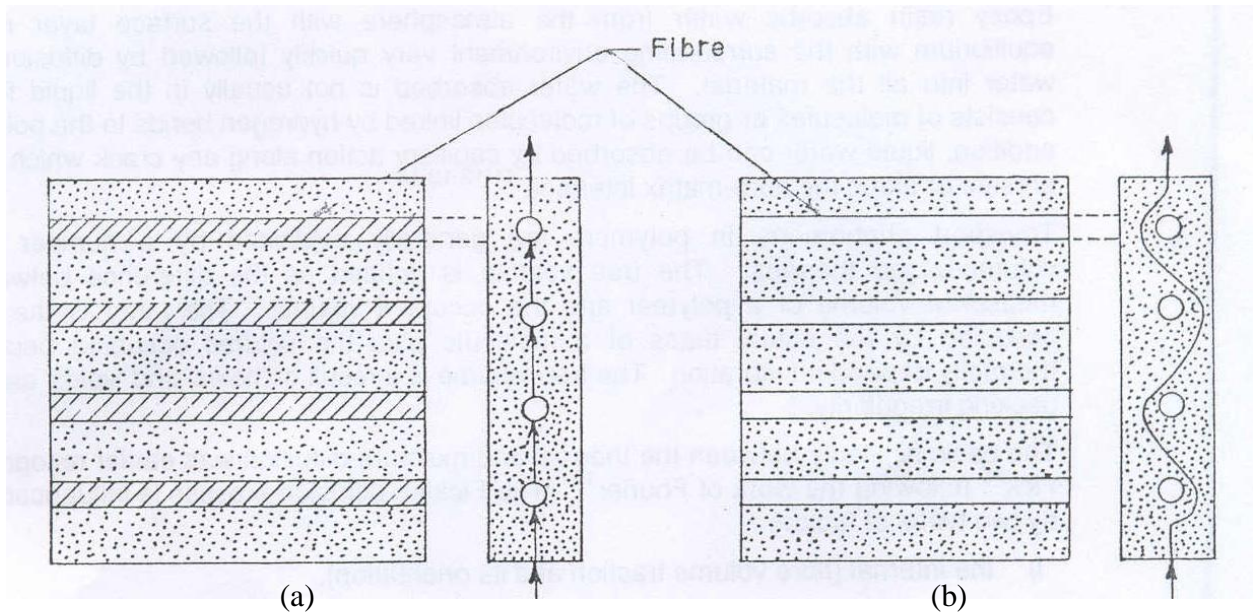


**Fig. 2.8: Typical diffusion path in polymeric composites composed of (a) permeable fibers and (b) impermeable fibers [17]**

#### **2.1.2.2.Effect of resin structure**

Proper choice of resin system is of paramount importance in the polymer composites as it decides not only moisture absorption capacity but also the kinetics. Moy et.al [65] has experimentally shown that highly cross-linked epoxy resins absorb less moisture than those having low cross-link density. Fig. 2.9 shows the significance of epoxy resin structure (functional groups, cross-linking etc.) in deciding moisture absorption characteristics of the system.

Springer [30] showed that on changing the catalyzing agent for the same fiber/matrix system, moisture diffusion kinetics changes.

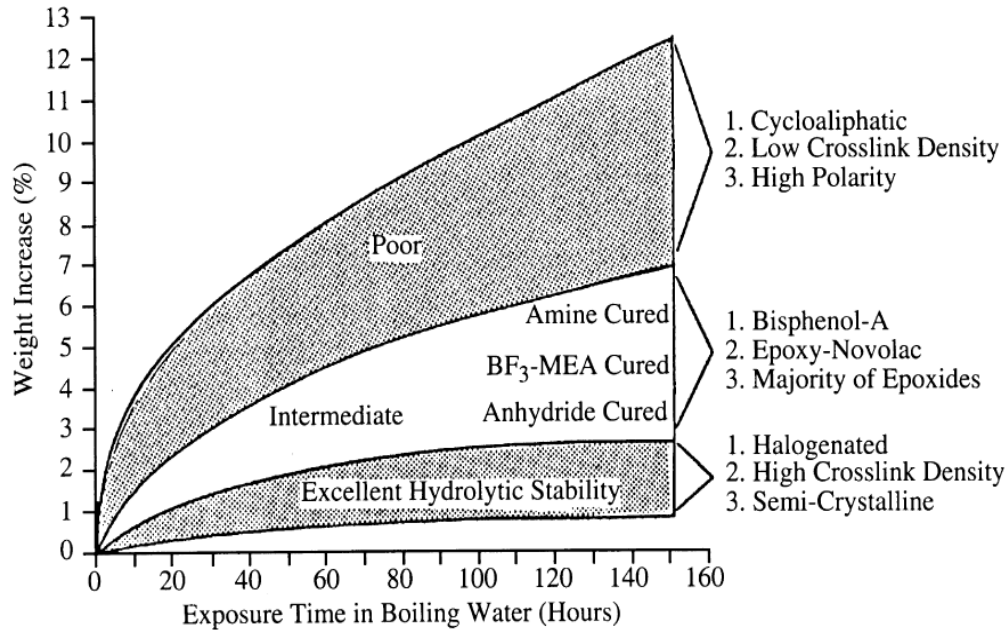


**Fig. 2.9: Structure dependence of stability of epoxy resins in boiling water [66]**

#### 2.1.2.3. Effect of interfacial adhesion

Silane coating is usually provided on the surface of glass fibers, which act not only as a protective coating but also as a coupling agent to promote the adhesion with polymer matrix.

The concept behind using silane coupling agents is to utilize chemical reactivity between the inorganic substrate and the organic resin, so as to develop proper adhesion at the fiber/matrix interface.

Fig. 2.10 shows the importance of silanizing agents of glass fibers on the moisture uptake kinetics of the polymeric composites [49]. Three reagents were used for silanization of glass fiber/epoxy composite, namely, 3-aminopropyltriethoxysilane (APTES), 3-aminopropylmethyldiethoxysilane (APDES) and 3-aminopropyldimethylmonoethoxysilane (APMES). The APMES reagent coupled FRP composite is found to have lowest saturation moisture content, whereas that coupled with APTES agent is found to undergo slowest moisture absorption kinetics.

Hence, it is important to create a healthy interphase/interface so that the threat to durability and reliability of the composite systems is minimized during their in-service performance.

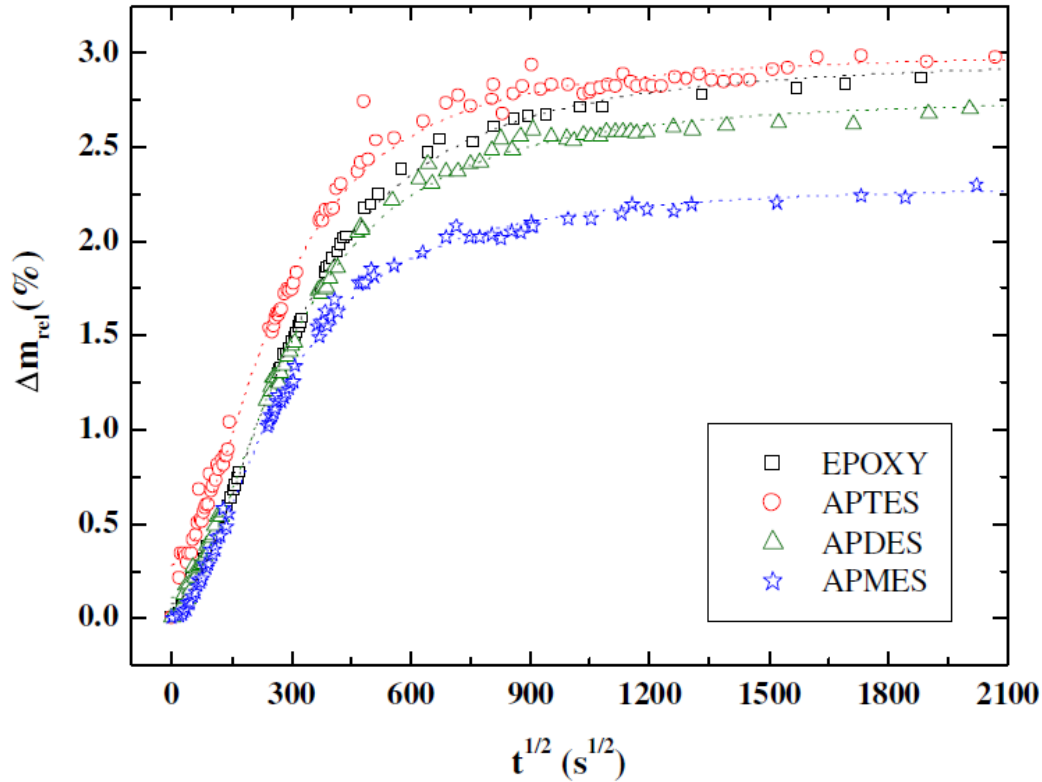


**Fig. 2.10: Effect of silanization on the moisture uptake profile of glass fiber/epoxy composites [49]**

### 2.1.3. Effect of Moisture Ingression on Mechanical Properties of FRP Composites

Plasticization adversely affects the properties of the polymer composite by inducing plastic deformation in the matrix and by lowering its glass transition temperature. Kelley et. al. have reported that there is a drop in glass transition temperature of about  $20^{\circ}\text{C}$  for each 1% moisture uptake [81].

Joshi [82] has investigated the effect of moisture on the interlaminar shear strength (ILSS) of carbon fiber/epoxy composites. He reported an initial increase in ILSS of about 10% upto 0.1 weight % absorbed moisture and a subsequent decrease by 25% at maximum moisture of approximately 2%.

The effect of water sorption on mechanical behaviour FRP composites has been investigated by many researchers [83-87]. It was reported that in case woven glass/epoxy composites

delamination load-carrying capability was reduced to 40% with 1.29% absorbed moisture [83]. Akay [84] reported that static and fatigue strength of carbon fiber/epoxy composite decreases when subjected to hygrothermal conditioning. Lassila et al. [85] have reported reduction in flexural strength of E-glass fibers reinforced polymer composites when exposed to water for 30 days.

Degradation of mechanical property under hygrothermal conditioning is often attributed to various degradation mechanisms leading to poor interfacial adhesion and change in failure mode due to moisture absorption in the polymeric composite [88-89].

#### 2.1.4. Effect of Moisture Ingression on Failure Modes of FRP Composites

Moisture induced degradation of FRP composites is the result of degradation of fibers, polymer matrix and/or the interface/interphase. Different reversible and irreversible chemical, physical and physico-mechanical degradation mechanisms take place as a result of environmental attack.

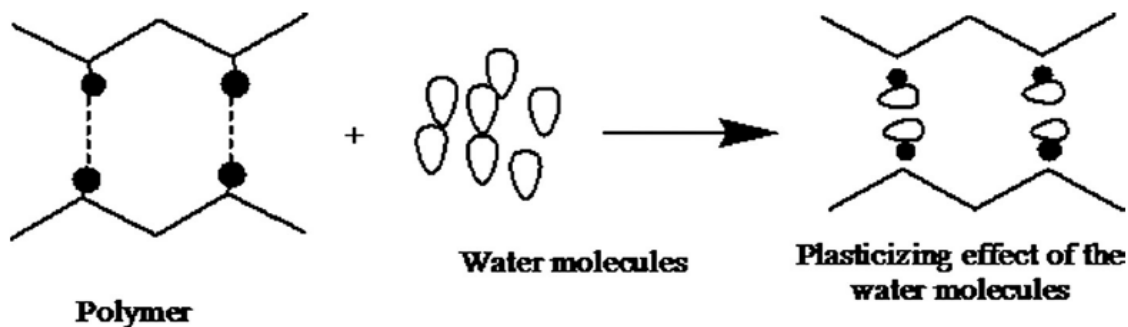


**Fig. 2.11: Schematic diagram of plasticization caused by moisture in polymer matrix [60]**

When moisture enters the polymer matrix, physical phenomena such as plasticization and swelling occur. In addition, chemical (hydrolysis and debonding) and physico-mechanical phenomena (micro-crack and micro-void formation) also occur in the composite, which can lead to degradation of not only the fibers and the matrix, but also the existing interface/interphase between them [67-79].

Plasticization process is schematically shown in Fig. 2.11, which is the result of interaction of water molecules with polymeric chains. Such interactions interrupt the existing hydrogen bonds in the polymeric matrix [68-70] and create new hydrogen bonds with the polymer matrix. This

phenomenon also accounts for the swelling of the polymer matrix occurring due to increase in bond-length between polymer chains.

Microvoid formation in the polymer matrix and at the interface is generally attributed to clustering of water molecules [72-73]. Also, the swelling caused by the absorbed moisture can induce internal stresses in the polymer, which may lead to formation of microvoids or micro-cracks. On the other hand, moisture induced swelling may also relieve residual stresses developed during the curing process.

However, plasticization and swelling are reversible phenomenon, whereas certain degradation phenomena are irreversible in nature such as hydrolysis, leaching, polymer relaxation, micro-cracking and microvoids formation.

Hydrolysis is the phenomena in which side groups are detached from the backbones of the polymeric chains. In general, hydrolysis is considered to be an irreversible degradation mechanism [71], but some literatures report that it is possible to reverse the hydrolyzing effect of diffusing water molecules.

Leaching is another mechanism by which break down of the fiber/matrix interphase region occurs and fibers and polymer get separated.

Composite materials are complex structures which may fail by a number of mechanisms which are not encountered in more homogeneous materials [91, 92]. Hence, the fractographic analysis of FRP composites is crucial in revealing the failure modes induced by moisture ingress. Alawsi et. al [80] studied the influence of exposure time on degradation mechanisms during accelerated humid ageing of E-glass/polyester composites. Fig. 2.13(a) shows the SEM image of the specimen which was not exposed to moisture, in which strong adhesion between fibers and matrix can be observed. But there is increasing loss of fiber/matrix adhesion with more time of exposure to humidity, which is highest for 2000 hours. Also, increasing deterioration of polymer matrix is observed as time of exposure was increased.



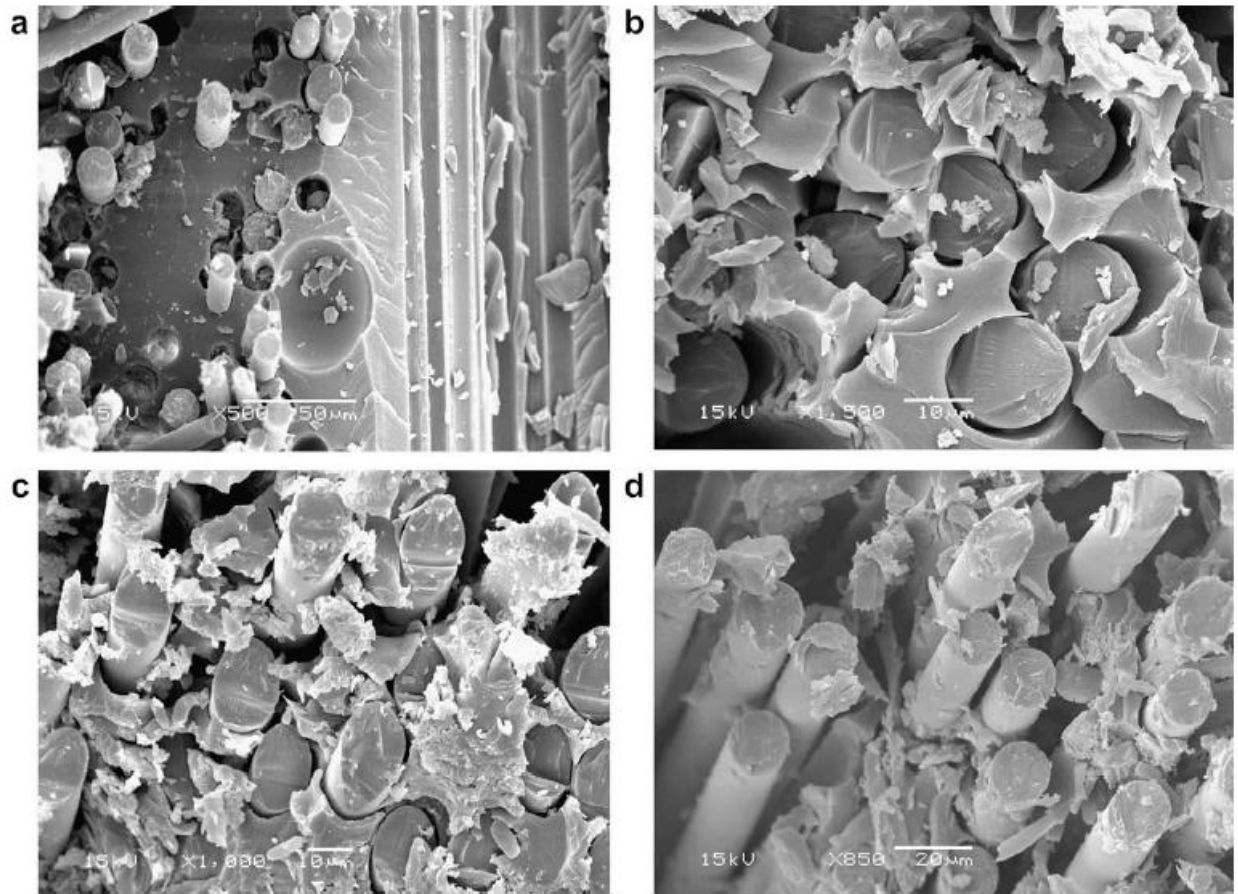


**Fig-13: Scanning electron micrographs of fracture surfaces of glass/polyester samples exposed to humid environment for (a) 0 hours (b) 500 hours (c) 1000 hours (d) 2000 hours [80]**

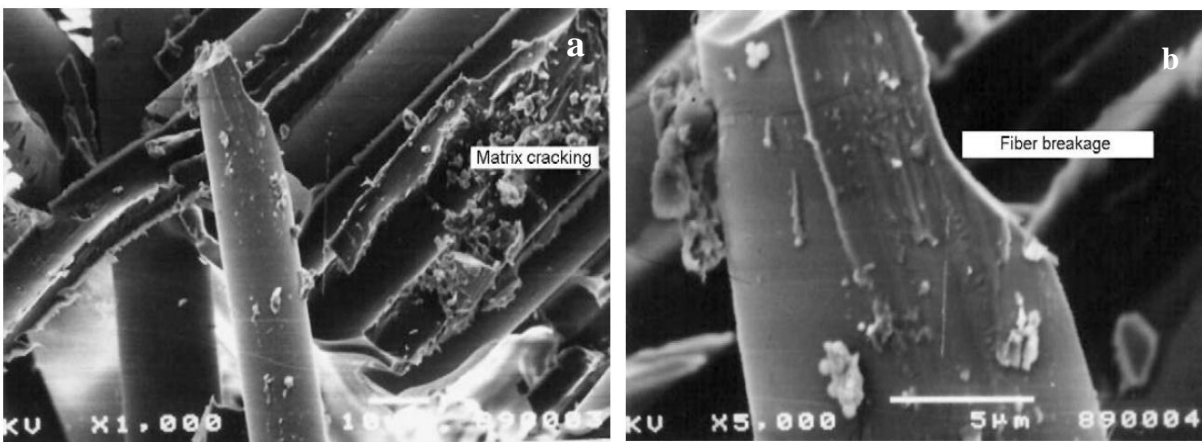


**Fig-14: Scanning electron micrographs of carbon/epoxy composites exposed to humidity, showing (a) matrix cracking and (b) fiber breakage [90]**



Ray [90] studied the effect of moisture ingress on carbon fiber/epoxy composites and observed fiber damage and matrix cracking in samples exposed to humid environment, as shown in Fig-14.

## **2.2. Effect of Thermal Spiking on FRP Composites**

Thermal spiking induces microcracking in composites; it is enhanced by the presence of moisture [93, 94]. In turn, this damage increases the moisture absorption capacity of composite lay-ups, typically by 100%. This phenomenon is of some concern in aerospace applications, where rapid temperature variations may occur during flight.

## **2.2. Effect of UV Radiation on FRP Composites**

UV light is the prime cause of breakdown and produces effects which are similar to thermal degradation. These involve the breaking of chemical bonds, giving rise to free radicals which result in permanent chain scission or in cross-linking, depending on the polymer involved, the wavelength of the UV and other factors [96]. Some of the groups formed may be chromophores. Unlike thermal degradation, UV degradation does not occur uniformly throughout the polymer, but particularly with opaque materials, the effects are felt on or near the surface. The two most commonly observed effects are loss of gloss and change in colour.

UV light can be divided into three types according to wavelength. The so called UV-A portion of the spectrum (400–315 nm) is the least harmful to organic polymers and forms about 6% of the sun's total radiation reaching the earth; UV-B (315–280 nm) is a more damaging part and forms about 0.1% of total; and UV-C (280 nm) is the most harmful of all to polymers. UV-C is, however, filtered out by the earth's atmosphere. UV radiation below about 350 nm is absorbed by window glass; UV-B is therefore effectively eliminated indoors apart from small amounts generated by artificial lighting. Atmospheric heat and moisture accelerate and change the nature of damage done by UV radiation to most exterior grade polymers, rather than act as primary causative agents themselves, unless the polymer is under high stress or has been badly fabricated. (For example, air occlusions beneath a polyester gel coat which pit and eventually break through.)

The most degrading environment for aramid fibers is ultraviolet light, which causes a discoloration and a loss in strength, with time [91]. Fortunately, the degradation products are self-screening, protecting the underlying polymer in the fiber, from degradation. It is therefore advisable to use matrix resins, which absorb ultraviolet light at the appropriate wavelength harmlessly, or use protective coatings [95]. Glass fibers on the other hand are much more susceptible to corrosion in aqueous environments. The most commonly used fibers in reinforced plastics by far are made from E-glass, which is susceptible to both acidic and alkaline environments where a reduction in performance by corrosion or extraction mechanisms is observed. Consequently a range of glass fiber reinforcements exists for specific applications. ECR glass is recommended for general corrosion resistance (especially acid resistance), and for alkali resistance, AR glass is preferred. The latter is also being developed for compatibility with polymer resins to provide both acid and alkali resistance. In many situations, it is satisfactory to use E-glass as the structural reinforcement in combination with a C-glass tissue reinforced surface resin. Optimum performance can also be achieved by employing C-glass surface tissues in combination with woven rovings rather than chopped strand mat. S and R glasses are employed where high performance is required, but they also provide enhanced durability over E-glass. As with moisture absorption, for chemical resistance the fibers should be carefully selected with a recommended surface finish.

## Chapter 3

### Motivation

In recent times, fibrous polymeric composites have received increased attention for a wide range of applications ranging from ladder rails to aircraft wings, from sports goods to space craft frames, from printed circuit boards to rocket motor cases, owing to unique combination of properties like low density, high strength to weight ratio, good anti-corrosion properties, fatigue resistance and low manufacturing costs. However, FRP composites encounter a variety of environments during their fabrication, storage and service life, which are capable of causing degradation in their expected in-service performance or even complete failure. Spacecrafts parts made up of composite materials are constantly under ultraviolet irradiation during service. In aircrafts, the body parts are subjected to humid condition caused by clouds or rain whereas in marine and pipeline application where the components are exposed to severe humidity conditions throughout their lifetime. Also, aircrafts especially vertical take-off and landing (VTOL) are highly susceptible to thermal spiking during take-off and landing. Although moisture ingress has significance effect on its reliability and performance, but the combined effects of high temperatures along with moisture conditioning, which are encountered in practice, are more deleterious on the properties of the composites than each individually. Hence, basic understanding of mechanical response and failure modes in service condition is highly necessary in such safety critical applications. Moreover, moisture uptake theory and mechanism in polymeric composites has been an active area of research for last few decades. But still accurate predictability of moisture absorption kinetics is under question due to complex sorption kinetics and huge scatter in experimental data.

It is a well-known fact that polymers are hygroscopic in nature and this necessitates proper understanding of the phenomena occurring during moisture ingress in polymeric composites. Also polymers are susceptible to high temperature as well as radiation induced damage. Also, it leads to change in glass transition temperature which adversely affects the mechanical properties. Moisture ingress and thermal spiking causes change in interfacial chemistry, which affects its load transfer characteristics and structural integrity. Hence, there is a need to predict the kinetics

of water diffusion in polymeric composites in order to predict their long term performance. Moreover, such environmental exposure causes damage to the polymeric composites which are irreversible and might lead to their failure.

In view of the increasing usage polymeric composite materials in various critical applications, there exists a urgent need to obtain a complete understanding of the relation between their in-service properties and environments to which they are exposed.

## Chapter 4

### Experimental Details

#### Materials Used

1. Woven Glass Fibers (FGP, RP-10)
2. Woven Carbon Fibers (TC-33)
3. Alumina Nanopowder (< 50 nm particle size)
4. Epoxy Resin (Lapox L-12) based on Bisphenol A
5. Hardener (Lapox K-6, AH-312)

Property	Epoxy	Glass fibres	Carbon fibres
Tensile strength (GPa)	0.11	3.4	4
Tensile Modulus (GPa)	4.1	72.3	240
Strain at failure %	4.6	4.8	1.6
Poisson's ratio	0.3	0.2	0.26
Density g/cm <sup>3</sup>	1.162	2.58	1.8

Table 4.1: Properties of epoxy resin, glass fibers and carbon fibers

#### Experimental Method

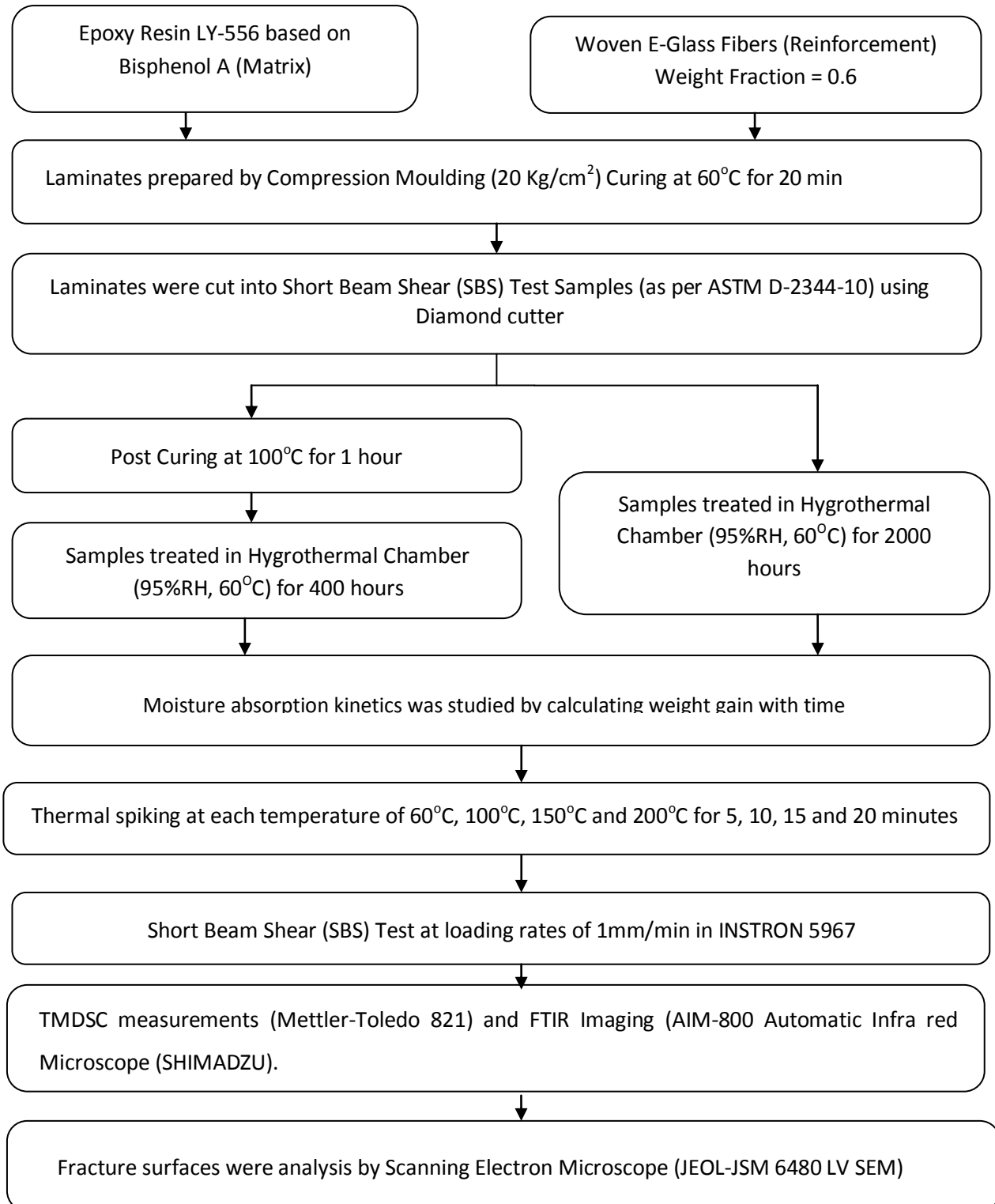
Woven E-glass fibers (FGP, RP-10) and woven carbon fibers (TC-33) were reinforced in epoxy resin (Lapox L-12) based on Bisphenol A and hardener Lapox K-6 (AH-312), for fabrication of glass/epoxy (weight fraction of glass fibers is 0.6), carbon/epoxyweight fraction of carbon fibers is 0.6) and glass/carbon/epoxy (weight fraction of glass and carbon fibers are 0.3 each) hybrid laminated composites. Also, alumina nano-fillers (3 weight percent of epoxy resin) were dispersed in epoxy resin by magnetic stirring and sonication, each carried out for one hour. This was used to fabricate GFRP laminate with alumina nano-fillers. Fabrication was done by hand lay-up method followed by compression moulding method at pressure of 20 kg/cm<sup>2</sup>, followed by curing at 60°C temperature for 20 minutes. Laminates were cut into Short Beam Shear (SBS)

Test Samples (as per ASTM D-2344-10) using diamond cutter. One lot of glass/epoxy specimens were subjected to post curing treatment at 100°C temperature for 1 hour. Hygrothermal conditioning of the specimen was done at 60°C temperature and 95% RH for about 400 hours. The other lot was subjected to hygrothermal conditioning at 60°C temperature and 95% RH environment for about 2000 hours. The carbon and hybrid composites were hygrothermally treated for about 2000 hours. Moisture absorption kinetics was studied by calculating weight gain with time. Thermal spiking was done at 60°C, 100°C, 150°C and 200°C for 5,10,15 and 20 minutes at each temperature.

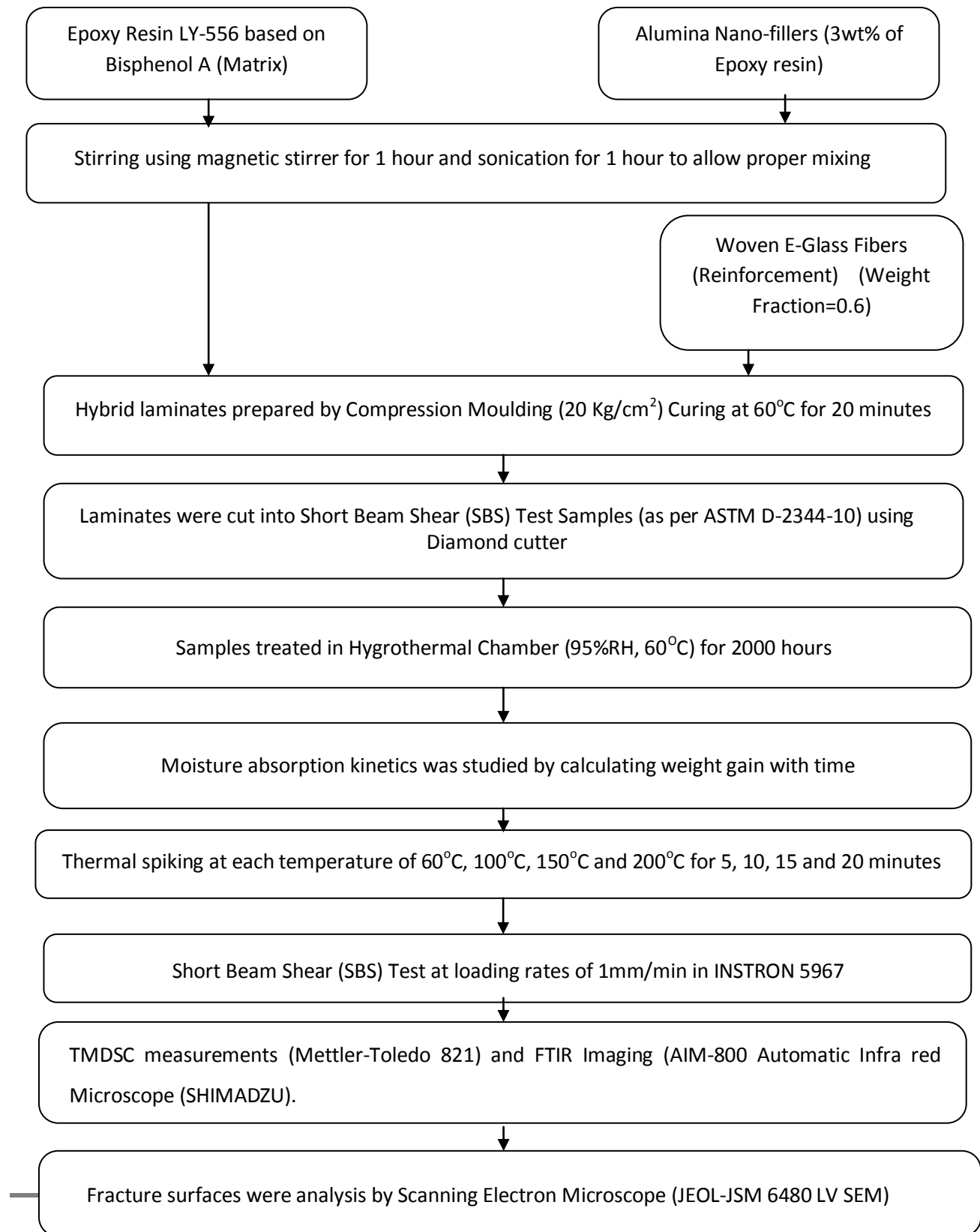
The specimens were dried in an oven at 50°C temperature for weight stabilization, followed by the 3-point bend test (ASTM standard D2344) using INSTRON 5967 at a crosshead speed of 1 mm/min. Some samples of each of above systems were also subjected to UV conditioning for 200 hours. Fracture surface analysis by Scanning Electron Microscope (JEOL-JSM 6480 LV SEM). The TMDSC (Temperature Modulated Differential Scanning Calorimetry) measurements were done by Mettler-Toledo 821. The FTIR imaging was performed in AIM-800 Automatic Infra red Microscope (SHIMADZU).

## 4.1. Effect of Hygrothermal Treatment and Thermal Spiking on FRP Composites

### 4.1.1. Glass Fibre Reinforced Composites

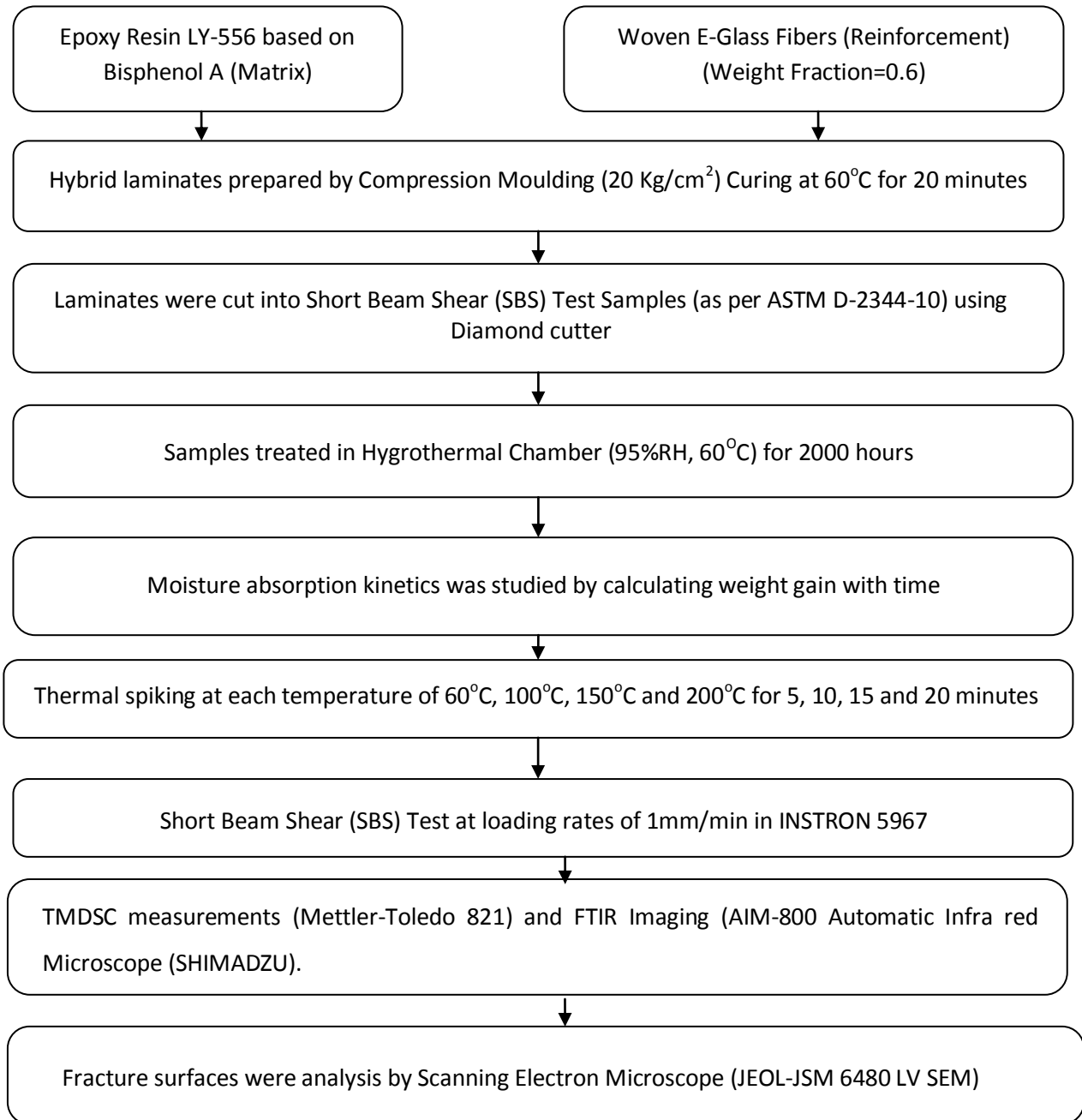


#### 4.1.2. Glass Fibre Composites with Nano-fillers

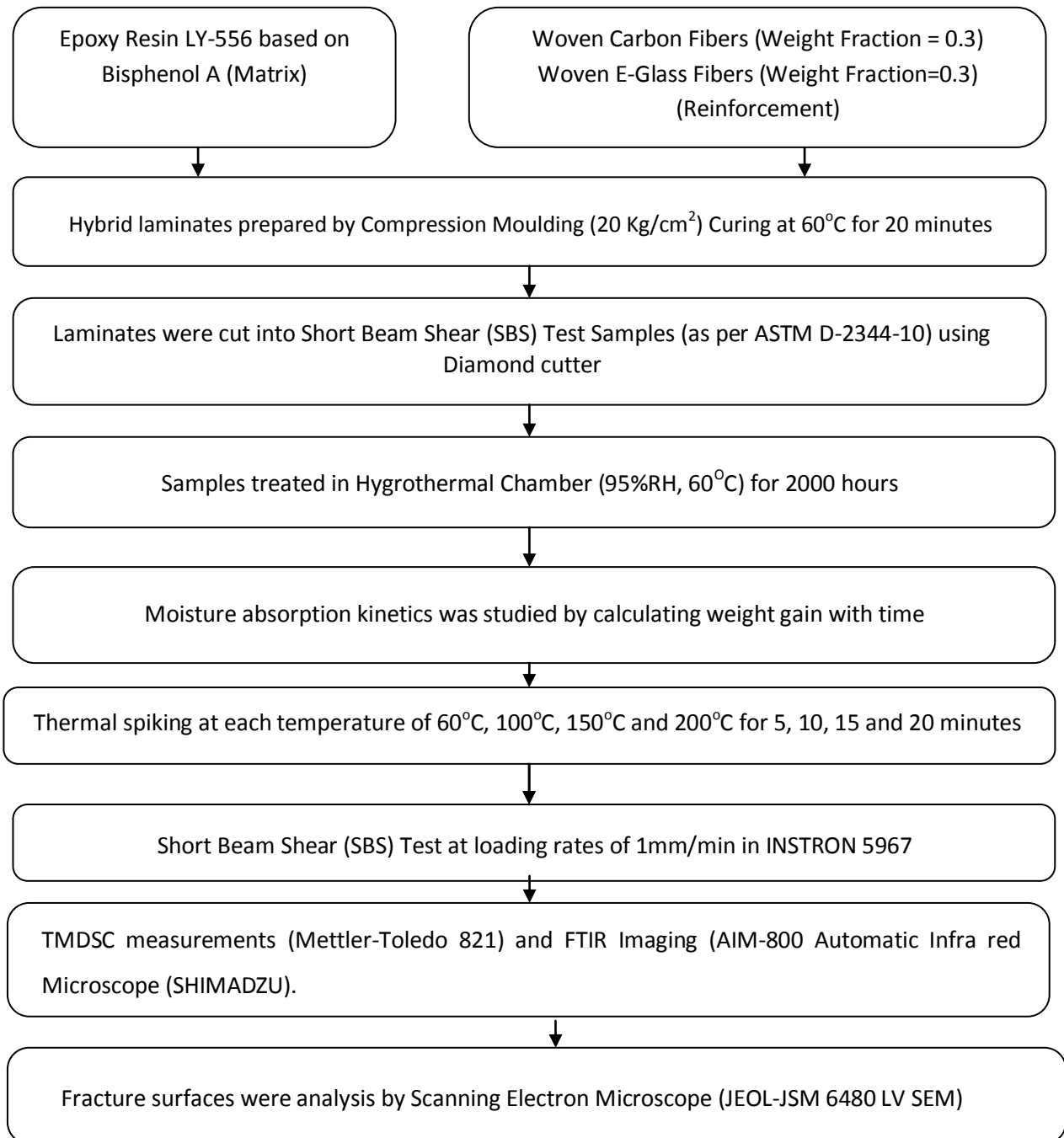




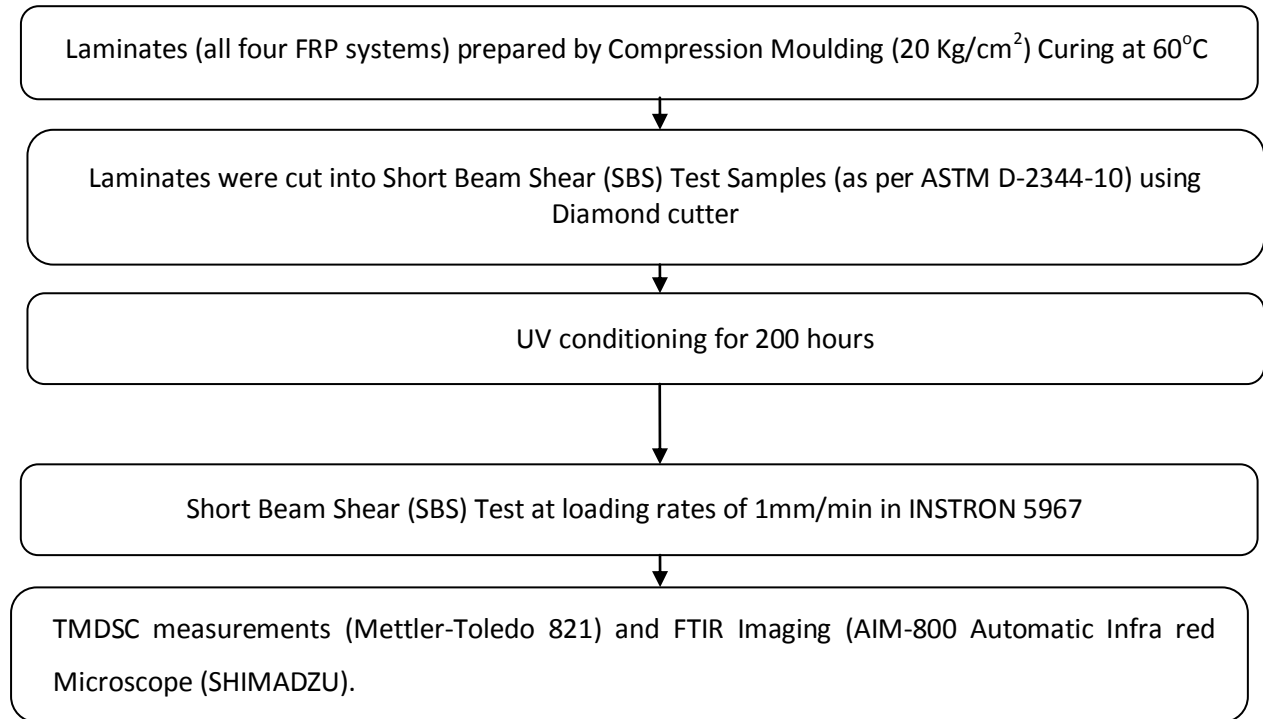
#### 4.1.3. Carbon Fibre Reinforced Composites



#### 4.1.4. Glass and Carbon Fibre Reinforced Hybrid Composites



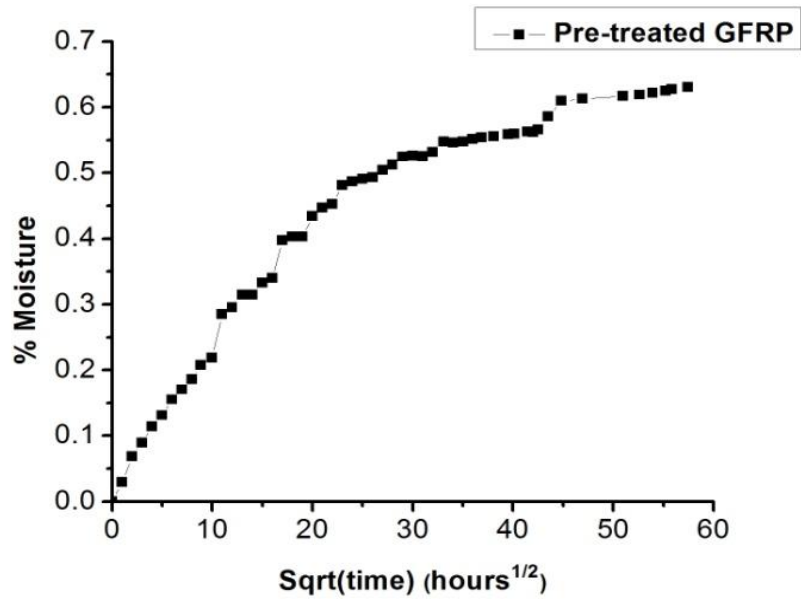
#### 4.2. Effect of UV Treatment on FRP Composites



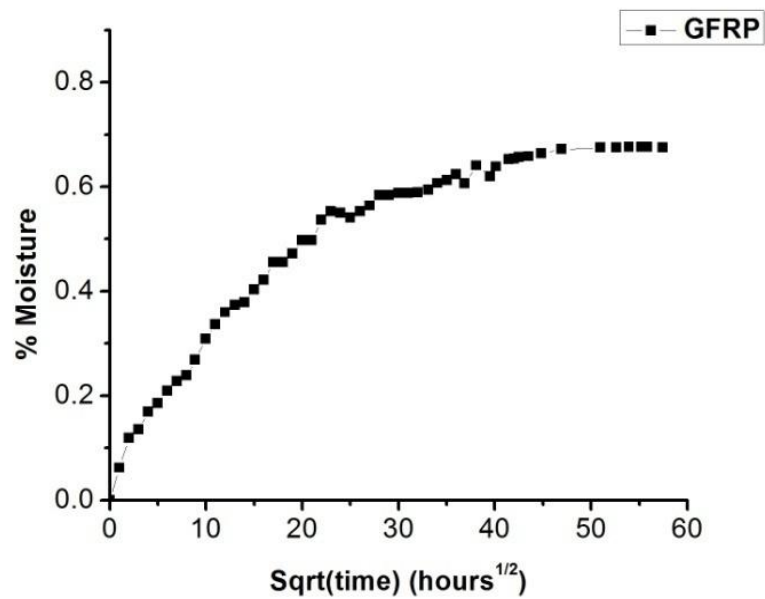
## Chapter 5

### Results and Discussion

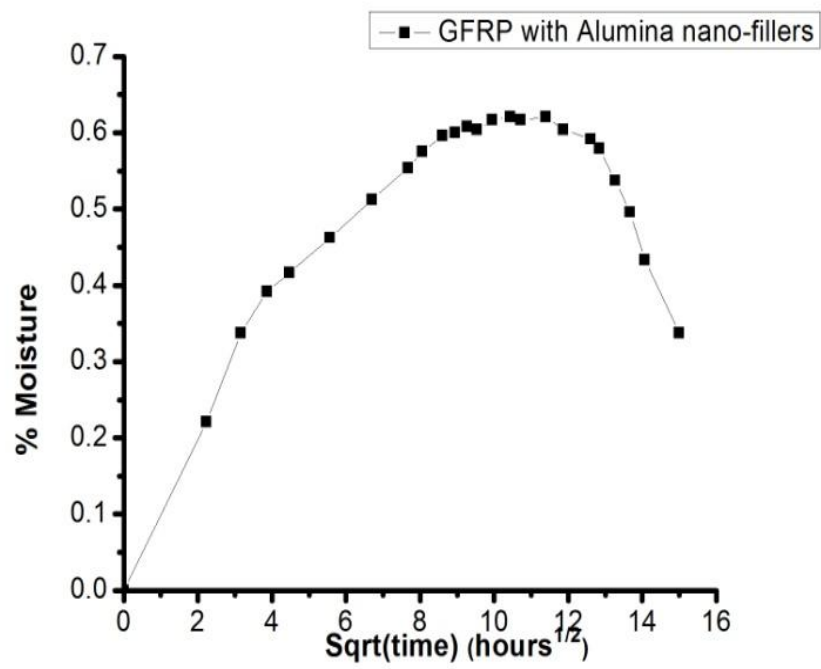
#### 5.1. Moisture Ingression Behaviour in FRP Composites



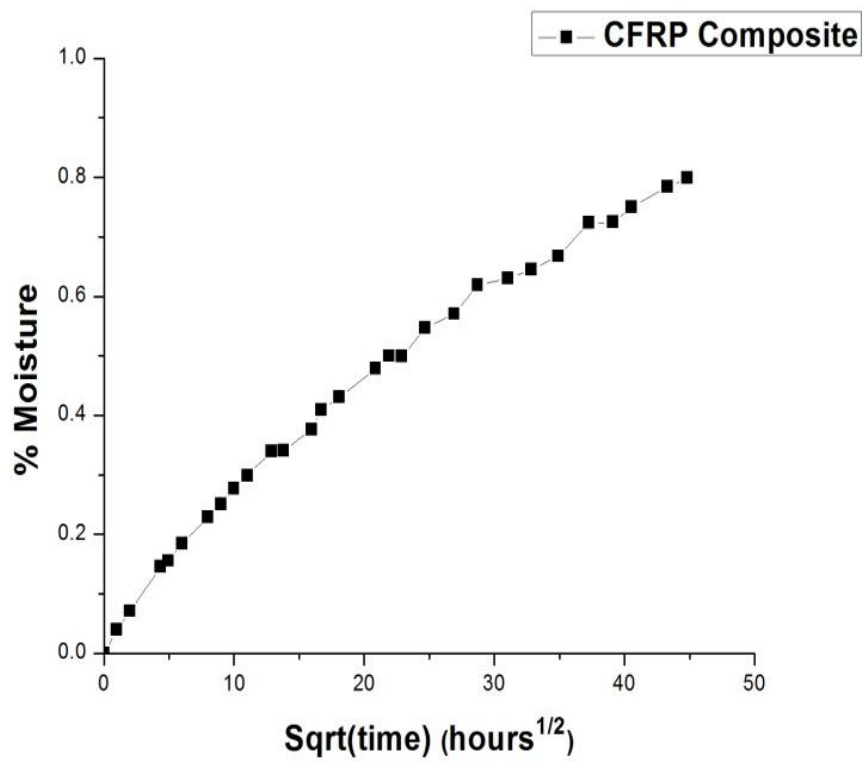
(a)



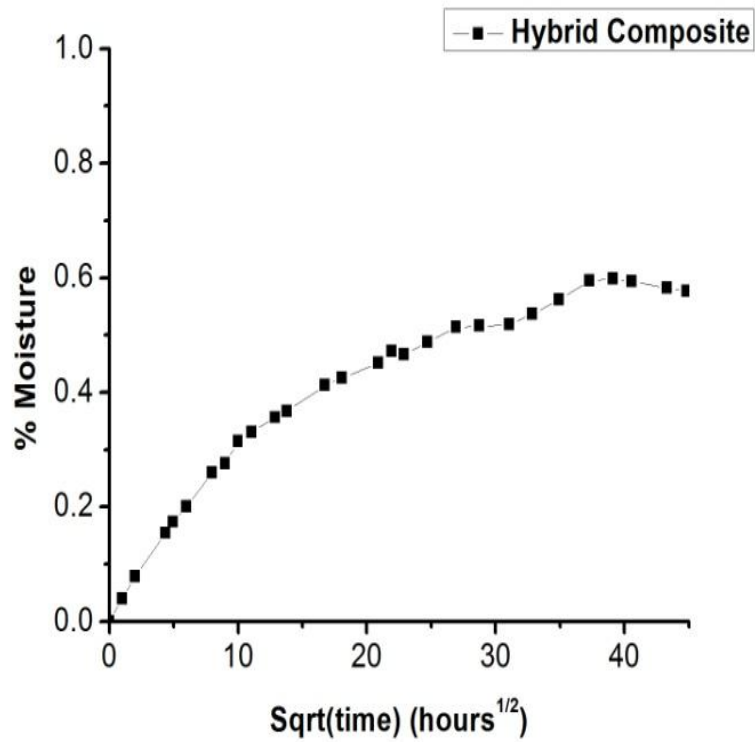
(b)



(c)



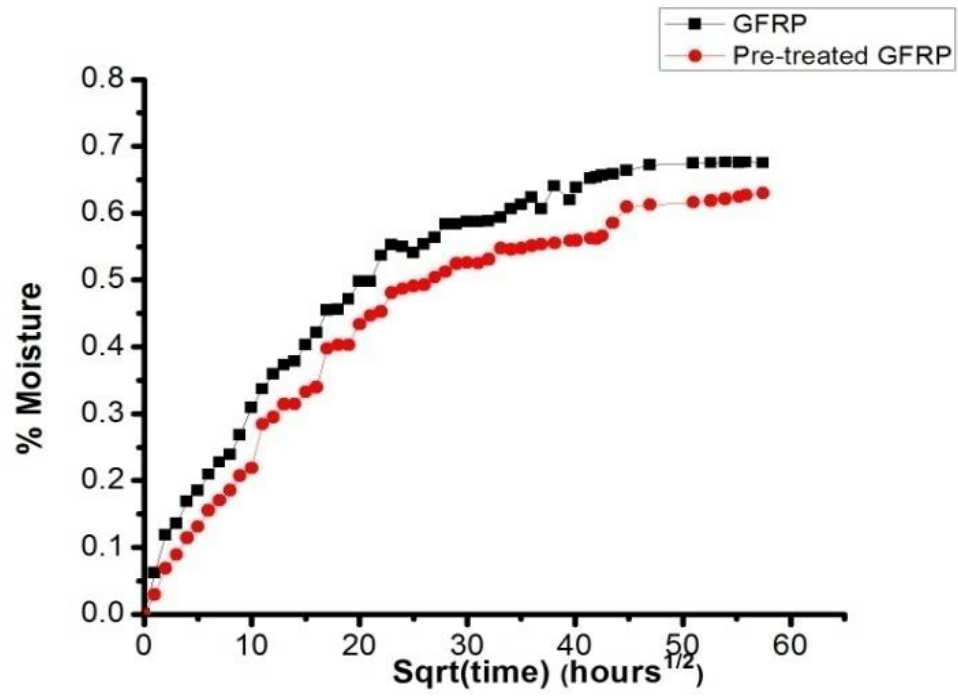
(d)



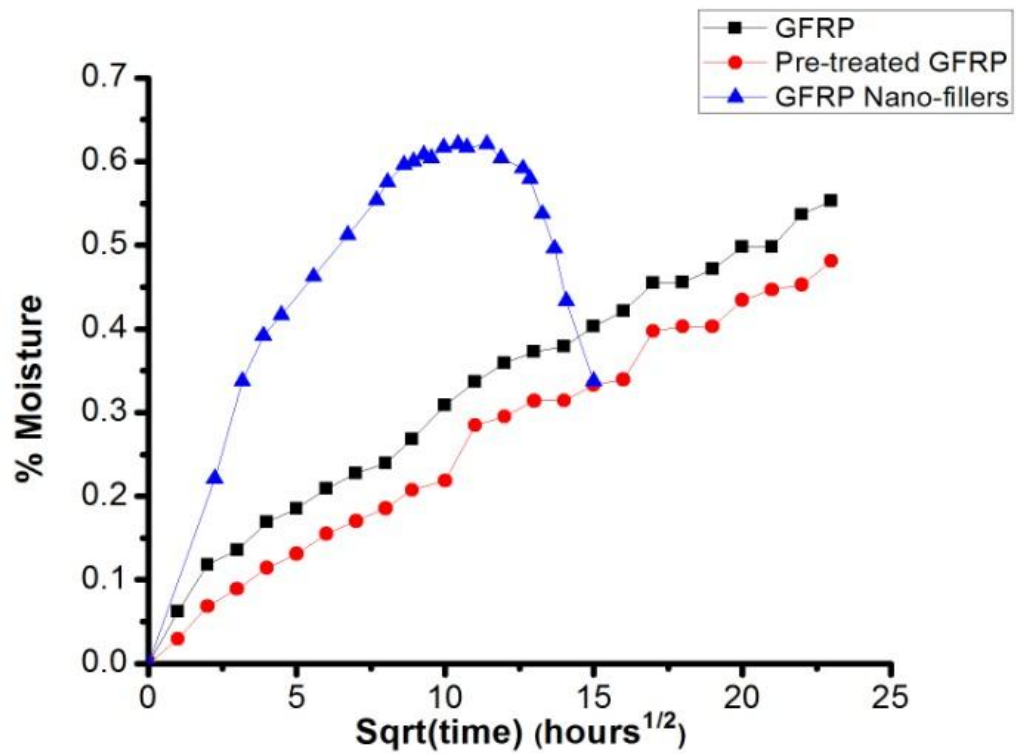
(e)

**Fig-5.1: Moisture uptake kinetics of (a) GFRP composite samples with post-curing treatment (b) GFRP composite samples without post-curing treatment (c) GFRP composite with alumina nano-fillers (d) CFRP composite samples and (e) Hybrid composite**

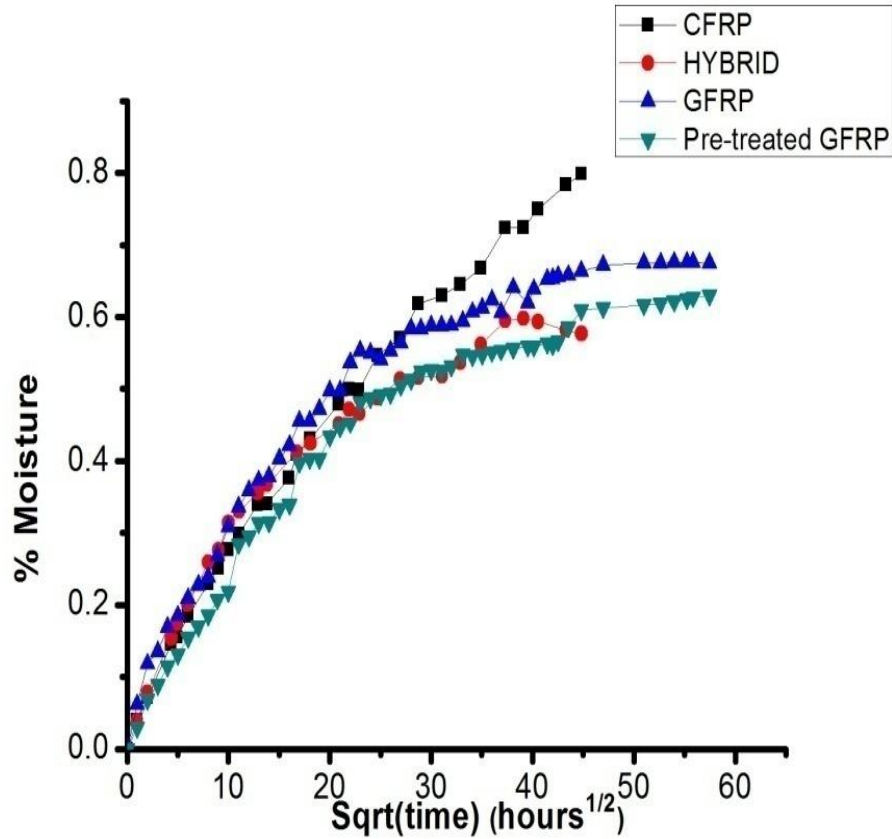
The moisture sorption kinetics of all of the fiber/epoxy systems initially follows Fickian behaviour. The GFRP and hybrid samples seem to follow dual-stage diffusion. But this can be confirmed only after further ageing.



(a)



(b)



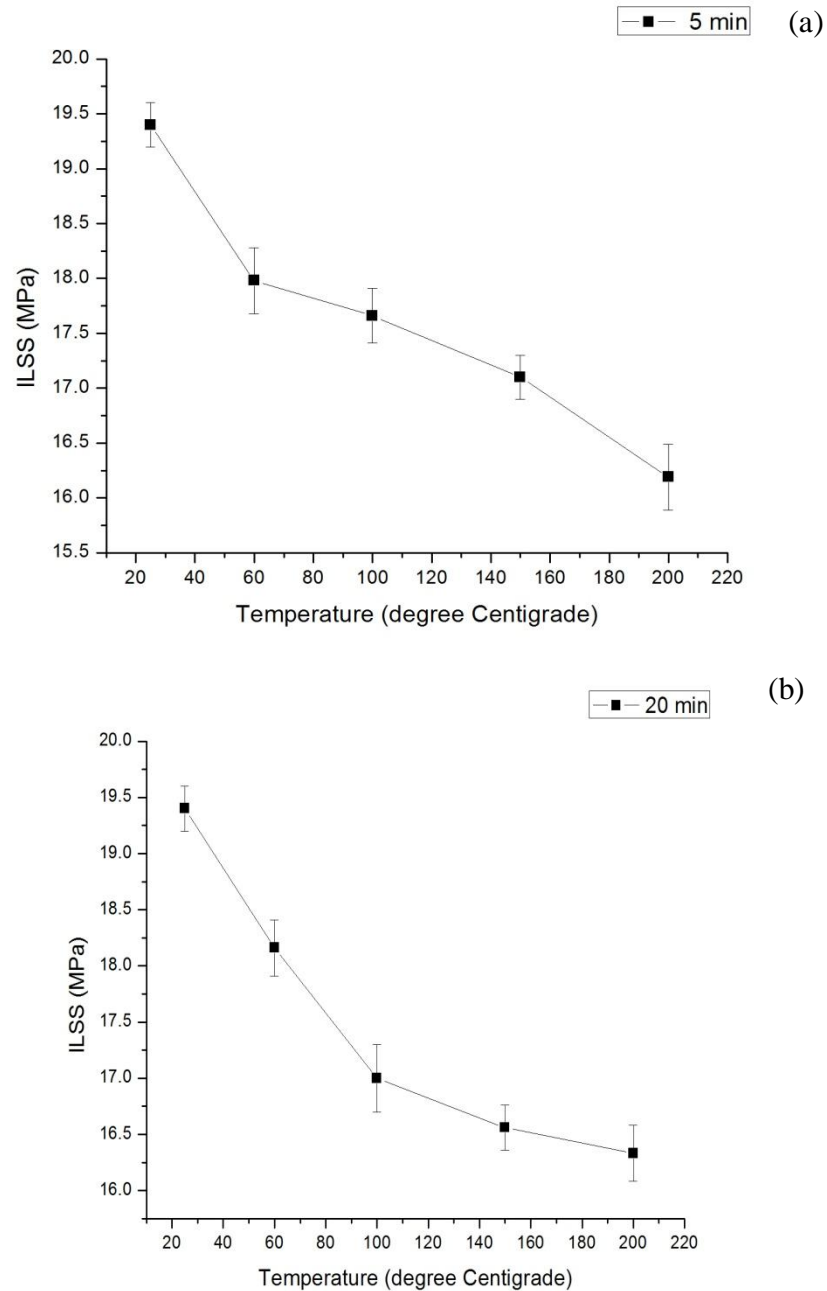
(c)

**Fig-5.2: Comparison of moisture uptake kinetics of (a) GFRP composite samples with and without post-curing treatment (b) GFRP composite samples with and without post-curing treatment and GFRP with alumina nano-fillers(c) GFRP composite samples with and without post-curing treatment, GFRP composite with alumina nano-fillers, CFRP composite samples and Hybrid composite**

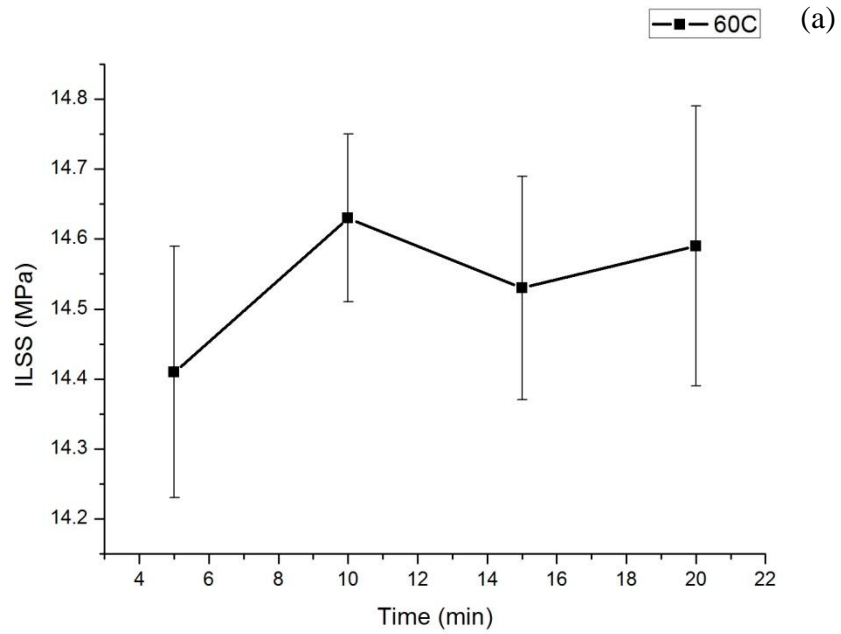
Initially, all FRP composites follow linear Fickian kinetics and linear portions of all FRP systems nearly overlap each other. Pre-treated GFRP composites show better resistance to moisture absorption than that not treated after curing. Moreover, GFRP composites with nano-fillers has maximum absorption rate in the initial linear part and undergoes permanent degradation after a very short time. However, carbon/epoxy composite follows linear kinetics for the longest time and hence; its behaviour may be accurately predicted by Fick's law.



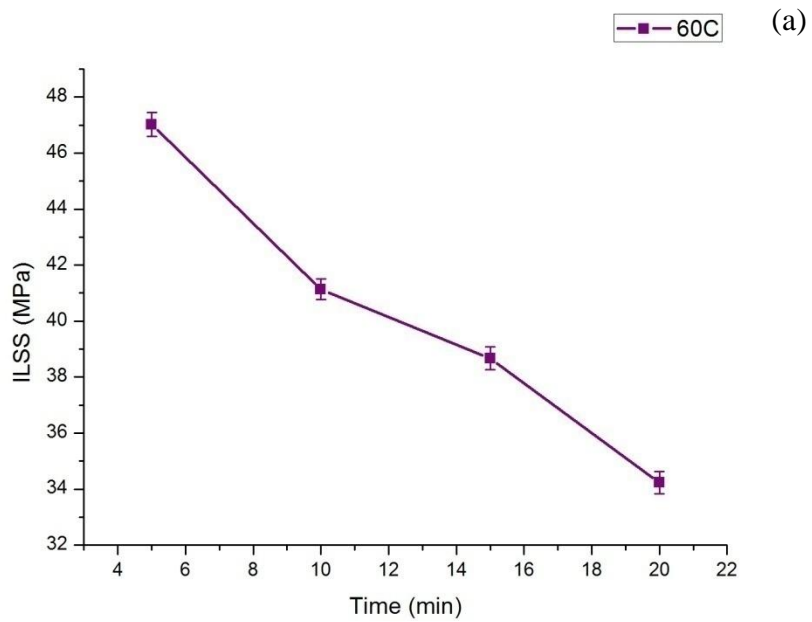
## 5.2. Effect of Moisture Ingression and UV radiation exposure on Interlaminar Shear Strength (ILSS) in FRP Composites

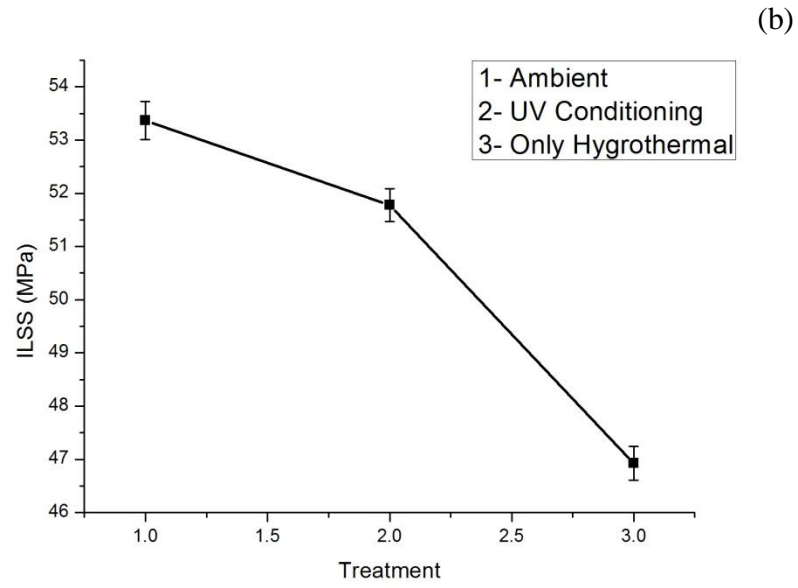


**Fig. 5.3: Variation of ILSS of GFRP composites with post-curing treatment with spiking temperature for times ( a) 5 minutes (b) 20 minutes**

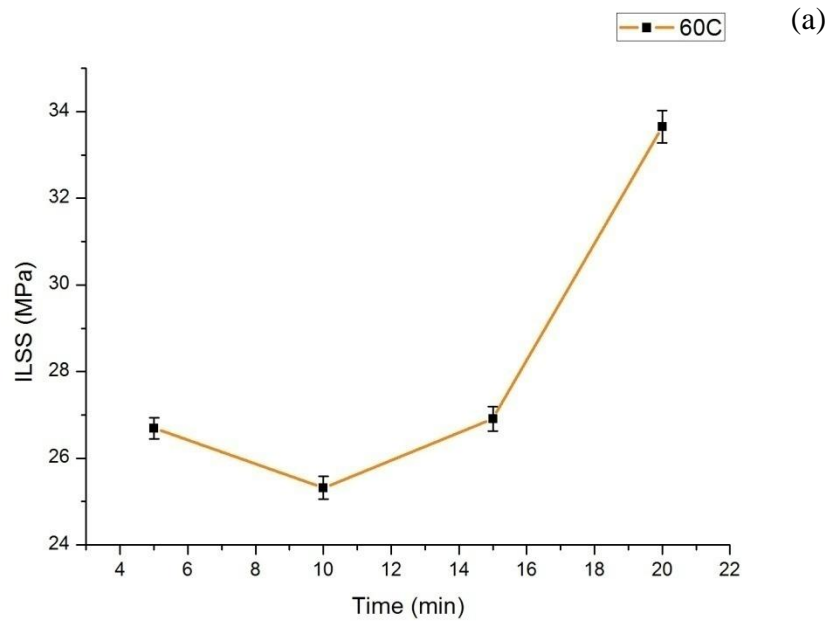


**Fig. 5.4: Variation of ILSS of GFRP composites without post-curing treatment with spiking times at 60°C**





**Fig. 5.5: Variation of ILSS of CFRP composites (a) with spiking times at temperature 60°C (b) with no treatment, hygrothermal treatment for 2000 hours and UV treatment**



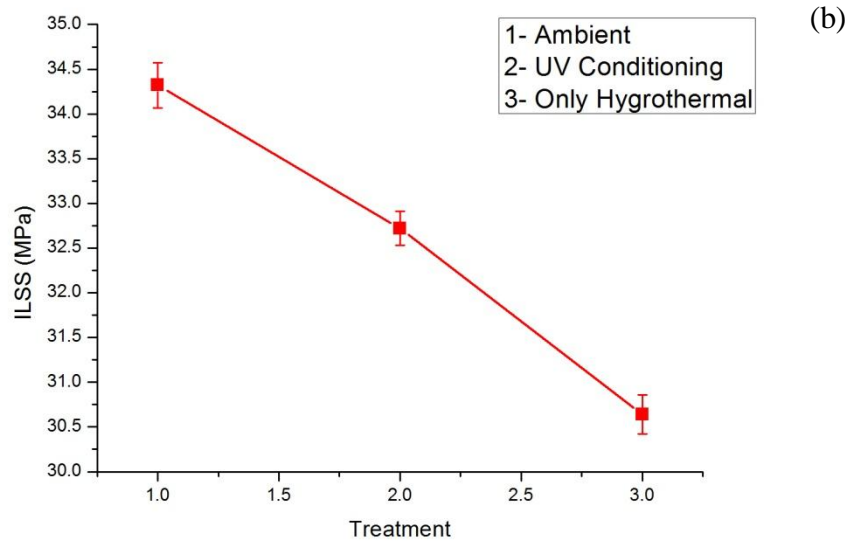


**Fig. 5.6: Variation of ILSS of Hybrid composites (a) with spiking times at temperature 60°C (b) with no treatment, hygrothermal treatment for 2000 hours and UV treatment**

As evident from above results, the interlaminar shear strength (ILSS) is found to decrease with increasing thermal spiking temperature. The decreasing trend of ILSS of the GFRP composite may be attributed to higher debonding tendency at higher temperature.

Due to humid ageing time of FRP composites, the interlaminar shear strength (ILSS) is found to decrease, which might be due to plasticization of polymer matrix. At lower spiking temperatures the interlaminar shear strength (ILSS) decreases. The possible reason might be the enhanced interfacial debonding due to nucleation of micro-cracks. The decrease in the interlaminar shear strength (ILSS) at higher temperatures of thermal spiking might be due to increase in viscous flow of the polymer matrix, which leads to enhanced debonding at interface.

### 5.3. Effect of Moisture Ingression and UV conditioning on Bond Structure in FRP Composites

FTIR-Imaging experiments were performed in this study to analysis the hygrothermally treated FRP composite as IR measurements are very sensitive to hydrogen bonds.

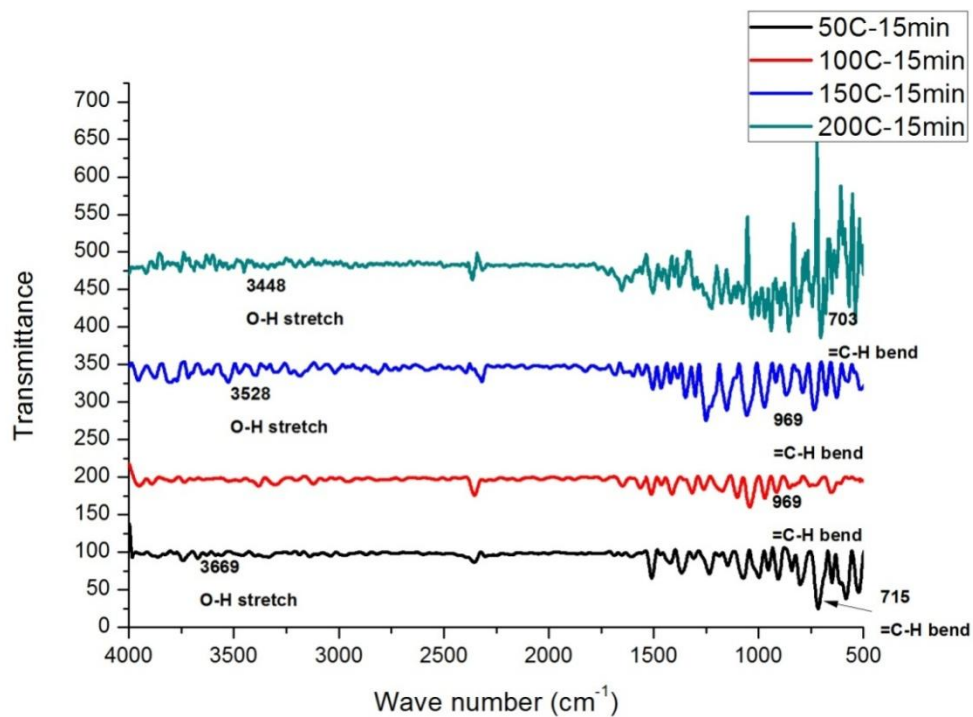


**Fig. 5.7: FTIR plot for GFRP specimens subject to hygrothermal treatment for 2000 hours and thermal spike for 15 minutes**

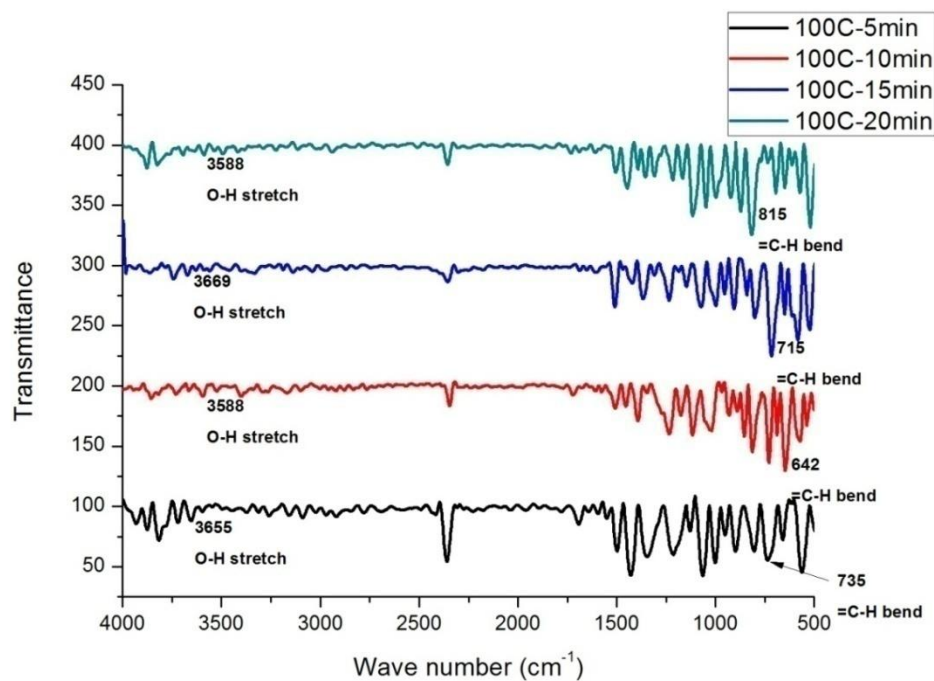


**Fig. 5.7 FTIR plot for GFRP specimens subject to hygrothermal treatment for 2000 hours and thermal spike at 100°C**

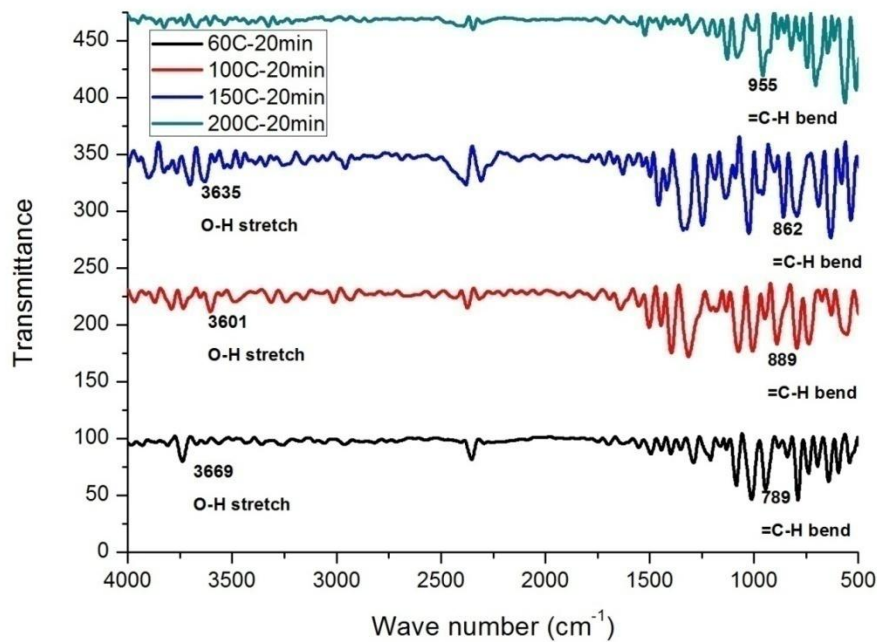


**Fig. 5.8 FTIR plot for CFRP specimens subject to hygrothermal treatment for 2000 hours and thermal spike for 20minutes**

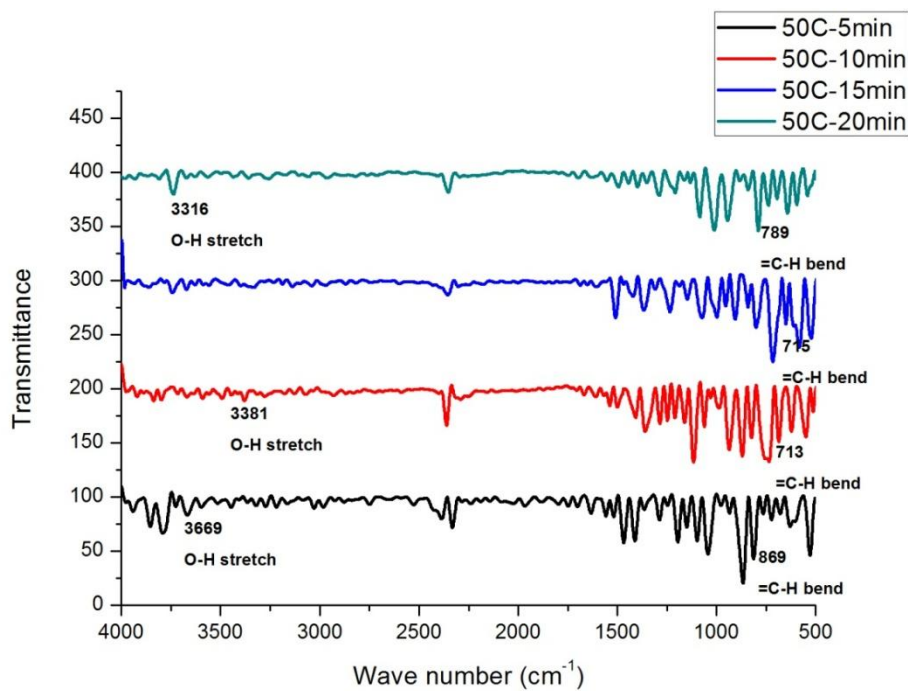


**Fig. 5.9 FTIR plot for CFRP specimens subject to hygrothermal treatment for 2000 hours and thermal spike at 60°C**

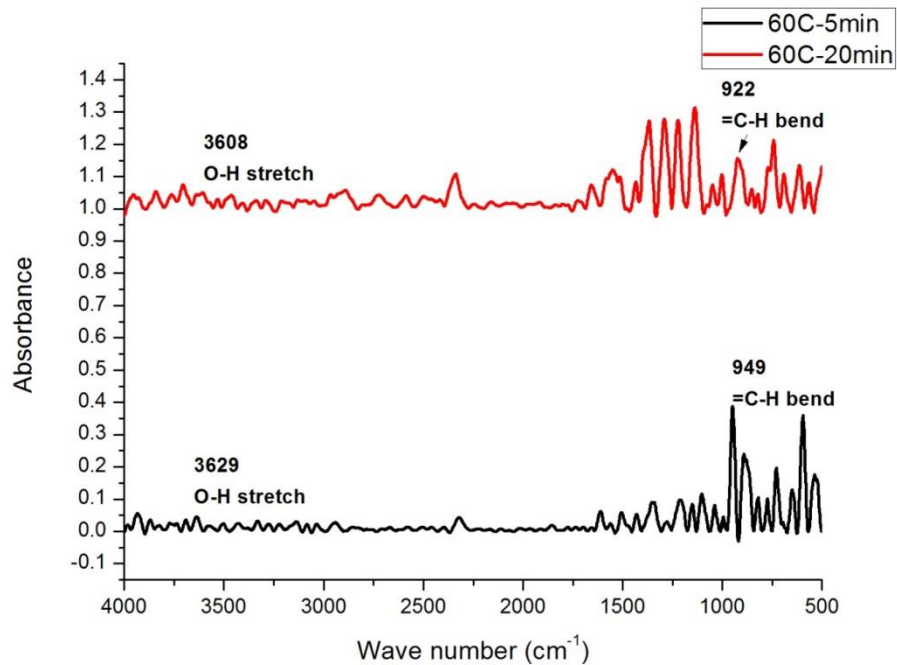


**Fig. 5.10 FTIR plot for GFRP specimens subject to hygrothermal treatment for 2000 hours and thermal spike at 60°C**

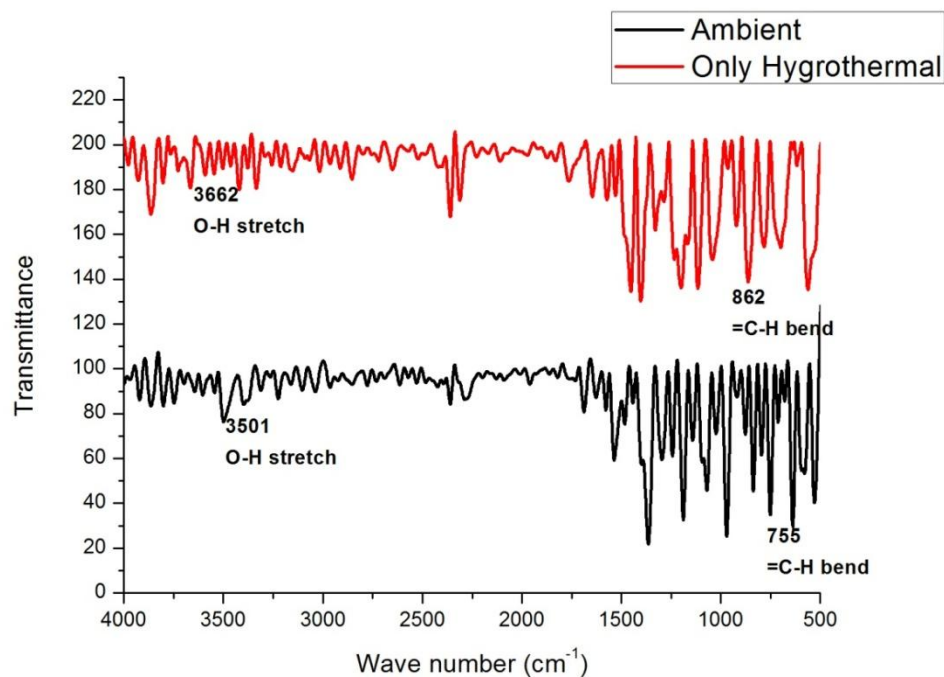


**Fig. 5.11 FTIR plot for Glass-Carbon-Epoxy composite specimens subject to hygrothermal treatment for 2000 hours and ambient specimens**

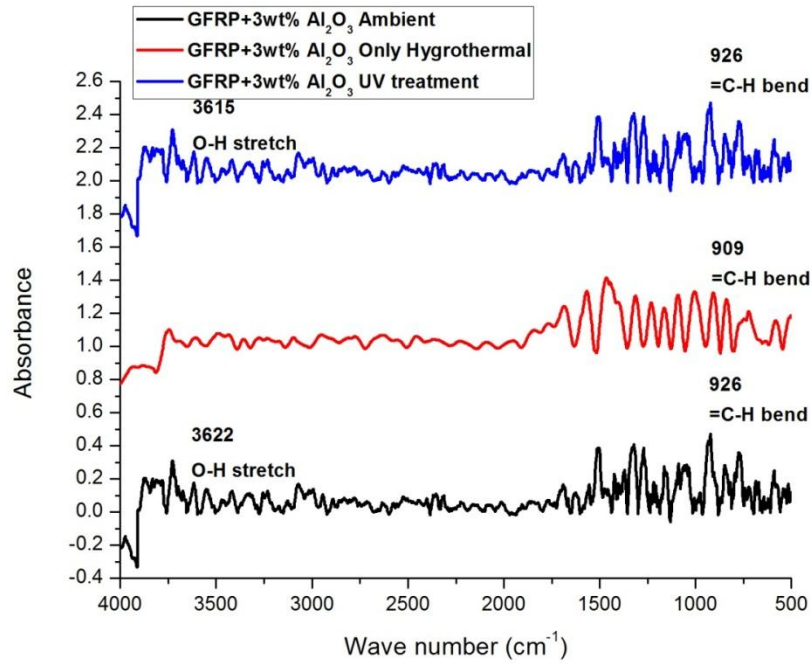


**Fig. 5.12 FTIR plot for GFRP+3 wt%  $\text{Al}_2\text{O}_3$  nano composite specimens subject to hydrothermal treatment, UV treatment and ambient conditions**

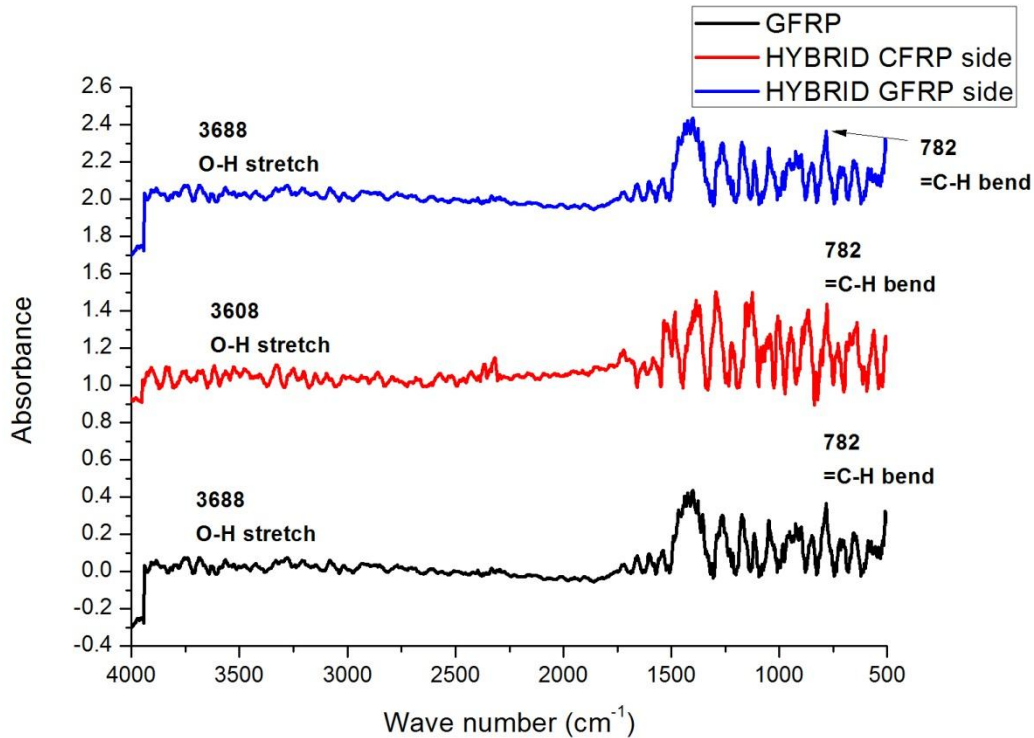


**Fig. 5.13 FTIR plot for Glass-Carbon-Epoxy composite and GFRP specimens subject to UV conditioning**



FTIR-Imaging experiments were performed in this study to analysis the hygrothermally treated FRP composite as IR measurements are very sensitive to hydrogen bonds.

Changes of frequency, intensity, and shape of the water-related bands have been interpenetrated in terms of bound and free water (up to four different water species in some systems), water clustering, water orientation, and water networking. The O-H vibration modes of liquid water lead to a very complicated vibration spectrum, complicated by both intermolecular and intra-molecular hydrogen bonding. Internal reflection FTIR Spectroscopy has been used to study the functional groups presents on the oxidized fiber surface. The larger size of the incident beam calls for novel experimental approaches.

#### 5.4. Effect of Moisture Ingression on Glass Transition Temperature ( $T_g$ ) in FRP Composites

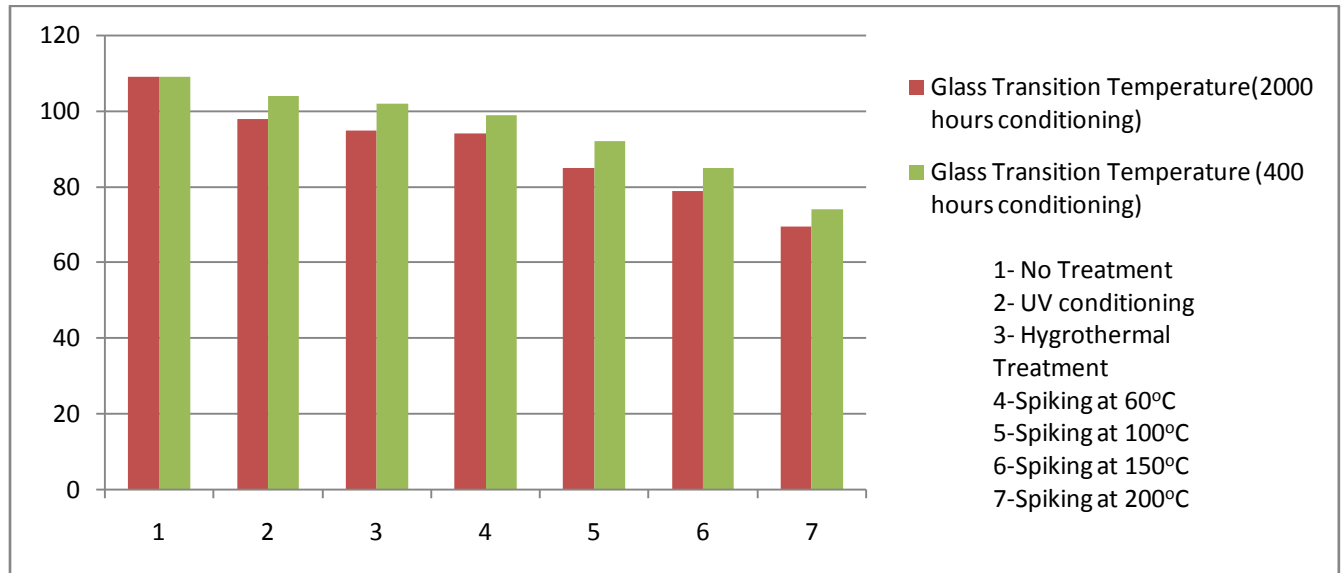


**Fig. 5.14: Variation of glass transition temperature of GFRP composites with hygrothermal treatment and thermal spiking at different temperatures.**

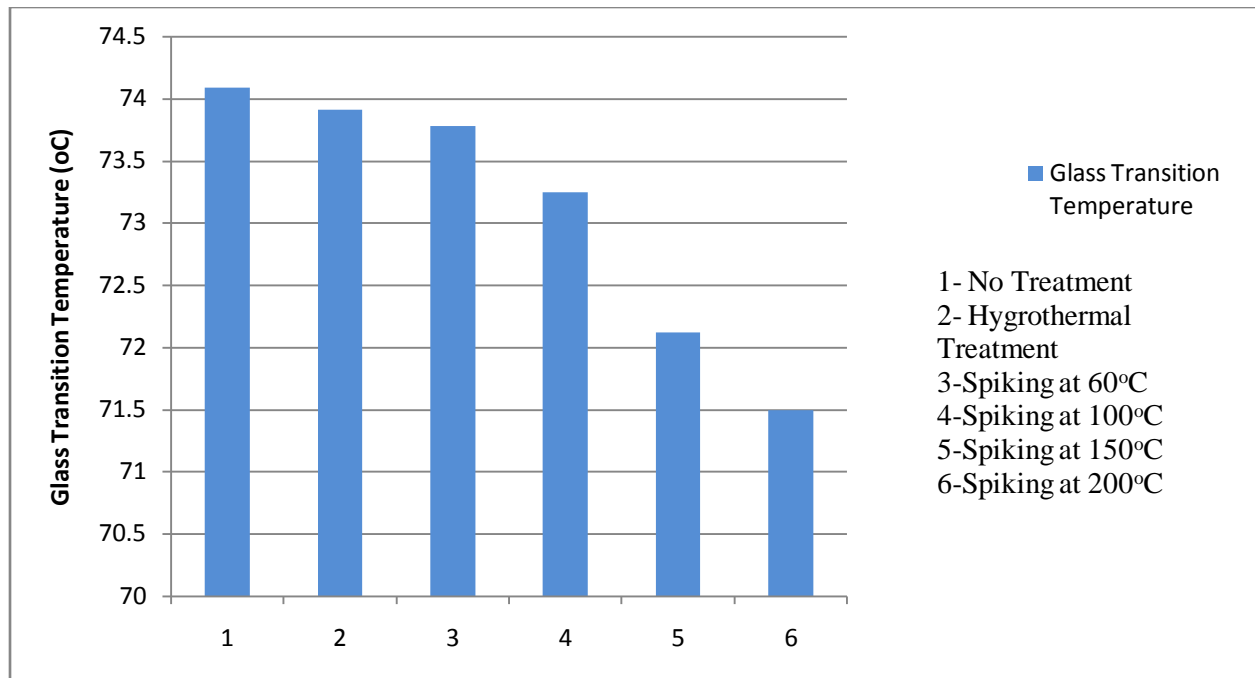


**Fig. 5.15: Variation of glass transition temperature of CFRP composites with hygrothermal treatment and thermal spiking at different temperatures.**

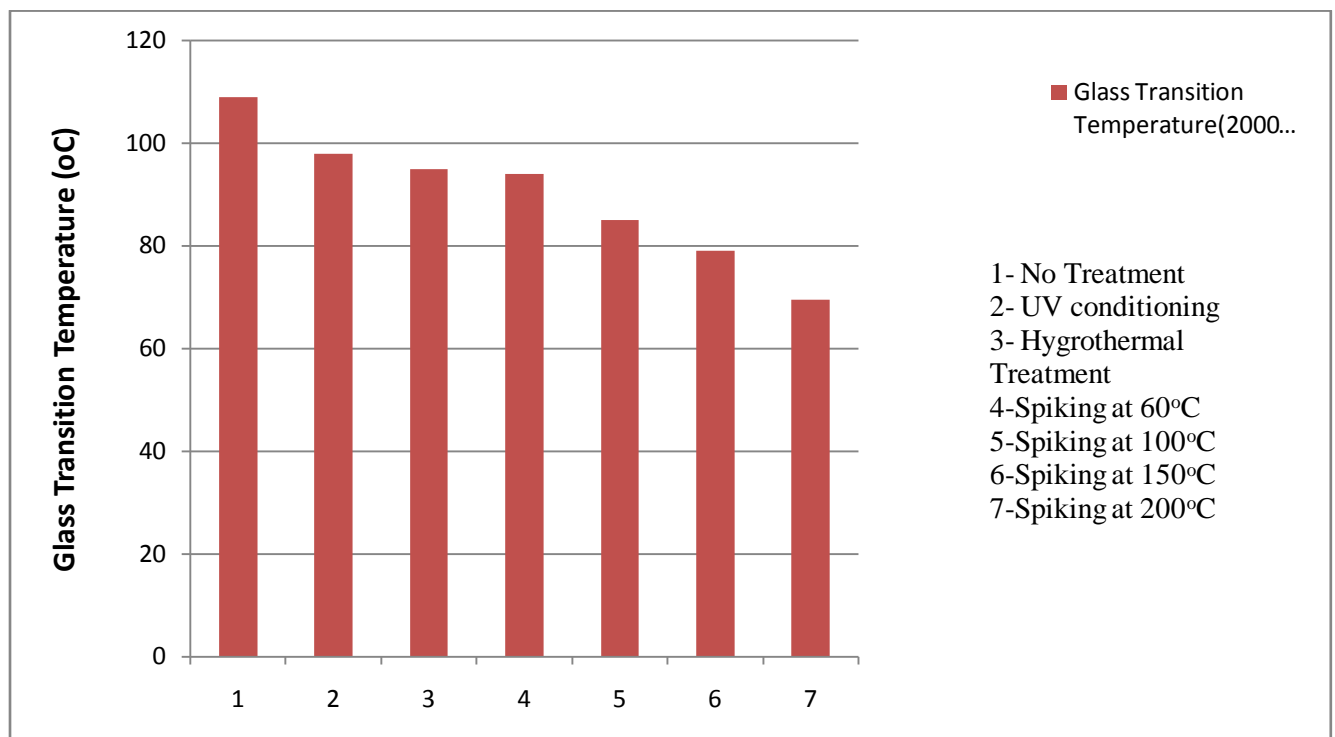


**Fig. 5.16: Variation of glass transition temperature of Hybrid composites with hygrothermal treatment and thermal spiking at different temperatures.**

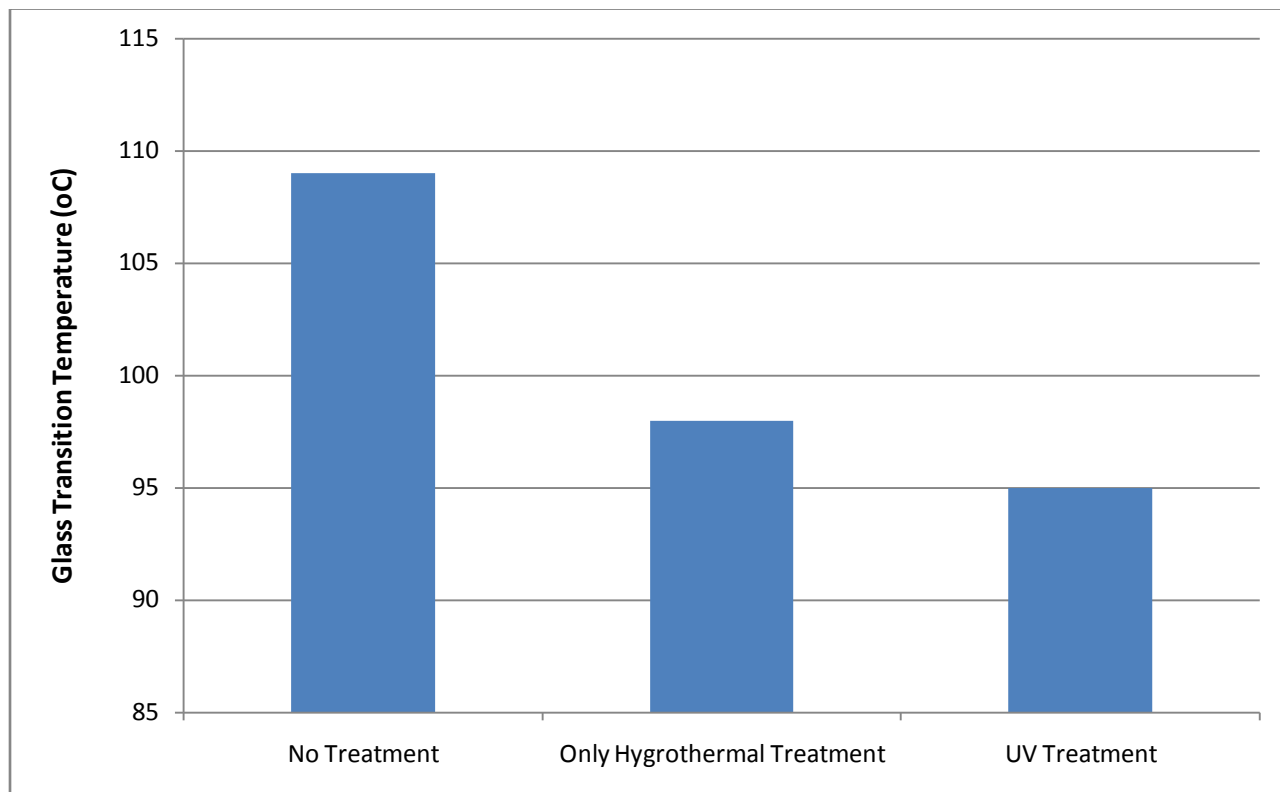


**Fig. 5.17: Variation of glass transition temperature of GFRP composites with nano fillers with hygrothermal treatment and UV treatment**

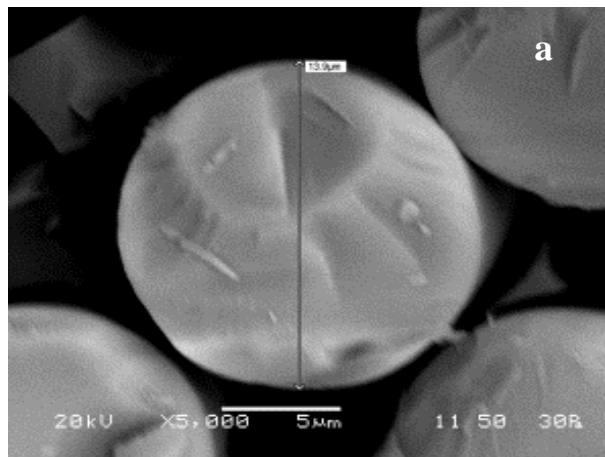
Glass transition temperature ( $T_g$ ) decrease due to moisture absorption. This can be attributed to plasticization of the polymer matrix.  $T_g$  decreases for low temperature spiking, which may be due to debonding but it decreases due to high temperature thermal spiking due to matrix softening.  $T_g$  decreases due to UV exposure.

## 5.4. Effect of Moisture Ingression on Failure Modes in FRP Composites

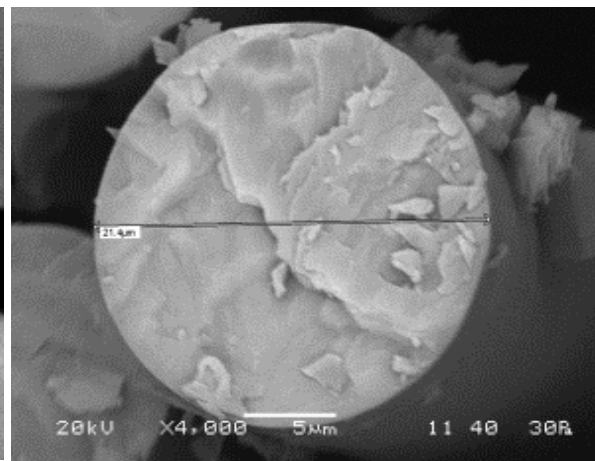
### 5.4.1. Glass/Epoxy Composites

#### 5.4.1.1. Failure Mode of Glass Fibers

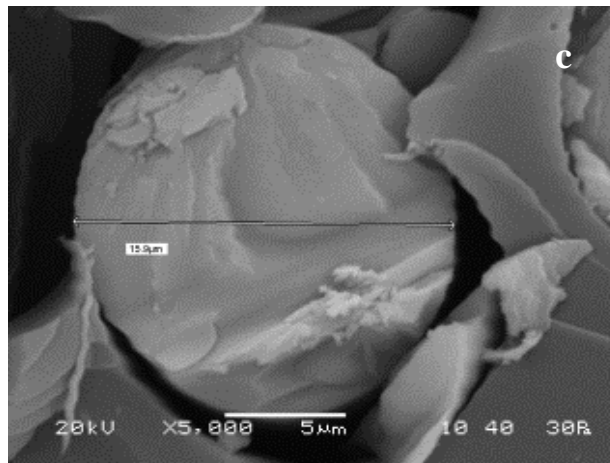
The SEM fractographs of the fractured fiber surfaces, as shown in Fig.5.5 clearly present evidence of brittle failure. The glass fibers were found to be swollen (around 7.5  $\mu\text{m}$ ) due to hygrothermal treatment, most likely in physisorbed and chemisorbed regions of interfaces because the chemically reacted region is quite resistant to hygrothermal attack. Moreover, the specimens with thermal spiking after hygrothermal treatment were found to have lower swelling (around 6  $\mu\text{m}$  for thermal spiking at 200°C) than those with only hygrothermal treatment.



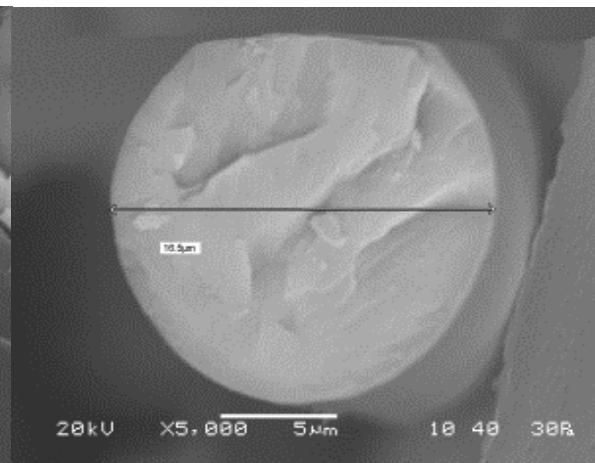
Fiber diameter=13.9 $\mu\text{m}$



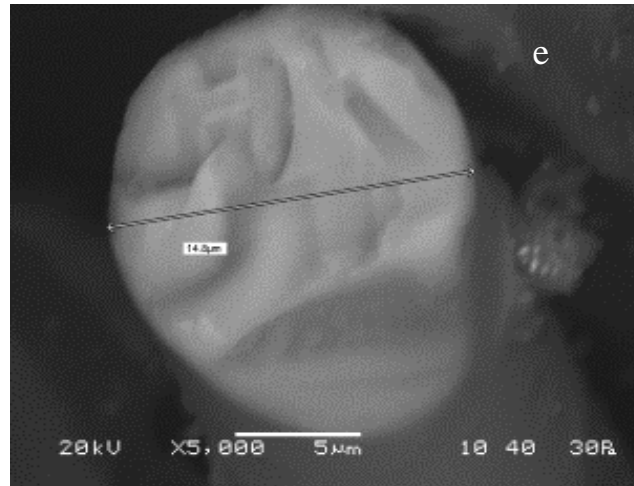
Fiber diameter=21.4 $\mu\text{m}$



Fiber diameter=15.9 $\mu\text{m}$



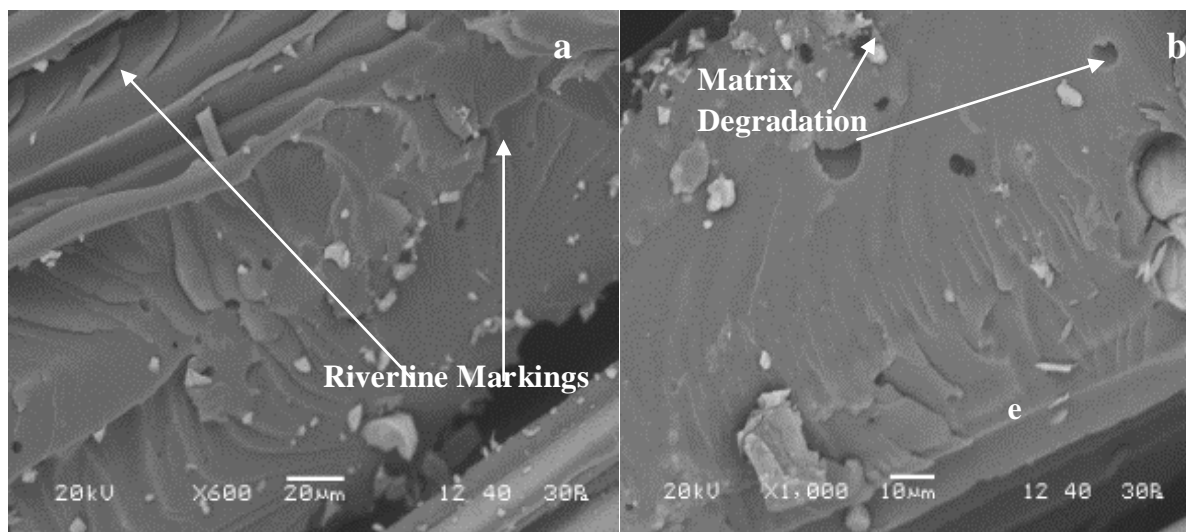
Fiber diameter=16.5 $\mu\text{m}$



Fiber diameter=14.8 $\mu$ m

**Fig. 5.18: Scanning electron micrographs of fractured E-glass fiber surfaces of GFRP samples tested at ambient temperature with (a) no treatment (b) hygrothermal treatment for 400 hours (c) thermal spiking at 60°C after hygrothermal treatment (d) thermal spiking at 100°C after hygrothermal treatment (e) thermal spiking at 200°C after hygrothermal treatment**

#### 5.4.1.2. Failure Mode of Epoxy Matrix



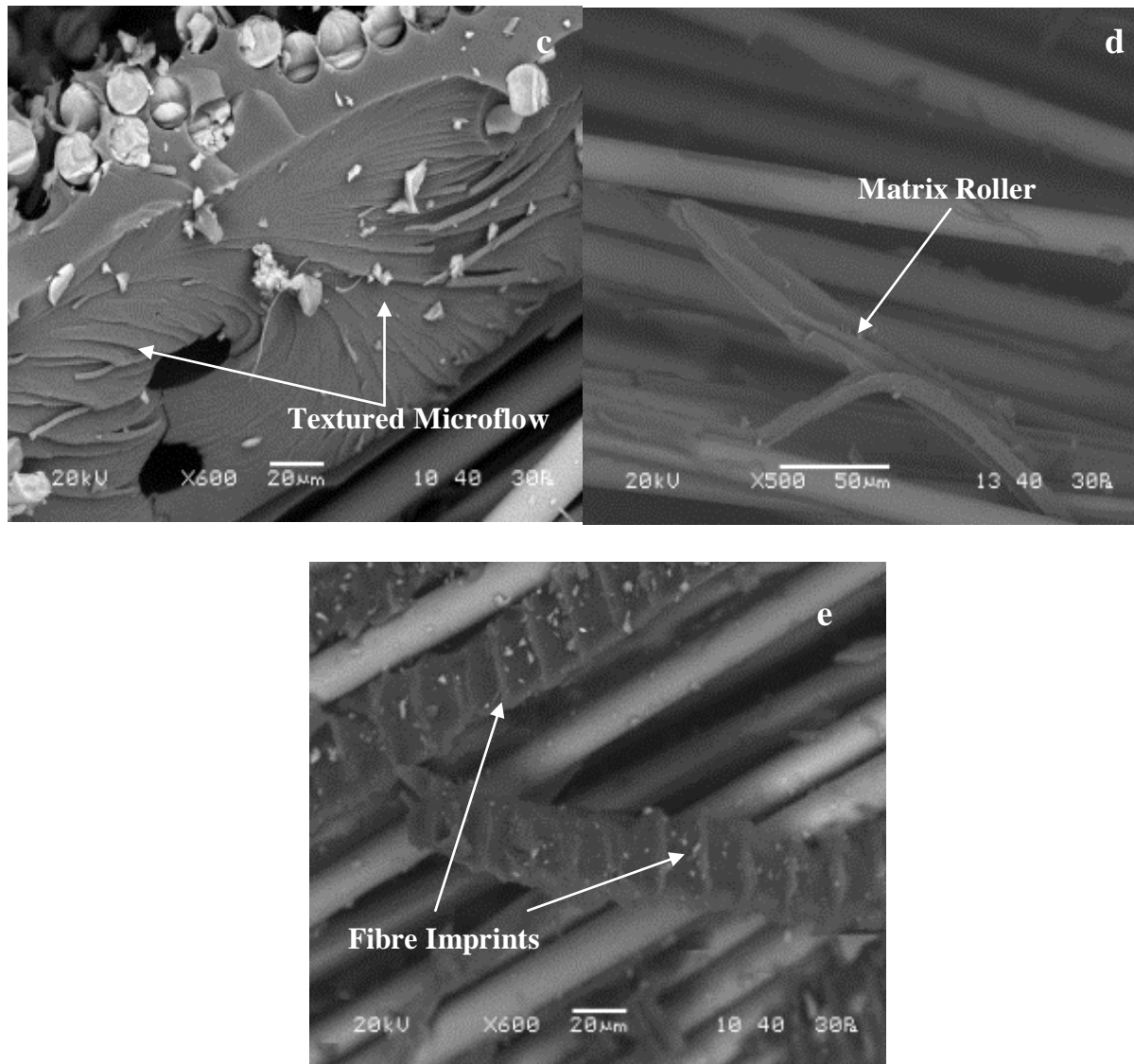


**Fig. 5.19: Scanning electron micrographs of epoxy matrix of GFRP samples tested at ambient temperature with (a) no treatment (b) hygrothermal treatment for 400 hours (c) thermal spiking at 60<sup>o</sup>C after hygrothermal treatment (d) thermal spiking at 100<sup>o</sup>C after hygrothermal treatment (e) thermal spiking at 150<sup>o</sup>C after hygrothermal treatment (f) thermal spiking at 200<sup>o</sup>C after hygrothermal treatment**

As shown in Fig.5.5, surface degradation of epoxy matrix due to moisture absorption is evident. Moreover, the hygrothermally treated specimen with no thermal spiking and thermal spiking at lower temperatures (60 <sup>o</sup>C and 100 <sup>o</sup>C) showed river line markings and textured micro-flow in

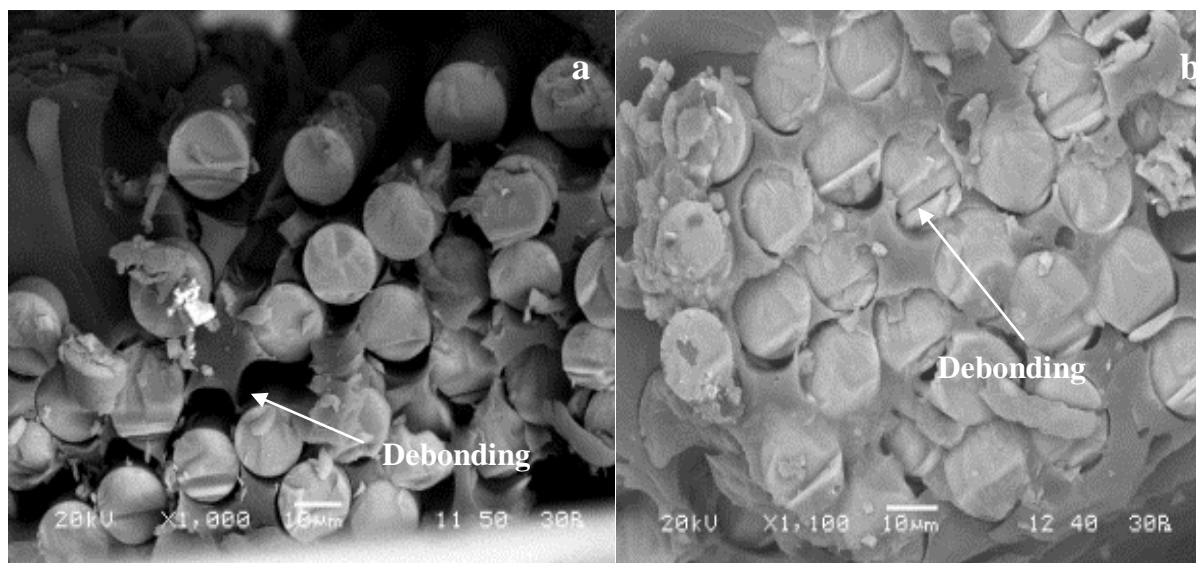


the epoxy matrix, whereas those thermally spiked at higher temperatures (150 °C and 200 °C) show formation of matrix roller. Riverlines are most valuable features in diagnosing crack growth. Direction of convergence of “riverlines” gives the direction of crack growth in the crack planes. Textured microflow is prevalent in brittle matrix systems

Also, it was observed that the samples which are thermally spiked at higher temperatures (150 °C and 200 °C), matrix is barely visible in the micrographs which might be due to burning of matrix.

#### 5.4.1.3. Failure Mode of Glass Fiber/Epoxy Interphase

At fiber/matrix interphase, debonding is observed to play a major role in failure of the FRP composites at all conditioning environments. However, the intensity of debonding and loss of adhesion at interphase is observed to depend on the environmental conditioning. As evident from Fig. 5.6, it was observed that in the samples which are thermally spiked at higher temperatures, matrix tends to stick to fibers due to increased viscous flow of polymer matrix. And due to this reason, the increase in tendency of fiber-matrix debonding was observed.



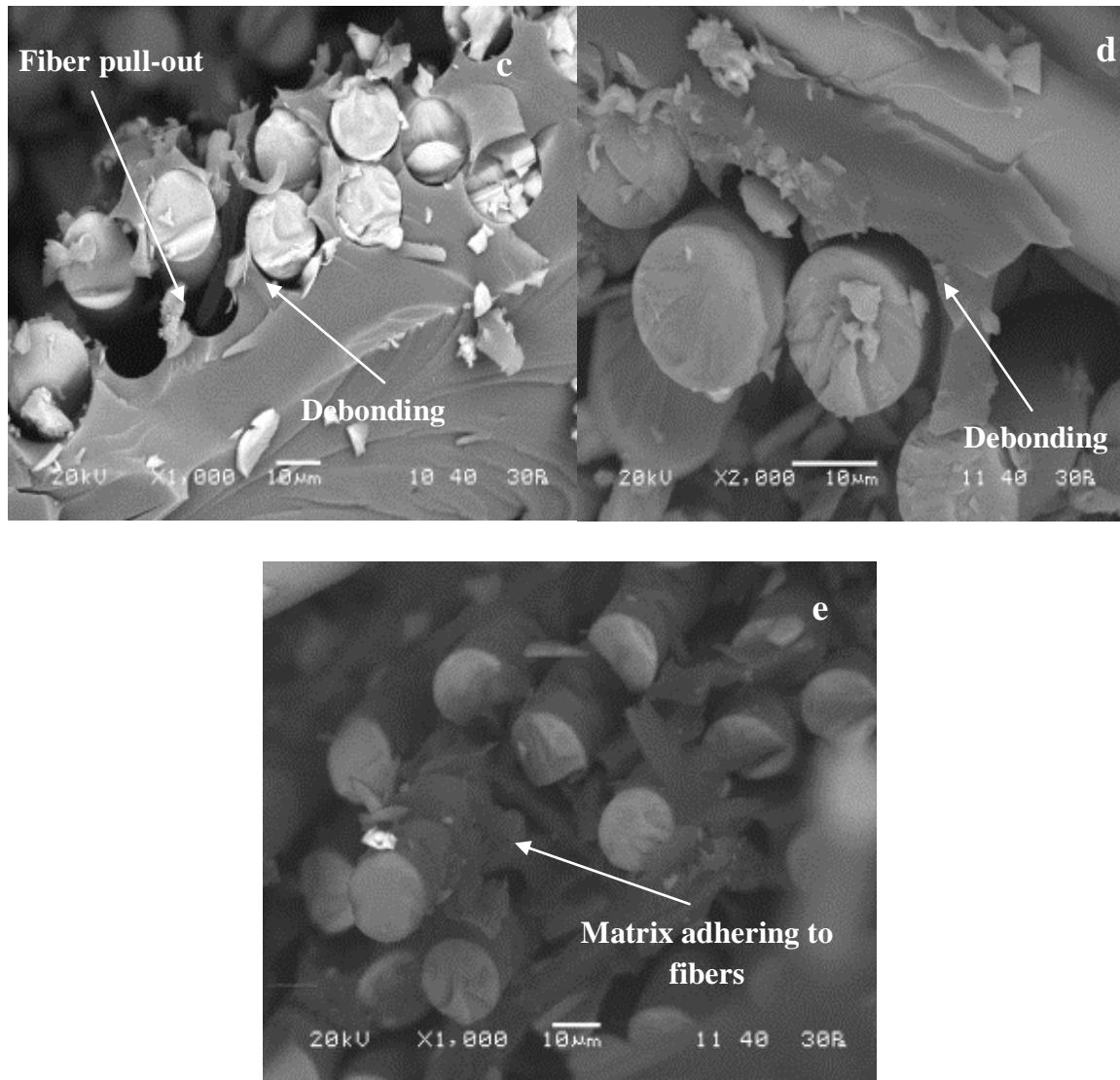


**Fig. 5.20: Scanning electron micrographs of fractured E-glass fiber surfaces of GFRP samples tested at ambient temperature with (a) no treatment (b) hygrothermal treatment for 400 hours (c) thermal spiking at 60°C after hygrothermal treatment (d) thermal spiking at 100°C after hygrothermal treatment (e) thermal spiking at 200°C after hygrothermal treatment**



### 5.4.2. Carbon/Epoxy Composites

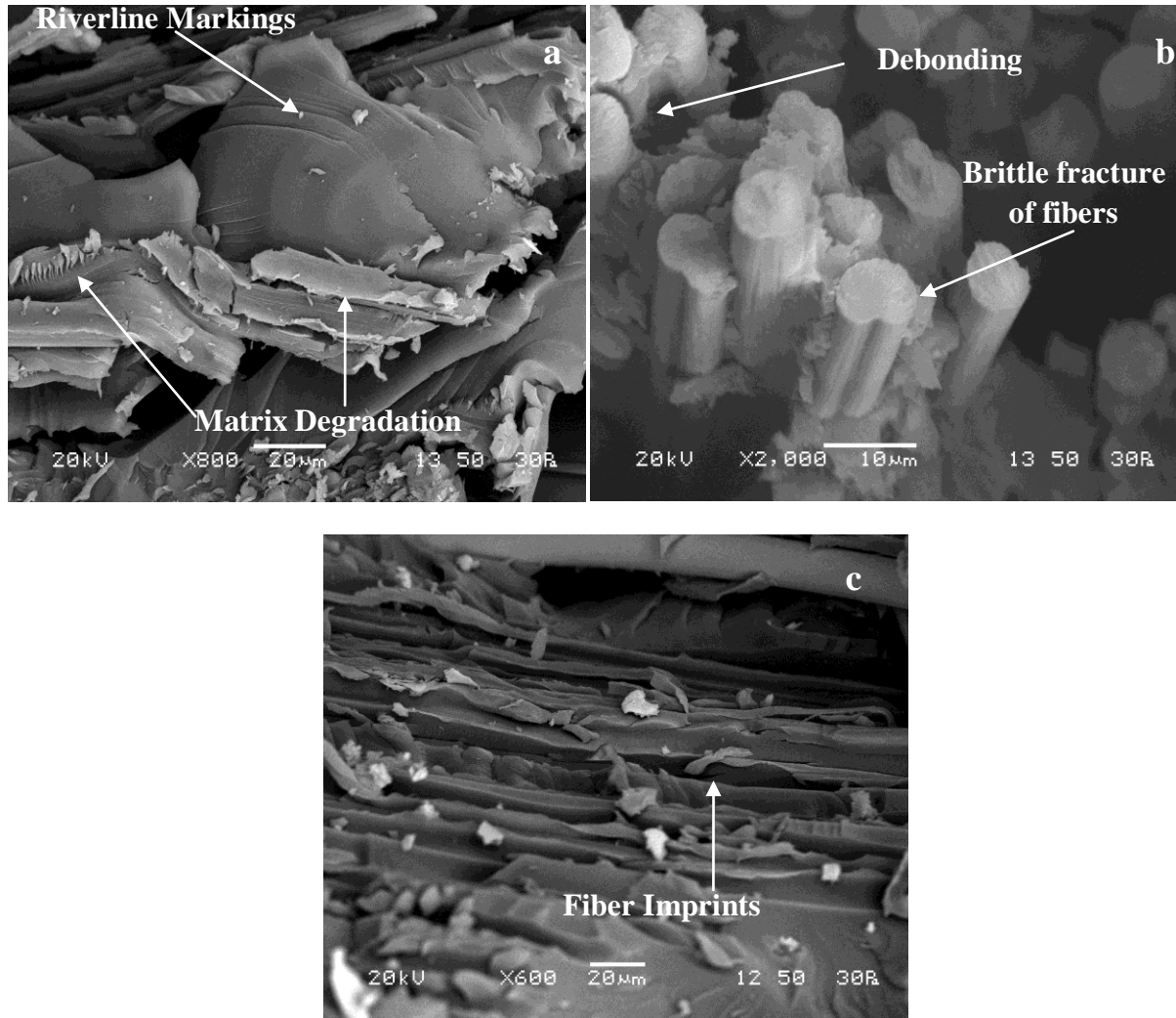


**Fig. 5.21: Scanning electron micrographs of fractured CFRP samples tested at ambient temperature subjected to hygrothermal treatment for 2000 hours showing (a) matrix failure modes (b) brittle failure of fibers and interfacial debonding (c) massive fiber imprints on matrix**

Fig. 5.7 shows the SEM fractographs of carbon/epoxy composites subjected to hygrothermal conditioning at 60°C and 95%RH for 2000 hours. Matrix degradation is caused due to moisture absorption. Other modes of failure observed are brittle failure of carbon fibers, interfacial debonding and fiber imprints on epoxy matrix.

### 5.4.3. Glass/Carbon/Epoxy Hybrid Composites

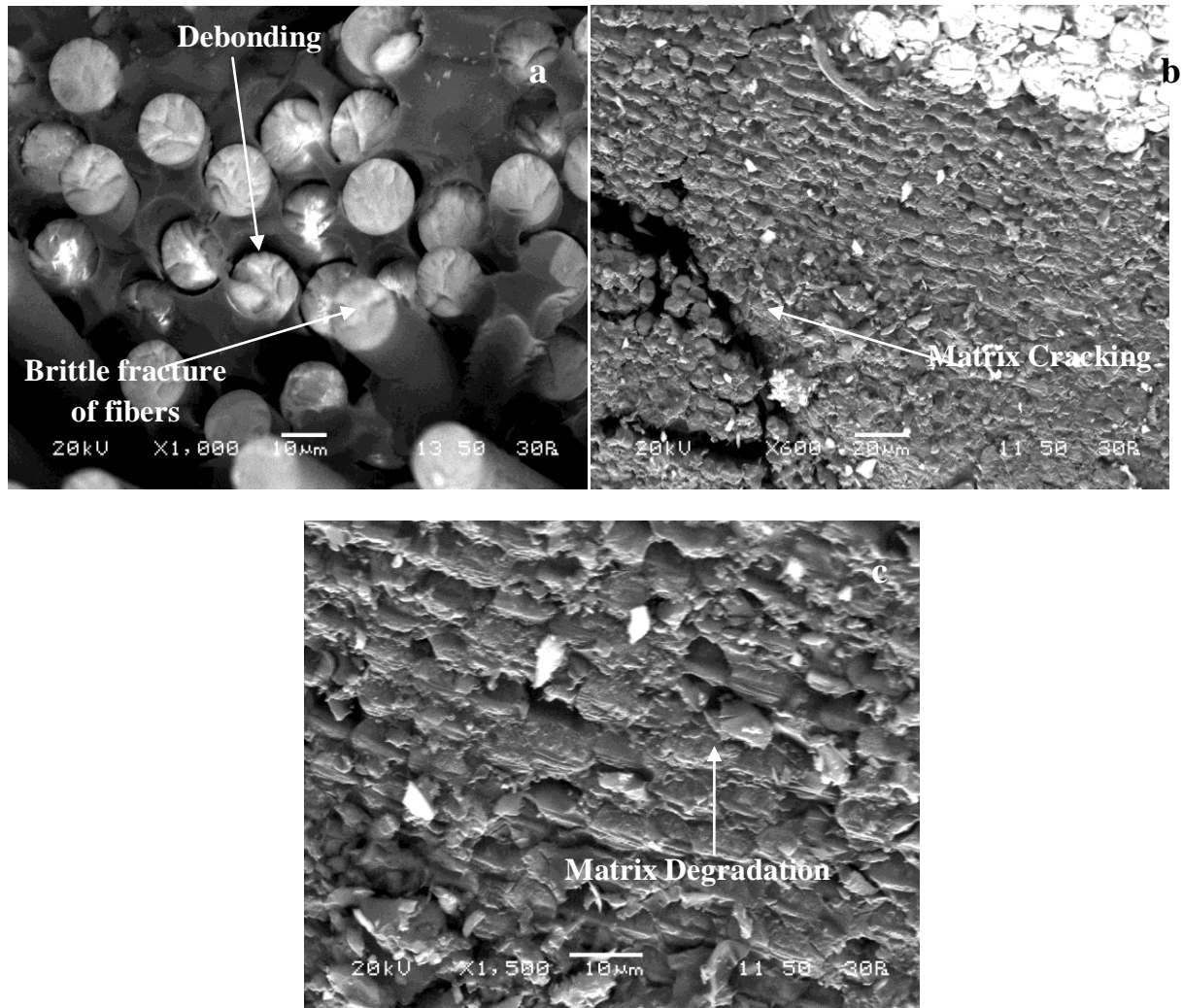


**Fig. 5.22: Scanning electron micrographs of fractured hybrid composite samples tested at ambient temperature subjected to hygrothermal treatment for 2000 hours showing (a) brittle failure of fibers and interfacial debonding (b) matrix cracking (c) matrix degradation**

Matrix degradation is quite prominent in case of hybrid composites as compared to glass/epoxy or carbon/epoxy composites. The possible reason might be the difference in coefficient of thermal expansion of glass and carbon fibers, between which the layer of epoxy matrix is sandwiched. Matrix cracking is also evident in this case which might be due to the same reason. Other modes of failure observed are brittle failure of carbon fibers and interfacial debonding.

#### 5.4.4. Glass/Epoxy Composites with alumina nano-fillers

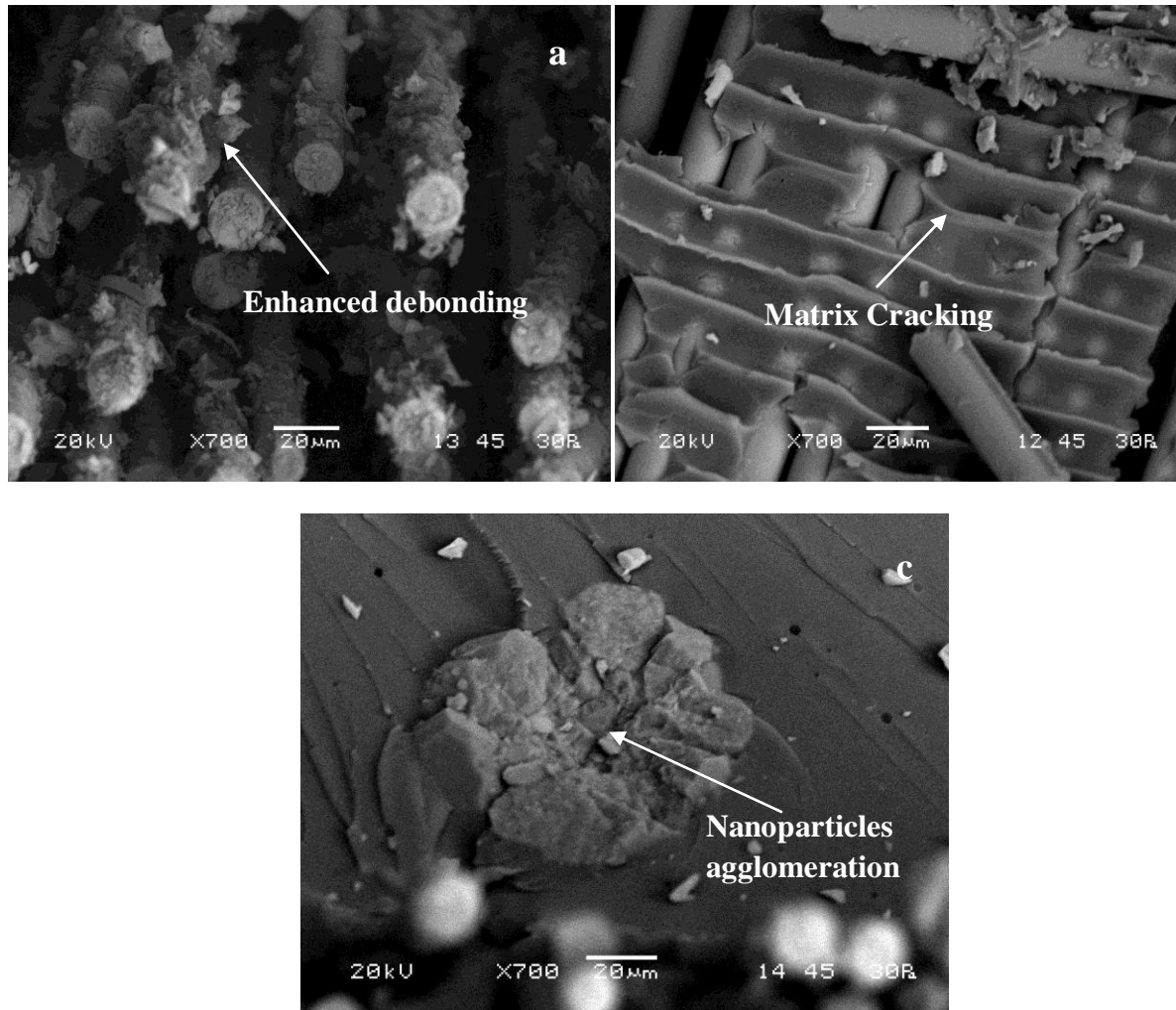


**Fig. 5.23: Scanning electron micrographs of fractured GFRP samples with alumina nano-fillers, tested at ambient temperature with (a) brittle failure of fibers and interfacial debonding (b) matrix degradation (c) agglomerated nano-particles**

As evident from Fig. 5.9, nano-particle agglomeration suggests that the dispersion of alumina nano-fillers in epoxy resin was not proper and better stirring and sonication is needed to be employed. Also, matrix cracking and enhanced debonding at fiber/matrix interphase was observed, which is possibly due to poor interfacial adhesion between the epoxy matrix and alumina nano-fillers. As a measure of correction, wetting reagents might be added to improve the adhesion between the matrix and fillers.

## Chapter 6

### Conclusion

#### *Moisture Ingression Kinetics*

The moisture sorption kinetics of none of the fiber/epoxy systems was found to follow Fickian behaviour entirely. Initially, all FRP composites follow linear Fickian kinetics for short exposure times, but for longer exposure times non-Fickian behaviour is observed. GFRP composites with nano-fillers has maximum absorption rate in the linear part and undergoes permanent degradation after a very short time. Carbon/epoxy composite follows linear kinetics for the longest time and hence, its behaviour may be predicted by Fick's law. Pre-treated GFRP composites show better resistance to moisture absorption.

#### *Effect on the interfacial properties of FRP Composites*

ILSS decrease due to moisture absorption. This can be attributed to plasticization of the polymer matrix. ILSS decreases for low temperature spiking, which may be due to debonding but it decreases due to high temperature thermal spiking due to matrix softening.

#### *Effect on the glass transition temperature of FRP Composites*

Glass transition temperature ( $T_g$ ) decrease due to moisture absorption. This can be attributed to plasticization of the polymer matrix.  $T_g$  decreases for low temperature spiking, which may be due to debonding but it decreases due to high temperature thermal spiking due to matrix softening.  $T_g$  decreases due to UV exposure.

#### *Effect on the failure modes of FRP Composites*

Study of SEM fractographs revealed the failure modes in the FRP composites. After moisture ingress, plasticisation and swelling (about 6  $\mu\text{m}$ ) are induced, this in turn leads to nucleation of micro-cracks and microvoids. Matrix degradation and matrix cracking are observed due to moisture intake. Fiber/matrix adhesion is gradually lost when spiking temperature is increased. Thermal spiking at higher temperature changes matrix failure modes to matrix roller formation. Glass fibers in the hygrothermally treated composites show swelling (most likely in physisorbed



and chemisorbed regions of interfaces) which decreases on subsequent thermal spiking. The fractured glass fiber surfaces show evidence brittle failure. Fiber/matrix adhesion is gradually lost when spiking temperature is increased. When thermally spiked at higher temperatures; matrix tends to stick to fibers due to increased viscous flow of polymer matrix.

The result of the study provides an improved understanding of the degradation of interfacial and thermal properties as well as the failure modes of FRP composites under the influence of thermal spike and humid ageing.

## **Chapter 7**

### **Scope of Future Work**

There exists a wide scope of future work in view of the present investigation. The future investigations can be focused on the study in variation of mechanical and thermo-physical behaviour of glass/epoxy, carbon/epoxy, hybrid and nano-filler incorporated composites cyclically exposed to different environments along with hygrothermal environments, such as - thermal conditionings (thermal spikes and shocks), cryogenic conditioning, vacuum conditionings and different radiation environments (such as UV and microwave).

Further investigation can be done to evaluate of efficiency of different methods to improve the properties of FRP composites such as - different types of hybridization methods and addition of different types of nano-fillers in the polymer matrix in different volume fractions. The effect of varying volume fraction of reinforcements and nano-fillers can be investigated.

## References

1. Pickering K. Properties and Performance of Natural-Fibre Composites, Woodhead Publishing Limited, 2008.
2. <http://www.mar-bal.com/applications/history-of-composites/> as retrieved on 10<sup>th</sup> March 2014.
3. <http://www.crowleaircadets.co.uk/Docs/acp33vol1.pdf> as retrieved on 17th March 2014.
4. Callister WD. Materials Science and Engineering-An Introduction, John Wiley and Sons, 2001.
5. Boyle MA, Martin CJ. Epoxy resins, ASM Handbook, Vol.21, ASM International, 2010.
6. Chawla KK. Composite Materials: Science and Engineering, Springer, 2013.
7. Kelly Z. Comprehensive Composite Materials: Polymer Matrix Composites, Elsevier Science Publication, 2000.
8. Hull D, Clyne TW. An Introduction to Composite Material, Cambridge University Press, 1996.
9. Rothon R. Particulate-filled Polymer Composites, Rapra Technology Limited, 2003.
10. Kim, JK, Mai, YW. Engineered Interfaces in Fiber Reinforced Composites, Elsevier Science Publication, 1998.
11. Strümpfer R, Maidorn G, Garbin A, Ritzler L, Greuter F. PolymPolym Compos 1996; 45: 299.
12. Alfrey T, Gurnee EF, Lloyd WG. J PolymSci 1966; C12:249.
13. Fick A, AnnPhysik Chemic 1855; 170: 59.
14. Fourier J.P., Theorie Analytique de la chaleur, Paris 1822, English Translation by Freeman, A., Dover Publication, 11.
15. Crank J, Park GS, Diffusion in Polymers, Academic Press Inc. London, 1968.
16. Shen CH, Springer GS. J Compos Mater 1976; 10: 2.
17. Ray BC, Biswas A, Sinha PK. Metals Materials and Processes, 1991; 3: 99.
18. Jiang X, Kolstein H, Bijlaard F, Qiang X. Compos A 2014; 57: 49.
19. Loos AC, Springer GS. J Compos Mater 1979; 13: 131.

20. Shirrell CD. Adv Compos Mater Environ Effects, ASTM STP 1978; 658: 21.
21. Mohlin T. In: Springer GS (ed) Environmental effects of composite materials, Technomic, Lancaster, PA, 1984; 3: 163.
22. Loos AC, Springer GS. In: Springer GS (ed) Environmental effects of composite materials. Technomic, Westport, CT, 1981: 34.
23. Yoosefinejad A, Hogg, PJ. In: Visconti CI (ed) Proceedings of ECCM eighth European conference on composite materials, Naples, Woodhead Publishing, Italy, 1998; 1: 151.
24. Henson MC, Weitsman YJ. Stress effects on moisture transport in an epoxy resin and its composite. In: Proceedings of the third Japan-US conference on composite materials, Japan Society of Composite Materials, Tokyo, 1986: 775.
25. Althof W. Proceedings of the 11th National SAMPE Conference, SAMPE, Azusa, 1979; 11: 309.
26. Nicolais L, Drioli E, Hopfenberg H, Caricati G. J MembrSci 1978; 3: 231.
27. Clark DL. Texas A&M University Report MM 4665-83-16, 1983.
28. Khan LA, Nesbit A, Day RJ. Compos A2010; 41: 942.
29. Weitsman Y. Compos A 2006; 37: 617.
30. Shen CH, Springer GS. In: Springer GS (ed) Environmental effects of composite materials. Technomic, Westport, CT, 1981: .
31. Lo SY, Hahn HT, ChiaoTT. In: Hayashi T, Kawata K, Umekawa S (eds) Proceedings of the fourth international conference on composite materials (ICCM/4). Progress in science and engineering of composites, Tokyo, 1982; 2: 987.
32. Yao J, Ziegmann G. J Compos Mater 2007; 41: 993.
33. Davies P, Choqueuse D, Mazeas F. In: Reifsnider KL, Dillard DA, Cardon AH (eds) Progress in durability analysis of composite systems. Balkema, Rotterdam, 1998: 19.
34. Chateauminois A, ChabertB, Soulier JP, Vincent L. In: Tsai SW, Springer GS (eds) Proceedings of the eighth international conference on composite materials (ICCM/8), Honolulu. 1991: 12.
35. Gao J, Weitsman YJ. University of Tennessee Report MAES 98-4.0 CM, 1998.
36. Lagrange A, Melennec C, JacquemetR.. In: Cardon AH, Verchery G (eds) Durability of polymer based composites systems for structural applications, Elsevier, 1991: 385.



37. Dewimille B, Thoris J, Mailfert R, Bunsell AR. In: Bunsell AR (ed) *Advances in composites materials; Proceedings of the Third International Conference on Composite Materials*, Paris, France. Pergamon, Paris, 1980: 597.
38. Nakanishi Y, Shindo A. In: Hayashi T, Kawata K, Unlekawa S (eds) *Proceedings of the fourth international conference on composite materials (ICCM/4)*, Tokyo. ISBS, Beaverton, 1982; 2: 1009.
39. Imaz JJ, Rodriguez JL, Rubio A, Mondragon I. *J Mater SciLett* 1991; 10: 662.
40. Gupta VB, Drzal LT, Rich MJ. *J ApplPolymSci* 1985; 23: 4467.
41. Mohlin T. In: Springer GS (ed) *Environmental effects of composite materials*, Technomic. Lancaster, PA, 1984; 3: 163.
42. Van den Emde CAM, Van den Dolder A. In: Cardon AH, Verchery G (eds) *Durability of polymer based composite systems for structural applications*, Elsevier Applied Science, New York, 1991: 408.
43. Apicella A, Migliaresi C, Nicolais L, Iaccarino L, Roccotelli S. *Composites* 1983; 14: 387.
44. French MA, Pritchard G. In: Cardon AH, Verchery G (eds) *Durability of polymer based composite systems for structural applications*, Elsevier, Amsterdam, 1991: 345.
45. Kootsookos A, Mouritz AP. *Compos SciTechnol* 2004; 64: 1503.
46. Ramirez F, Carlsson L, Acha B. *J Mater Sci* 2008; 43: 5230.
47. Fukuda H. In: Loo TT, Sun CT (eds) *Proceedings of the international symposium on composite materials and structures*, Beijing, 1986: 50.
48. Nicolais L, Apicella A, Del Nobile MA, Mensitieri G. In: Cardon AH, Verchery G (eds) *Durability of polymer based composite systems for structural applications*, Elsevier Applied Science, New York, 1991: 99.
49. Olmos D, Lo´pez-Moro´n R, Gonza´lez-Benito J. *Compos SciTechnol* 2006; 66:2758.
50. Manocha LM, Bahl OP, Jain RK. In: Hayashi T, Kawata K, Umekawa S (eds) *Proceedings of the fourth international conference on composite materials (ICCM/4)*, Progress in Science and engineering of Composites, Tokyo, 1982; 2: 957.
51. Carter HG, Kibler KG. *J Compos Mater* 1978;12: 118.
52. Lee MC, Peppas NA. *J ApplPolymSci* 1993; 47: 1349.
53. Perreux D, Suri C. *Compos SciTechnol* 1997; 57: 1403.
54. Merdas I, ThomINETTE F, Tcharkhtchi A, Verdu J. *Compos SciTechnol* 2002; 62: 487.

55. Kumosa L, Benedikt B, Armentrout D, Kumosa M. *Compos Part A Appl Sci Manuf* 2004; 35: 1049.
56. Popineau S, Rondeau-Mouro C, Sulpice-Gaillet C, Shanahan MER. *Polymer* 2005;46: 10733.
57. Ferreira JM, Pires JTB, Costa JD, Errajhi OA, Richardson M. *Compos Struct* 2007;78:397.
58. Helbling CS, Kharbari VM. *J Reinf Plast Compos* 2008;27:613.
59. Saponara VL. *Compos Struct* 2011; 93: 2180.
60. Grace LR, Altan MC. *Compos A* 2012; 43: 1187.
61. Grace LR, Altan MC. *Polym Compos* 2013; 34: 1144.
62. Pritchard G, Speake SD. *Composites* 1987; 18: 227.
63. Jiang X, Kolstein H, Bijlaard F. *Mater Des* 2012; 37: 304.
64. Jiang X, Kolstein H, Bijlaard F. *Compos B* 2013; 45: 407.
65. Moy P, Karasz F. *Polym Eng Sci* 1980; 20: 315.
66. Buehler FU, Seferis JC. *Compos A* 2000; 31: 741.
67. Hammiche D, Boukerrou A, Djidjelli H, Corre Y, Grohens Y, Isabelle P. *Constr Build Mater* 2013; 47: 293.
68. Kwei TK. *J Appl Polym Sci* 1966; 10: 1647.
69. Nissan AH. *Macromolecules* 1975; 9: 840.
70. Mijovic J, Zhang H. *J Phys Chem B*. 2004; 108: 2557.
71. Antoon MK, Koenig JL. *J Macromol Sci R M C* 1980; C19: 135.
72. Ishida H, Koenig JL. *Polym Eng Sci* 1978; 18: 128.
73. Lowry HH, Kohman GT. *J Phys Chem* 1927; 31: 23.
74. Kim JK, Mai YW, *Engineered interfaces in fiber reinforced composites*, Elsevier, New York, 1998.
75. Plonka R, Mader E, Gao SL, Bellmann C, Dutschk V, Zhandarov S. *Compos Part A- Appl S* 2004; 35: 1207.
76. Dibenedetto AT, Lex PJ. *Polym Eng Sci* 1989; 29: 543.
77. Walker P. *J Adhes Sci Technol* 1991; 5: 279.
78. Pisanova E, Mader E. *J. Adhes Sci. Technol.* 2000; 14: 415.
79. Ishida H. *Polym Compos* 1984; 5: 101.

80. Alawsi G, Aldajah S, RahmaanSA. *Mater Des* 2009; 30: 2506.
81. Kelley FN, Bueche F. *J PolymSci* 1961;50: 549.
82. Joshi OK. *Composites* 1983; 14: 196.
83. Collings TA, Stone DEW. *Compos Struct* 1985; 3: 41.
84. Akay M. *Composites* 1992; 23:101.
85. LassilaLVJ, Nohrstrom T, Vallittu PK. *Biomaterials* 2002; 23: 2221.
86. Chu W, Karbhari VM. *J Mater Civil Eng*, 2005; 17: 63.
87. Wan YZ, Wang YL, Huang Y, Zhou FG, He BM, Chen GC, Han KY. *Compos SciTechnol* 2005; 65: 1237.
88. Whitney JM, HusmanGE. *ExpMech* 1978; 18: 185.
89. Drzal LT, Madhukar M. *J Mater Sci* 1993; 28: 569.
90. Ray BC. *J Colloid InterfSci* 2006; 298: 111.
91. Ray BC, RathoreD. *AdvColloidInterfac* 2014; doi: 10.1016/j.cis.2013.12.014.
92. Ray BC, Rathore D. *Polym Compos* 2014; doi 10.1002/pc
93. Hahn HT. *J Eng Mater Technol* 1987; 109:3.
94. Collings T, Stone D. *Compos Struct* 1985; 3:341.
95. Wigington GD. Paper 15-C, Proceedings 46th Annual Conference, Composites Institute, New York, 1991.
96. Rabek JF. *Polymer Photodegradation*, London, Chapman and Hall, 1995.

## Appendix I

### List of papers presented/communicated based on this project

#### In Journal

**Soumya Mishra**, Dinesh Kumar Rathore and Bankim Chandra Ray, “*A Recent Understanding on Theories of Moisture Ingression and its Effect on FRP Composites*”, Journal of Advanced Research in Manufacturing, Material Science & Metallurgical Engineering, Advance Research Publications (Accepted)

#### In Conferences

**Soumya Mishra**, Sanghamitra Sethi and B.C. Ray, “*Failure Behaviour of GFRP Composites: Effect of Thermal spike and Humid Ageing*”, **International Conference on Functional Materials (ICFM), February 2014**, Indian Institute of Technology, Kharagpur.

**Shivangi Sahu**, Sanghamitra Sethi and B.C. Ray, “*Effect of Hygrothermal Conditioning and Thermal Spike on Mechanical Performance of GFRP Composites*”, **International Conference on Functional Materials (ICFM), February 2014**, Indian Institute of Technology, Kharagpur.